Title
Transient thresholding in the HIV Tat fate-selection circuit

Author
Aull, Katherine Hoffman

Publication Date
2016

Peer reviewed|Thesis/dissertation

Transient thresholding in the HIV Tat fate-selection circuit

by

Katherine Hoffman Aull

DISSERTATION

Submitted in partial satisfaction of the requirements for the degree of

DOCTOR OF PHILOSOPHY

in

Biological and Medical Informatics

in the

GRADUATE DIVISION

of the

UNIVERSITY OF CALIFORNIA, SAN FRANCISCO

Acknowledgements

This research was made possible by the sharp insights and patience of my advisor, Leor Weinberger, who guided this work through its many iterations. I am also indebted to the generosity of the UCSF research community, and the many professors and staff scientists who willingly contributed expertise, reagents, and advice. These community members include Matthew Thomson for systems biology analysis; Eric Collisson, Melanie Ott, and Eric Verdin for their deep knowledge of the model systems; and Marielle Cavrois and Kurt Thorn for training on the instrumentation.

I also greatly benefited from discussions, about research and life, with an intelligent and diverse set of labmates and classmates. Special thanks are due to Brandon Razooky, who made the key initial observations that inspired my research and contributed many useful reagents, and to my classmate and co-TA Juan Perez-Bermejo, who taught me to play Magic and continues to be a good friend. Current and former GIVI members Ibs Ali, Roy Dar, Maike Hansen, Jon Klein, Tim Notton, Anand Pai, Elizabeth Tanner, Noam Vardi, and Winnie Wen, among others, provided helpful input; Cynthia Bolovan-Fritts and Kim Osborn told me where everything was.

This research was also made possible by the love and support of my partner Phil Yam, who remains my best friend and my rock, and by my parents and cheerleaders, Jan and Ken Aull. I am also grateful for my Magic and board gaming communities, particularly Jenny and Josh Lin, for keeping my life supplied with fun and perspective. It takes a village to raise a PhD.

Statement of Published Materials

The text of Chapter 3 in this thesis is adapted from Aull, K.H., Thomson, M., and Weinberger, L.S. (2016). Transient thresholding in the HIV Tat fate-selection circuit. (in submission). The senior author Leor Weinberger directed and supervised the research that forms the basis for Chapter 3 in this thesis. Matthew Thomson aided in the development and presentation of the analysis.

Abstract

Human Immunodeficiency Virus type 1 (HIV) is a lentivirus that infects CD4+ T cells, causing progressive immune dysfunction (AIDS). Although effective treatments exist, HIV is able to form a 'latent reservoir' in long-lived memory immune cells that is transcriptionally silent and invisible to both the immune system and conventional antivirals. The HIV fate decision between latency and replication is controlled by the sole HIV promoter, LTR, and its gene product and non-cooperative monomeric activator, Tat. It remains unclear how the Tat-LTR positive-feedback circuit generates an activation threshold to prevent 'leaky' Tat expression from transactivating the LTR, thereby enabling maintenance of the latent state. Threshold generation in gene regulatory networks (GRNs) is typically achieved through deterministic bistability, which is absent here. Without some form of non-linear activation (e.g. self-cooperativity), expression noise should trigger runaway Tat feedback and thus HIV replication. Despite this, HIV latency is apparently stable, even under strong activating conditions. Using flow cytometry and single-cell imaging, I find that HIV LTR exhibits a transient threshold in response to Tat. The molecular threshold at early times is ~40,000 Tat proteins per cell, but largely disappears after 40 hours, explaining the lack of bistability and hysteresis. Further, I demonstrate that slow 'toggling' between active and inactive promoter states can generate an activation threshold without cooperativity. Cellular signaling can modulate toggling frequency and thereby adjust this threshold. These results indicate a potential role for promoter toggling as a mechanism for tunable threshold generation in GRNs. Finally, I propose a class of general stochastic models for multi-step transactivation of a toggling promoter, and argue for its relevance to LTR, which is known to exhibit intrinsic bursts of transcription at multiple time scales. This work may advance the predictive modeling of Tat-LTR and similar GRNs in higher eukaryotes.

Table of Contents

Chapter 1: Hypotheses 1

1.1. The HIV LTR promoter exhibits a transient threshold in response to Tat 1

1.2. Toggling provides a mechanism for creating activation thresholds 2

1.3. Tat increases the intensity and duration of LTR expression bursts 2

Chapter 2: Introduction 4

2.1. The problem of partial HIV reactivation 5

2.2. Evidence for cellular control of HIV latency 6

2.2.1. Cellular activation increases LTR expression 7

2.2.2. The resting cell state restricts LTR expression 9

2.2.3. Epigenetic effects restrict LTR expression 11

2.3. Evidence for viral control of HIV latency 14

2.3.1. The HIV fate decision occurs shortly after infection 15

2.3.2. Latency may increase the odds of HIV transmission 16

2.3.3. Tat feedback is sufficient to maintain LTR activity 17

2.3.4. The LTR sequence drives transcriptional pausing 19

2.4. Background on transcriptional noise 20

2.4.1. Intrinsic noise as a driver of cell-to-cell variability 20

2.4.2. Evidence for hour-scale "bursts" of transcription 21

2.4.3. LTR noise can be tuned to control HIV latency 22

2.5. Background on classic bistable fate decisions 23

2.5.1. Competing negative feedback loops 23

2.5.2. Self-cooperative positive feedback loops 24

2.5.3. Bimodality from non-cooperative positive feedback 25

Chapter 3: Transient thresholding in the HIV Tat fate-selection circuit... 26

3.1. Abstract 26

3.2. Introduction 27

3.3. Materials and Methods 30

3.3.1. Cell lines and reagents 30

3.3.2. Flow cytometry data collection and analysis 31

3.3.3. Immobilization of cells for time-lapse imaging 31

3.3.4. Microscope setup and imaging conditions 32

3.3.5. Image segmentation analysis to generate single-cell trajectories 33

3.3.6. Quantitation of Tat-Dendra molecular number by GFP molecular ruler 34

3.4. Results 35

3.4.1. The HIV LTR-Tat circuit lacks hysteresis and bistability 35

3.4.2. Single-cell flow cytometry analysis of the HIV LTR-Tat dose-response function shows a threshold-like response that is transient in time 37

3.4.3. Time-lapse microscopy analysis verifies the threshold-like LTR response to Tat at early times after activation 40

3.4.4. Transcriptional activation by TNF effectively accelerates the transient lifetime of the LTR activation threshold 43

3.5. Discussion 44

3.6. Acknowledgements 48

3.7. Supporting Materials 49

Chapter 4: Promoter toggling generates a tunable threshold in gene activation 53

4.1. Abstract 53

4.2. Introduction 53

4.3. Results 55

4.3.1. Non-cyclic promoter toggling is sufficient to create a threshold in gene activation but not mean expression 55

4.3.2. A threshold generated by promoter toggling can be tuned by cell state 64

4.3.3. Cyclic promoter toggling can generate a threshold in mean expression without bistability 68

4.4. Discussion 72

4.5. Model Definitions 74

4.5.1. Extended open-loop model with transactivator and three promoter states. 74

4.5.2. Simplified model with transactivator-dependent k-off and k-max. 75

4.5.3. Detailed model with mRNA and non-linear transactivator production. 76

4.5.4. Feedback models with non-cooperative and cooperative activation. 77

4.5.5. Open-loop model with transactivator-dependent nucleosome remodeling. 78

4.5.6. Feedback model with transactivator-dependent nucleosome remodeling. 79

4.6. Methods 80

4.6.1. Stochastic simulations 80

4.7. Analytic Forms 80

References 86

Table of Figures

Figure 1: HIV replication is controlled by the viral Tat-LTR positive-feedback circuit. 2

Figure 2: The HIV LTR-Tat positive-feedback circuit lacks hysteresis and bistability. 36

Figure 3: The LTR promoter exhibits a transient threshold in its response to Tat. 40

Figure 4: Time-lapse microscopy verifies that the LTR exhibits an activation threshold at early times. 42

Figure 5: Transcriptional activation by TNF effectively accelerates the transient lifetime of the LTR activation threshold. 44

Figure 6: At early times, the open-loop Tat-LTR circuit exhibits a threshold in both activation and mean expression. 49

Figure 7: Extraction and QC of single-cell trajectories from time-lapse images. 50

Figure 8: Correcting for photobleaching in Tat-Dendra trajectories. 51

Figure 9: Quantitation of Tat-Dendra by HSV-GFP molecular standard. 51

Figure 10: The non-physiological activator TSA and the cytokine TNF have distinct effects on threshold parameters. 52

Figure 11: Non-cyclic promoter toggling is sufficient to create a threshold in gene activation but not mean expression. 60

Figure 12: Design constraints for a toggling promoter model with threshold-like activation. 61

Figure 13: A biochemically detailed model with mRNA and inducible transactivator produces comparable output. 62

Figure 14: Intensity of Dox-induced Tat-Dendra increases super-linearly with time. 63

Figure 15: The extended model exhibits a threshold in activation but not mean expression. 63

Figure 16: Unscaled dose-response plots showing LTR response to TNF. 65

Figure 17: A threshold generated by promoter toggling can be tuned by cellular activation. 66

Figure 18: Toggling models show optimal sensitivity to cell state when transactivator decay matches toggling rate. 67

Figure 19: Toggling models with cooperative feedback are poorly responsive to cell state. 68

Figure 20: Cyclic toggling can generate a threshold in mean expression without bistability. 70

Figure 21: The cyclic nucleosome toggling model exhibits a threshold in both activation and mean expression. 71

Figure 22: The cyclic nucleosome toggling model has greater state persistence but does not exhibit permanent hysteresis or bistability. 71

Figure 23: Characteristic curves for toggling models at baseline and activated states. 85

Chapter 1: Hypotheses

1.1. The HIV LTR promoter exhibits a transient threshold in response to Tat

Infection with Human Immunodeficiency Virus (HIV) persists for a lifetime, even in the era of highly active antiretroviral therapies (HAART) that reduce viral blood titers to undetectable levels. Upon infection of CD4+ T lymphocytes, HIV undergoes a fate decision between active replication and proviral latency (Figure 1). In latently infected cells, HIV remains hidden within the cellular genome; the integrated provirus either does not express viral transcripts, or does so minimally and non-productively (Chun et al., 1995). Consequently, latent HIV cannot be detected by the immune system, nor can it be targeted by HAART or other standard therapeutic approaches. Stochastic reactivation of latent HIV leads to the rebound of HIV viremia upon interruption of HAART (Richman et al., 2009). The potential clinical utility of a treatment that depletes this 'latent reservoir' has attracted considerable interest, but these efforts have met with limited success (Deeks, 2012; Shang et al., 2015). Better understanding of the mechanisms that stabilize latent HIV would improve the likelihood of developing such a treatment.

A central puzzle of HIV latency and reactivation is that the genetic circuit responsible for controlling this process appears to be too simple to generate two deterministically stable states (Weinberger, 2015). The HIV LTR promoter, which controls all HIV transcription, is activated by its gene product Tat in a simple non-cooperative positive-feedback loop. This circuit should not have an activation threshold; in parameter ranges where activation is possible, leaky expression from the LTR should inevitably trigger Tat positive feedback, leading to HIV replication (Figure 2A). Despite this, the latent state of HIV is stable (Crooks et al., 2015; Siliciano et al., 2003), and can persist even when the state of the host cell strongly favors

replication (Ho et al., 2013). ***Therefore, I hypothesize that HIV latency results from an intrinsic threshold 'hardwired' into the LTR promoter itself.*** This hypothesis is supported by work submitted for publication (Aull et al., 2016), reproduced in Chapter 3.

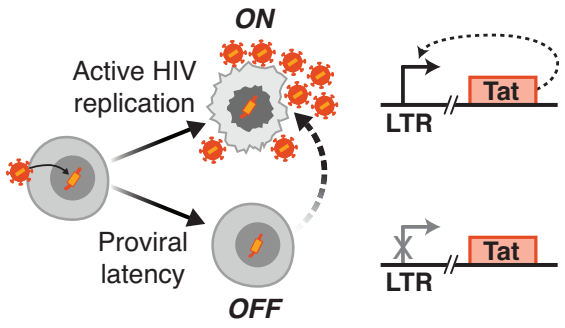

Figure 1: HIV replication is controlled by the viral Tat-LTR positive-feedback circuit. Schematic of the HIV fate decision between active replication (ON) and latent (OFF) states. Transactivation of LTR, the sole promoter of HIV, by its gene product Tat drives further Tat production and HIV replication. LTR is quiescent during latency. Figure adapted from (Dar et al., 2014).

1.2. Toggling provides a mechanism for creating activation thresholds

Stochastic fate decisions, in which genetically identical cells produce different phenotypic outcomes, are driven by the inherent noise of biological systems (Raj and van Oudenaarden, 2008). Transcription, at least in higher eukaryotes, does not occur with uniform probability; rather, mRNA is produced in sharp bursts, with the promoter otherwise inactive (Symmons and Raj, 2016). This structured noise may have functional consequences. ***I hypothesize that hours-long periods of LTR inactivity allow small bursts of Tat to decay, while larger amounts persist and trigger positive feedback during subsequent bursts.*** Thus, even in the absence of a deterministic method for establishing an activation threshold, LTR is able to suppress its response to 'leaky' Tat expression and maintain the latent state of HIV.

1.3. Tat increases the intensity and duration of LTR expression bursts

The mechanistic origins of transcriptional bursting are not well understood (Symmons and Raj, 2016). One recently identified source of confusion is that the bursting occurs at multiple

time scales (Featherstone et al., 2016; Tantale et al., 2016). Studies based on directly imaging transcriptional foci in eukaryotic cells typically report bursts at the scale of a few minutes, with variable intensity among the bursts (Chubb et al., 2006; Corrigan et al., 2016; Larson et al., 2011). By contrast, studies that track expression of reporter genes over time typically report burst cycles of a few hours, with the promoter 'toggling' between discrete active and inactive states (Harper et al., 2011; Suter et al., 2011; Zoller et al., 2015). Studies of LTR expression that infer burst parameters from statistical properties of the distributions of single-cell mRNA or protein measurements also give results consistent with lengthy toggling cycles (Dar et al., 2012; Dey et al., 2015; Skupsky et al., 2010). ***I propose general stochastic models for the multi-step transactivation of a toggling promoter that unify these diverse observations.*** This model features a slow, Tat-independent toggling step to an "open" state, which can then undergo a rapid Tat-binding step to reach the active state. By this arrangement of steps, Tat can both increase the probability of expression and, by keeping the promoter in the active state, decrease the odds that the LTR will toggle back to the inactive state. In Chapter 4, I argue that this model has natural properties that are desirable for a promoter in a genetic circuit like that of HIV, including an intrinsic activation threshold and a large dynamic range.

Chapter 2: Introduction

Acquired Immune Deficiency Syndrome (AIDS) is the result of a progressive, ultimately fatal immune dysregulation caused by infection with Human Immunodeficiency Virus (HIV). In the absence of treatment, roughly half of those infected with HIV type 1, the most prevalent form, will progress to AIDS within ten years (Mandell et al., 2010). Roughly 39 million people have died of AIDS in the period 1981-2014, mostly in sub-Saharan Africa (UNAIDS, 2015). There is no shortage of anti-HIV pharmaceuticals; over 30 mechanistically diverse agents have been approved for clinical use, and when used in combination, these are capable of routinely lowering HIV blood titers to undetectable levels. Despite this, HIV is generally incurable, with infected persons requiring treatment for life (Mandell et al., 2010). The cost and complexity of administering the necessary antiviral cocktails (HAART) means that many go without HIV treatment, especially in countries with limited medical infrastructure (UNAIDS, 2015).

A major obstacle to curing HIV is the presence of a 'latent reservoir' of inactive, genomically integrated provirus that is invisible to the immune system and presents no conventional drug targets (Figure 1). Due to the stability of latent HIV and the longevity of the memory CD4+ T cells that harbor it, the half-life of the latent reservoir has been estimated at 44 months (Crooks et al., 2015; Finzi et al., 1999; Siliciano et al., 2003), thus natural attrition is not sufficient to cure the virus on any practical time-scale. Even when infected persons have been successfully treated, having no detectable viral load for years, interruption of treatment results in HIV viremia in as little as two weeks (Davey et al., 1999; Imamichi et al., 2001). However, latent HIV is rare, being present in roughly 1 in 10^6 target cells *in vivo* (Chun et al., 1997; Eriksson et al., 2013;

Finzi et al., 1997; Wong et al., 1997). If this relatively small reservoir could be eliminated, a cure for HIV would become a practical reality.

2.1. The problem of partial HIV reactivation

Proponents of the "shock and kill" approach to HIV treatment hope to identify a mechanism by which the latent reservoir can be reactivated on demand. This new treatment modality would be applied in combination with conventional HAART, preventing a new reservoir from forming. Ideally, this approach would purge HIV from the body, meaning that infected persons would be truly cured and could discontinue treatment (Deeks, 2012; Richman et al., 2009).

An article from the Siliciano Lab (Ho et al., 2013) highlights the difficulty of this proposition. The standard test for HIV reactivation, a viral outgrowth assay (VOA), measures the proportion of resting CD4+ T cells that release infectious virus after stimulation (Finzi et al., 1997; Siliciano and Siliciano, 2005). Even under maximal T cell activation, the strongest known stimulus to HIV replication, the proportion of patient-isolated CD4+ T cells that were positive by VOA was 300 times less than the proportion of these same cells found to contain latent HIV by single-cell PCR (Eriksson et al., 2013). These non-inducing proviruses were previously assumed to be defective, but direct sequencing revealed that a full 11.9% were intact. Further, when populations of $2x10^5$ patient-isolated CD4+ T cells that did not produce virus on the first round of stimulation were allowed to recover and then treated again, another 24.6% of these showed active replication (Ho et al., 2013). Based on these results, Ho et al. argues that the true size of the latent reservoir is 60 times greater than revealed by VOA. This result is more remarkable given that the activating stimulus is far too strong to apply *in vivo*; potential treatments that have entered early-stage clinical trials give a much weaker result (Bullen et al., 2014), even when used

in combination (Laird et al., 2015). A better understanding of the fundamental mechanisms of HIV latency will be required to make progress.

2.2. Evidence for cellular control of HIV latency

HIV is a lentivirus, with its compact genome of only 9.7 kb containing one promoter and nine overlapping ORFs. The functions of all fifteen viral gene products have been comprehensively documented, yielding no evidence of a virally encoded transcriptional program for maintaining the latent state. Thus, research on HIV latency has focused on identifying cellular determinants of HIV fate, with the goal of relieving barriers to HIV reactivation and purging the latent reservoir (Siliciano and Greene, 2011).

The gene-regulatory circuit that controls HIV should, in the absence of cellular restrictions, inevitably trigger viral replication. The sole promoter of HIV, the long terminal repeat (LTR), is activated by its gene product Tat, forming a positive feedback loop. Tat binds as an obligate monomer to the RNA hairpin formed by stalled transcription at the LTR promoter, relieving the stall and driving expression of the full viral transcript, including Tat (Siliciano and Greene, 2011). Unlike multimeric activators, which can exhibit an activation threshold based on weak binding activity below the association constant, a positive feedback circuit based on a monomeric activator can only have one stable state (Dill and Bromberg, 2010). The theory of activation thresholds is further detailed in Chapter 3 (see Figure 2A). Briefly, if the HIV Tat-LTR feedback loop is capable of activation, it should always activate once any leaky expression has occurred, thus triggering replication. An enduring mystery of HIV research is how the virus exploits its host cell to achieve both latency and replication without devoting any obvious regulatory mechanisms to the task.

2.2.1. Cellular activation increases LTR expression

HIV preferentially replicates in activated CD4+ T cells (Spina et al., 1995; Stevenson et al., 1990; Zack et al., 1990; Zhou et al., 2005). Once the HIV genome became available, and its LTR promoter was identified, researchers quickly noted the similarities between LTR and a class of activation-induced lymphocytic promoters, typified by the interleukin-2 receptor (IL-2Rα, or CD25) and activating cytokines such as TNF-α, IL-2, IL-6, and IL-8 (Böhnlein et al., 1988; Civil et al., 1999). All of these promoters, as well as LTR, have a CD28-responsive element (CD28RE) that is required for expression. CD28 refers to the co-stimulatory receptor which, in combination with the antigen-specific receptor CD3, leads to activation of targeted CD4+ T cells (Murphy and Weaver, 2017). These CD28RE promoters are not expressed in resting memory T cells, the cell type most likely to harbor latent HIV.

Expression of CD28RE promoters is controlled by a suite of activation-induced transcription factors that have densely packed, and in some cases interacting, binding sites located within the CD28RE. The most important of these activating factors are NF-κB (Duh et al., 1989; Nabel and Baltimore, 1987; West et al., 2001), NFAT and AP-1 (Duverger et al., 2013; Kinoshita et al., 1997; Rooney et al., 1995), and SP1 (Perkins et al., 1993; Ross et al., 1991; Suñé and García-Blanco, 1995). Removing either of the two NF-κB binding sites or the first SP1 binding site gives the largest reductions in LTR transcription (Burnett et al., 2009).

Given that activating cytokines such as TNF-α and IL-2 are known to stimulate CD28RE promoter expression, these agents were the first to be proposed as a method for reactivating latent HIV (Chun et al., 1998b). However, in HIV-infected persons stabilized on HAART, treatment with IL-2 alone (Abrams et al., 2009; Davey et al., 1999; Dybul et al., 2002; Stellbrink

et al., 2002), IL-2 plus interferon γ (Lafeuillade et al., 2001), and IL-2 plus anti-CD3 antibody (Prins et al., 1999; van Praag et al., 2001) did not reduce the latent reservoir and also caused serious adverse effects by overstimulating the immune system. Concerns over similar toxicity have limited the use of cytokine mimics, such as Protein Kinase C (PKC) agonists, that also activate CD28RE (Delagrèverie et al., 2016).

Recent clinical trials of cell state activating treatments have focused on more tolerable agents. Major classes include Toll-like receptor (TLR) agonists, which stimulate receptors involved in nonspecific pathogen recognition (Novis et al., 2013; Scheller et al., 2006); the cytokine IL-7, which is involved in T cell homeostasis and also increases CD4+ T cell count (Levy et al., 2009; Wang et al., 2005); and disulfiram, an FDA-approved compound used to treat alcohol dependence, which can activate NF-κB through the Akt pathway (Doyon et al., 2013; Xing et al., 2011). Neither TLR agonists (Winckelmann et al., 2013), nor IL-7 (Katlama et al., 2016; Vandergeeten et al., 2013), nor disulfiram (Elliott et al., 2015; Spivak et al., 2014) have proved effective in patients, though more trials are ongoing (Delagrèverie et al., 2016).

The use of activating treatments also risks creating the opposite response, in which the immune cells become refractory to stimulation. These ‘exhausted’ cells can also be produced by the chronic immune activation associated with HIV infection, and are more likely to harbor latent HIV (Autran et al., 2013; Barouch and Deeks, 2014; Klatt et al., 2013). Evidence suggests that organ transplant recipients put on immunosuppressants show a reduction in latent HIV (Stock et al., 2014). Restoration of exhausted immune cells via inhibition of programmed cell death protein-1 (PD-1) may similarly reduce the latent reservoir (Said et al., 2010; Velu et al.,

2015). Inhibitors of PD-1 and PD-1 ligand are currently being tested in several highly anticipated clinical trials (Delagrèverie et al., 2016).

Overall, it is likely that disrupting the HIV latent reservoir by immune activation will cause more harm than good. Consequently, those seeking an effective "shock and kill" therapy for HIV have largely turned their attention to the mechanisms that restrict LTR expression in non-activated cells (Ruelas and Greene, 2013; Siliciano and Greene, 2011).

2.2.2. The resting cell state restricts LTR expression

Resting CD4+ T cells present numerous obstacles for HIV replication (Pan et al., 2013). These obstacles include barriers to infection, such as depletion of internal nucleotide pools by SAMDH1 (Baldauf et al., 2012; Descours et al., 2012) and hypermutation of the HIV genome by APOBEC3G (Yu et al., 2004), which prevent efficient reverse transcription and integration of the intact HIV provirus (Korin and Zack, 1998; Pierson et al., 2002; Zack et al., 1992; Zhou et al., 2005). When infection does occur, resting CD4+ T cells are unable to support expression from the LTR promoter, thus HIV remains latent (Agosto et al., 2007; Swiggard et al., 2005).

In the resting CD4+ T cell, many of the activating transcription factors that target LTR are sequestered or inactivated (Ruelas and Greene, 2013). The active form of NF-κB, the p50/RelA heterodimer, is sequestered in the cytoplasm by IκBα. NFAT is also retained in the cytoplasm by heavy phosphorylation. Instead, the NF-κB binding site of LTR is occupied by the inactive p50/p50 homodimer, which lacks a transactivation domain and which recruits repressive histone deacetylases (HDACs) to the LTR (Williams et al., 2006). Other repressive transcription factors with LTR binding sites, such as YY1 and LSF, are also involved in recruiting HDACs (Coull et

al., 2000; Romerio et al., 1997). The absence of activating transcription factors from LTR, and the presence of repressors, limits transcriptional initiation at the promoter.

If HIV transcription does occur in the resting CD4+ T cell, the mRNA is likely to be sequestered as well, being retained in the nucleus instead of exported to the cytoplasm for translation. This defect in nuclear export can be reversed by overexpression of polypyrimidine tract binding protein (PTB), which is also produced upon cellular activation (Lassen et al., 2006). HIV mRNA encodes the viral activator Tat, which is required for efficient transcriptional elongation from the LTR promoter. In the absence of Tat, 87% of initiated transcripts terminated prematurely at positions +55 to +59 (Kao et al., 1987). Thus, blocking nuclear export of HIV mRNA further reduces the likelihood that latent HIV will generate enough Tat protein to maintain expression of LTR and successfully enter the active replication state.

The mechanism of Tat activation of LTR is complex, but a key step is the Tat-dependent recruitment of P-TEFb to the LTR (Ott et al., 2011; Wei et al., 1998). Recruitment of P-TEFb is impaired in resting CD4+ T cells, where P-TEFb is partially sequestered in an inactive complex with 7SK RNA and HEXIM-1 (Yang et al., 2001). Active P-TEFb phosphorylates the regulatory domain of RNA Pol II (Kim et al., 2002; Parada and Roeder, 1996) and its repressive cofactors NELF and DSIF (Bourgeois et al., 2002; Fujinaga et al., 2004; Ivanov et al., 2000), releasing the transcriptional stall at LTR and enabling productive elongation.

P-TEFb provides a potential mechanism for targeted HIV latency reactivating agents that do not require activation of the resting cell. The most promising class of agents, bromodomain (BET) inhibitors, block the binding of BRD4 and related BET proteins to P-TEFb and have been shown to increase LTR activity (Banerjee et al., 2012). The mechanism of activation is

controversial, but it is believed that BRD4 competes with other potential binding partners of P-TEFb, including Tat (Bisgrove et al., 2007; Li et al., 2013) but also Tat-independent factors (Boehm et al., 2013) including NF-κB (Barboric et al., 2001). BET inhibitors are being developed as a cancer treatment, and synergize with other HIV latency reactivating agents *in vitro*, but have not yet been clinically tested in HIV-infected persons (Delagrèverie et al., 2016).

2.2.3. Epigenetic effects restrict LTR expression

Because HIV integrates into the genome of its host cell, LTR is subject to epigenetic regulation, just as other cellular promoters are. The prospect of reactivating latent HIV by altering the repressive chromatin environment of its genomic location has garnered intense research interest. The major therapeutic agents that have been clinically tested in HIV-infected persons are histone deacetylase (HDAC) inhibitors (Delagrèverie et al., 2016), though a diverse set of epigenetic mechanisms have been implicated in the formation and maintenance of HIV latency (Ruelas and Greene, 2013; Siliciano and Greene, 2011).

Histone acetylation plays a role in fine-tuning expression of regulated eukaryotic promoters. In activated CD4+ T cells, the CD28RE factors NF-κB (Zhong et al., 2002) and NFAT (García-Rodríguez and Rao, 1998) recruit the histone acetyl transferase (HAT) p300/CBP to the LTR, resulting in localized opening of the chromatin and increased transcriptional activation. Notably, p300/CBP also interacts with the viral activator Tat, and provides functionally important acetylations to the Tat protein (Ott et al., 1999). In resting CD4+ T cells, the p50/p50 NF-κB homodimer (Williams et al., 2006) and other repressive factors (Coull et al., 2000; Romerio et al., 1997) recruit HDACs to the LTR instead, promoting a closed chromatin state that is less likely to be transcribed.

HDAC inhibitors were quickly identified as potential HIV latency reactivating agents *in vitro* (Laughlin et al., 1993; Van Lint et al., 1996). The first HDAC inhibitor tested *in vivo* was valproic acid (VPA), an FDA-approved anticonvulsant that targets Class I HDACs (Phiel et al., 2001). Class I HDACs are the predominant type found at the LTR in resting CD4+ T cells (Keedy et al., 2009). While an early trial of VPA in HIV-infected persons gave promising results in three of the four cases (Lehrman et al., 2005), the ensuing wave of follow-up trials failed to demonstrate any depletion of the HIV latent reservoir following VPA treatment (Archin et al., 2010; Archin et al., 2008; Routy et al., 2012; Sagot-Lerolle et al., 2008; Siliciano et al., 2007; Steel et al., 2006).

Another, more potent HDAC inhibitor, suberoylanilide hydroxamic acid (SAHA) or vorinostat, is an FDA-approved cancer treatment. Vorinostat can reactivate HIV from resting CD4+ T cells derived from HIV-infected persons on HAART (Banerjee et al., 2012; Elliott et al., 2014). Romidepsin is another, yet more potent HDAC inhibitor with greater Class I specificity, also FDA-approved for cancer treatment. In clinical trials, romidepsin triggered reactivation of HIV mRNA from resting CD4+ T cells and detectable HIV viremia (Søgaard et al., 2015). However, in clinical trials, vorinostat (Barton et al., 2014; Elliott et al., 2014; Ke et al., 2015), the chemically related compound panobinostat (Rasmussen et al., 2014), and also romidepsin (Søgaard et al., 2015) all failed to deplete the HIV latent reservoir. Trials of these agents, alone and in combination with anti-HIV therapeutic vaccines, are ongoing (Delagrèverie et al., 2016).

DNA methylation serves as a longer-term method of gene silencing. This modification is common in heterochromatic regions of mammalian DNA, occurring largely at CpG dinucleotides (Deaton and Bird, 2011; Razin and Cedar, 1977). Many promoters, including LTR, have an

'island' of CpG sites that facilitate silencing by DNA methylation (Bednarik et al., 1990). Whether methylation of the LTR is a major driver of HIV latency *in vivo* remains controversial. In cell line models (Bednarik et al., 1990; Blazkova et al., 2009; Kauder et al., 2009; Pearson et al., 2008) and primary CD4+ T cells infected *in vitro* (Kauder et al., 2009; Tyagi et al., 2010), latent HIV is hypermethylated at the LTR promoter. Inhibition of DNA methylation with 5-aza-2'deoxycytidine restores the impaired response of LTR to cellular activation (Blazkova et al., 2009; Kauder et al., 2009). However, recent studies of latently infected CD4+ T cells derived from aviremic HIV-infected persons on HAART do not reveal hypermethylation of LTR in the natural context (Blazkova et al., 2012; Ho et al., 2013). While it remains possible that methylation is involved in the maintenance of HIV latency (Blazkova et al., 2009), it is unlikely to be the dominant mechanism of latency establishment.

The effect of genomic location on HIV activity has also been investigated. HIV integrates semi-randomly into the host genome, with a bias towards actively expressed genes (Han et al., 2004; Schröder et al., 2002). This bias is attributed to LEDGF/p75, a host cell chromatin tethering factor and required cofactor for HIV integration (Marshall et al., 2007; Shun et al., 2007), which specifically targets genes localized to nuclear pores (Marini et al., 2015). An early hypothesis was that HIV latency was the unintended result of integration within transcriptionally disfavored regions of the genome. However, latent HIV integration sites in a Jurkat CD4+ T cell model are not only enriched for globally repressed heterochromatic sites, including centromeric repeats (Jordan et al., 2003), but also for sites within highly expressed genes (Lewinski et al., 2005). A comparison of five *in vitro* models, using primary cells and cell lines, reveals no consistent predictors of HIV latency based on genomic integration site (Sherrill-Mix et al.,

2013). In latently infected CD4+ T cells from aviremic persons on HAART, most integration sites are within actively transcribed regions (Han et al., 2004; Ho et al., 2013).

The unexpected presence of latent HIV in actively transcribed genomic regions has prompted the investigation of transcriptional interference (Shearwin et al., 2005) as a mechanism for suppressing LTR expression. For primary CD4+ T cells *in vitro*, there was a modest 1.8-fold bias in latent HIV found in the same orientation as the host gene, rather than the reverse orientation (Shan et al., 2011). If the provirus is integrated in the same orientation as the host gene, 'read-through' by RNA Pol II may displace nascent assemblages of transcriptional machinery on LTR, thus preventing its expression (Greger et al., 1998). In a Jurkat CD4+ T cell model, this interference can be stopped by blocking transcription of the upstream host gene (Lenasi et al., 2008). Alternately, if the provirus is integrated in the reverse orientation, the RNA Pol II complexes from LTR may collide with those of the host gene, causing early arrest of transcription (Lewinski et al., 2005). However, it is unclear how these site-specific effects could cause the general phenomenon of latency, nor how strong activating stimuli could produce a partial response (Ho et al., 2013), given that binding of activated NF-κB effectively blocks transcriptional interference (Lenasi et al., 2008).

2.3. Evidence for viral control of HIV latency

Given the complex relationship between expression of the HIV LTR promoter and numerous cellular factors acting at the global *trans* and locus-specific *cis* levels, and the lack of latency-specific transcripts that maintain LTR repression, researchers have long supposed that cell state is the predominant driver of HIV latency. The prevailing hypothesis has been that latency is an evolutionary accident, resulting when HIV infects an activated CD4+ T cell that is in the process

of transitioning to the quiescent memory cell state (Coffin and Swanstrom, 2013; Siliciano and Greene, 2011). However, this hypothesis had not been empirically tested, and recent experimental results have failed to support it (Razooky et al., 2015). Emerging evidence suggests that the 'bet-hedging' phenotype of HIV, in which both latency and active replication are potential outcomes of infection, increases overall fitness and is actively maintained by features of the Tat-LTR circuit (Rouzine et al., 2015; Weinberger, 2015).

2.3.1. The HIV fate decision occurs shortly after infection

Latency is established early during acute infection, likely within days of initial HIV exposure (Chun et al., 1998a). In a macaque model, treatment with HAART three days post intra-rectal exposure to SIV was unable to prevent establishment of the latent reservoir (Whitney et al., 2014), and in a recent human case, the child of an untreated HIV+ mother was ultimately not protected by antiviral treatment initiated within 30 hours of birth (Ledford, 2014). To directly measure the kinetics of the HIV fate decision *in vitro*, dual-reporter viruses were developed, with a fluorescent LTR marker and a second constitutive marker that also reveals latently infected cells. In established cell lines, the majority of HIV infections result in *immediate* latency (Calvanese et al., 2013; Dahabieh et al., 2013).

The simplicity of this dual-reporter *in vitro* system excludes several common explanations for HIV latency. While the cell lines used are still not fully uniform, the complex immune dynamics present *in vivo* are absent. Further, the rapid onset of latency precludes a major role for epigenetic silencing, which acts on timescales of a week or more in T cells (Tyagi et al., 2010). The most likely conclusion is that the Tat-LTR positive-feedback circuit provides the necessary

conditions for the short-term establishment of latency in HIV-targeted cells (Razooky et al., 2015; Weinberger, 2015).

2.3.2. Latency may increase the odds of HIV transmission

In the era of HAART, latency provides an advantage by preventing the clearance of established HIV infections (Richman et al., 2009). HAART is nevertheless a recent invention, and cannot account for the ancient origins of latency, which appears to be a common feature of the lentiviral clade (VandeWoude and Apetrei, 2006). Indeed, latency should decrease replicative fitness, as it decreases the viral load and thus the probability of transmission.

In a recent modeling study, Rouzine et al. (2015) argues that this decrease in viral load is balanced by an increased probability that the new infection will become self-sustaining. Over 90% of HIV infections occur via mucosal routes (e.g., genital or oral contact), and these sites are depleted in HIV-targeted immune cells (Haase, 2011). A latency-deficient HIV strain might therefore "burn out" by replicating in an environment where the probability of transmission is low. However, if the virus temporarily enters latency, then reactivates in a target-rich environment such as a lymph node, systemic infection will likely occur. The model of Rouzine et al. (2015) thus calculates the optimal frequency of latent infections at 50%. This figure is not dissimilar to published estimates of HIV latency rates, which indicate that roughly half of all infections become latent in both established cell lines and activated primary CD4+ T cells (Calvanese et al., 2013; Chavez et al., 2015; Dahabieh et al., 2013).

This model assumes that HIV transmission is a rare event, which is well attested. Infections typically expand from a single founder sequence; the diversity of HIV sequences found within

the infected person emerges *in situ* (Kearney et al., 2009; Keele et al., 2008). Less than 1% of unprotected sex acts successfully transmit HIV (Fraser et al., 2007; Gray et al., 2001; Wawer et al., 2005), and in primates, mucosal challenge experiments with large doses of SIV often fail to establish systemic infections (Haase, 2011; Miller et al., 2005).

The evidence that latency increases the probability of transmission is more speculative. It was recently shown that sexual transmission of HIV does not select for latency-deficient strains with higher replicative capacity, but rather for consensus-like LTR variants with a substantial probability of latency (Deymier et al., 2015). Given the high mutation rate of HIV, which has a labile RNA genome and experiences roughly one mutation per replication event (Cuevas et al., 2015; Perelson, 2002), it would be extraordinary if HIV were unable to solve the latency "problem" over evolutionary time. Therefore, HIV latency is very likely to be adaptive.

2.3.3. Tat feedback is sufficient to maintain LTR activity

Tat plays a central role in the control of HIV replication. While the LTR does respond to cell state, even strong activating stimuli (e.g., TNF-α) only increase LTR expression roughly 2-fold, while Tat increases LTR expression over 50-fold (Razooky and Weinberger, 2011; Weinberger et al., 2005; Weinberger et al., 2008). When Tat activity is disrupted by mutation (Emiliani et al., 1998; Yukl et al., 2009) or by direct inhibition (Mousseau et al., 2015), HIV is unable to exit latency. Conversely, when the HIV-infected cells constitutively express Tat, latency is greatly reduced (Donahue et al., 2012). Inducible Tat expressed in *trans* is able to reactivate latent HIV in short-term infections with a Tat-deleted virus (Razooky et al., 2015), and exogenous Tat reverses long-term latency in cell line models (Jordan et al., 2003; Weinberger et al., 2008).

To directly test the hypothesis that cellular silencing is sufficient to break Tat-LTR positive feedback and push HIV into latency, Razooky and Pai et al. (2015) activated primary CD4+ T cells, infected them with single-round (*env* mutant) HIV, then allowed the cells to relax to the resting memory state. Strikingly, while expression of the activation markers CD25 and CD69 declined to baseline levels within a week, only 11.6% of actively transcribed HIV loci had turned off after 13 days without stimulation. This result indicates that Tat feedback is sufficient to overcome progressive cellular silencing and maintain expression of the Tat-LTR feedback loop, despite the less favorable conditions for LTR expression (Razooky et al., 2015).

Naively, it seems obvious that Tat would control HIV replication, since Tat plays an indispensable role in the complex biochemistry of LTR activation (Ott et al., 2011). In genetics terms, the absence of Tat, and therefore of LTR transcriptional elongation, is 'epistatic' to activating factors that promote LTR transcriptional initiation. The broader point is that, since Tat is sufficient to drive LTR activity, HIV evolution should be able to tune the fate decision between latency and active replication for optimal fitness by changing the feedback properties of the Tat-LTR circuit, all without changing the host cell. For example, a shorter-lived or less active variant of Tat would increase latency, while a more active variant would reduce latency.

A synthetic biology study directly tested the hypothesis that tuning the strength of Tat-LTR feedback can affect latency (Razooky et al., 2015). By adding an FKBP degron tag, the rate of Tat degradation can be reversibly decreased, with this shorter-lived Tat providing weaker positive feedback to LTR. As predicted, increasing the half-life of Tat from the FKBP-shortened 2.5 hours to its native 8 hours was sufficient to reactivate the majority of latent isoclones tested (Razooky et al., 2015). Tat-LTR feedback was similarly weakened by the orthogonal method of

SirT1 overexpression, which decreases the proportion of active Tat in the cell (Weinberger et al., 2008). Tat is only functionally active when acetylated (Kiernan et al., 1999; Ott et al., 1999); its activity is controlled by a futile cycle of acetylation by p300 and deacetylation by SirT1 (Pagans et al., 2005). Overexpression of SirT1 was sufficient to increase the probability of latent infection (Weinberger et al., 2008).

These synthetic biology studies also provide direct evidence that a minimal circuit containing only LTR and Tat is sufficient to generate 'phenotypic bifurcation', in which isoclonal cell lines hosting, e.g., a lentiviral LTR-GFP-IRES-Tat construct produce bimodal distributions of GFP activity (Weinberger et al., 2005). This minimal Tat-LTR feedback circuit has none of the standard indicators of bistability (as detailed in Chapter 3), and is likely monostable OFF (Weinberger and Shenk, 2007). However, stochastic modeling suggests that 'noise' in LTR expression can be amplified by Tat positive feedback to create the observed bifurcations (Weinberger et al., 2005; Weinberger and Shenk, 2007), potentially sustaining a transient pulse of LTR activity for long enough to enable HIV replication (Weinberger, 2015).

2.3.4. The LTR sequence drives transcriptional pausing

Positioned nucleosomes are a major source of the intrinsic noise in eukaryotic transcription, especially for non-constitutive promoters (Symmons and Raj, 2016), which typically have a high-occupancy nucleosome near the transcriptional start site (TSS) that can intermittently pause expression (Tirosh and Barkai, 2008). In the case of LTR, there are two characteristic positioned nucleosomes, which occur regardless of integration site: nuc-1, which is adjacent to the TSS and blocks elongation of RNA Pol II, and nuc-0, which is ~450 bases upstream and interferes with transcription factor binding (Van Lint et al., 1996; Verdin et al., 1993). These nucleosomes can

be remodeled by epigenetic factors, including histone acetyl transferases (HATs) recruited by activated NF-κB and NFAT (Bednarik et al., 1990; Kauder et al., 2009; Pearson et al., 2008) and by SWI/SNF complexes (Rafati et al., 2011). However, the dominant driver of baseline nucleosome positioning is the genomic sequence at that location (Struhl and Segal, 2013). The more nucleosome-bound the LTR becomes, the lower the frequency of expression bursts, and the higher the noise relative to the mean (Dey et al., 2015). Thus, by creating large, infrequent bursts of Tat expression, the LTR sequence itself likely drives the 'phenotypic bifurcation' of HIV latency (Weinberger, 2015).

2.4. Background on transcriptional noise

2.4.1. Intrinsic noise as a driver of cell-to-cell variability

Stochastic fate decisions, in which genetically identical cells produce different phenotypic outcomes, are driven by the inherent noise of biological systems (Raj and van Oudenaarden, 2008). Noise can be divided into two broad categories: 'extrinsic', which pertains to cell-to-cell differences in global factors such as environmental stimuli, cell size, stage in cell cycle, and availability of transcriptional components; and 'intrinsic', which pertains to variations in expression of a single promoter locus. The importance of intrinsic noise was elegantly demonstrated by Elowitz et al. (2002), who measured the expression of two identical *E. coli* promoters driving fluorescent proteins of different colors. In this system, correlated expression is due to extrinsic noise, while the remaining variation is due to intrinsic noise. This cell-to-cell intrinsic variability was clearly visible from the range of blended colors produced, especially under conditions that repress transcription (Elowitz et al., 2002).

The mechanisms that generate intrinsic noise are not completely understood. While the combination of low absolute numbers of mRNA and efficient translation amplifies intrinsic noise (Ozbudak et al., 2002), other processes contribute as well. In bacteria, transcription occurs in bursts (Golding et al., 2005), broadening the distribution of single-cell mRNA counts relative to the Poisson curve expected from independent single mRNA production events occurring with constant probability (So et al., 2011; Taniguchi et al.; Zong et al., 2010). The periodic buildup and release of DNA supercoiling likely accounts for the bursting observed in highly transcribed bacterial genes (Chong et al., 2014). For weaker promoters, these bursts likely involve relatively few mRNAs; some studies observed no noise effect attributable to bursting at the transcriptional level (Cai et al., 2006; Yu et al., 2006).

In eukaryotes, which have additional layers of chromatin organization and regulation, the situation is even more complex. In *S. cerevisiae*, extrinsic noise dominates (Raser and O'Shea, 2004), but in higher eukaryotes, the intrinsic noise from large transcriptional bursts has a larger influence (Symmons and Raj, 2016). Due to strong intrinsic noise, expression of co-regulated genes (Shah and Tyagi, 2013), or even of matched alleles (Levesque and Raj, 2013), becomes largely uncorrelated within a single cell, and the mapping between cellular *trans* factors and locus-specific expression becomes abstract and probabilistic. There are numerous factors that influence bursting, but in general, *trans* factors regulate burst size and *cis* factors regulate burst frequency (Symmons and Raj, 2016).

2.4.2. Evidence for hour-scale "bursts" of transcription

Based on inference from mRNA and protein distributions, the average burst cycle of a mammalian promoter was estimated to require a few hours to complete, both in HIV LTR (Dar

et al., 2012; Dey et al., 2015; Singh et al., 2010) and in other promoters (Raj et al., 2006; Viñuelas et al., 2013). Similar results were obtained in live human tissues (Bahar Halpern et al., 2015). Instead of short-term activity bursts with a random distribution, as observed in bacteria, these state changes (which I refer to as "toggling") are longer-lasting and appear more structured. Toggling has been directly visualized by time-lapse microscopy using reporter genes (Featherstone et al., 2016; Harper et al., 2011; Suter et al., 2011). These measurements in diverse eukaryotic promoters confirm the generality of hour-scale toggling, and reveal further structures within the "noise"; for example, after exiting the active state, the promoters have a 'refractory period' in which they cannot be reactivated (Cesbron et al., 2015; Harper et al., 2011; Suter et al., 2011), and while active, the promoters have smaller-scale bursts of activity that may be comparable to those observed in bacteria (Featherstone et al., 2016; Tantale et al., 2016).

2.4.3. LTR noise can be tuned to control HIV latency

When noise is detrimental, promoter sequences can evolve towards more consistent gene expression (Batada and Hurst, 2007; Fraser et al., 2004). Given the unusually noisy expression of the HIV LTR promoter (Dar et al., 2012; Dey et al., 2015; Singh et al., 2010), it is likely that noise plays some kind of adaptive role. Altering the level of noise in gene regulatory networks is known to influence stochastic fate decisions (Balázsi et al., 2011).

LTR noise has been experimentally modified by removing key transcription factor binding sites in the minimal LTR-GFP-IRES-Tat model. The two NF-κB sites and first SP1 site had the largest impact on LTR output (Burnett et al., 2009), while mutations in the third SP1 site and TATA box most strongly increased the switching rate between ON and OFF states (Miller-Jensen et al., 2013). LTR noise is also increased by latency reactivating compounds such as

TNF-α, TSA, and JQ1. TNF-α and TSA increase both the frequency (Singh et al., 2010) and the size of LTR expression bursts, with burst frequency increasing at low expression levels and burst size increasing at higher expression levels (Dar et al., 2012). Unlike conventional activators, JQ1 does not increase mean LTR expression, and acts primarily through increasing burst size (Boehm et al., 2013). On the theory that previous screens may have missed 'noise enhancers' like JQ1, Dar et al. (2014) performed a screen of FDA-approved compounds, identifying several that increased LTR noise, plus several 'noise suppressors' with inverse effects. Despite not increasing mean LTR expression, these 'noise enhancers' synergized with TNF-α and prostratin in reactivating latent HIV from cell lines and primary CD4+ T cells (Dar et al., 2014).

2.5. Background on classic bistable fate decisions

Our understanding of the HIV fate decision between latency and active replication (Figure 1) will be informed by other well-studied examples of genetic circuits that produce two distinct bistable outcomes. Those gene regulatory networks (GRNs) based on transcriptional regulation fall into two distinct design patterns: competing negative feedback loops, and self-cooperative positive feedback with activation thresholds (Losick and Desplan, 2008; Mitrophanov and Groisman, 2008). As the HIV Tat-LTR circuit is likely controlled primarily by transcriptional regulation (Weinberger, 2015), such GRNs will be the focus of this discussion. Fate decisions based on post-transcriptional regulation and signaling networks use a more diverse range of ultrasensitive processes (Ferrell and Ha, 2014a, b, c; Ha and Ferrell, 2016).

2.5.1. Competing negative feedback loops

The most obvious analogy to HIV latency is the fate decision performed by phage λ, an *E. coli* virus and a key model system of early genetics research (Ptashne, 2004). Phage λ infection

may proceed to active replication and lysis, or alternately, the phage may integrate into the bacterial genome and form a 'lysogen' capable of reactivation at a later time. This fate decision is controlled by multiple overlapping feedback loops which bias the decision towards the optimal outcome for a given cell state. However, the core functionality is performed by a 'toggle switch', in which two repressors, Cro and CI, compete to repress one another. Each repressor is associated with a separate dedicated gene expression program, where Cro promotes lysis and CI promotes lysogeny; the competition between Cro and CI ensures that these programs are mutually exclusive (Arkin et al., 1998; Bednarz et al., 2014). A dedicated latency program is also present in some pathogenic human viruses, including herpesviruses (Farrell et al., 1991), though this feature is absent in HIV (Siliciano and Greene, 2011).

The 'dual-repressor toggle switch' has been replicated by synthetic biology, demonstrating the generality of this circuit (Gardner et al., 2000). As in the core circuit of phage λ, each repressor targets the promoter of the other. When three such modules are connected in a loop, the result is a 'repressilator' with periodic cycles of activity (Elowitz and Leibler, 2000).

2.5.2. Self-cooperative positive feedback loops

The classic example of a fate decision controlled by self-cooperative positive feedback is that of competence in *B. subtilis* (Maamar and Dubnau, 2005; Süel et al., 2006). Entry into the competent state is driven by the transcriptional activator ComK, which cooperatively binds its own promoter as a dimer of dimers (Hamoen et al., 1998). As in phage λ, this core circuit is tuned by several auxiliary feedback loops that respond to environmental stimuli. However, the bistable response of ComK is chiefly enabled by non-linearity attributable to self-cooperative binding (see also Figure 2A). When ComK is scarce, it is largely present as inactive monomers,

while ComK activity quickly increases as its concentration approaches the dimerization constant. This intrinsic threshold limits the ComK response to weak or transient stimuli. The choice of individual cells to enter the competent state remains stochastic, with 'noise' from the ComK promoter playing a key role (Maamar et al., 2007). The ComK circuit is similar to the Tat-LTR positive feedback loop that controls HIV replication, with one striking difference: Tat binds as a monomer and does not exhibit cooperativity (Weinberger and Shenk, 2007).

2.5.3. Bimodality from non-cooperative positive feedback

There is evidence that cooperative self-activation may be dispensable for generating bimodal expression from a positive feedback circuit in eukaryotes, though such a circuit would not exhibit true bistability. For example, To and Maheshri (2010) demonstrated bimodality in a synthetic positive feedback circuit in *S. cerevisiae*. This circuit was based around the Tet-OFF activator, which exhibits an effectively non-cooperative binding response (Tet-OFF dimerizes below effective concentrations). Theoretical studies predict that bimodality is possible with non-cooperative positive feedback only when transcription occurs in large, infrequent bursts, and when the activator increases the frequency of bursting (Friedman et al., 2006). Variants of the synthetic Tet-OFF feedback loop that exhibited smaller, more frequent bursts, or that increased the effective burst frequency by reducing the Tet-OFF degradation rate, did not exhibit bimodality (To and Maheshri, 2010). Many non-constitutive eukaryotic promoters 'toggle' between active bursts of expression and long periods of inactivity (Symmons and Raj, 2016), with the HIV LTR promoter being a clear example (Dar et al., 2012; Singh et al., 2010). The implications of LTR promoter toggling for HIV latency are discussed in Chapter 4.

Chapter 3: Transient thresholding in the HIV Tat fate-selection circuit

Chapter 3 was reproduced from Aull, K.H., Thomson, M., and Weinberger, L.S. (2016). Transient thresholding in the HIV Tat fate-selection circuit. (in submission). K.H.A. and L.S.W. designed the research; K.H.A. performed the research; K.H.A., M.T., L.S.W. analyzed data; K.A., M.T., L.S.W. wrote the paper.

3.1. Abstract

Threshold generation in fate-selection circuits is often achieved through deterministic bistability, which requires cooperativity (i.e., nonlinear activation) and associated hysteresis. However, the Tat positive-feedback loop that controls HIV's fate decision between replication and proviral latency lacks self-cooperativity and deterministic bistability. Absent cooperativity, it is unclear how HIV can temporarily remain in an off state long enough for the kinetically slower epigenetic silencing mechanisms to act—expression fluctuations should rapidly trigger active positive feedback and replication, precluding establishment of latency. Here, using flow cytometry and single-cell imaging, I find that the Tat circuit exhibits a transient activation threshold, which largely disappears after ~40 hours accounting for the lack of deterministic bistability and hysteresis. The molecular threshold at early times is ~10^4 Tat transactivator molecules per cell and cellular signaling can modulate the transient threshold value. Existing models appear unable to reproduce this transient threshold effect, and I discuss models that, given further data, may recapitulate this phenomenon.

3.2. Introduction

Thresholds allow biological systems to either respond to, or disregard, a signaling input based on the input's strength or level. Such thresholds are critical for cellular decision making and are often a key design feature of gene-regulatory circuits, enabling the regulatory circuit to be robust to spurious signals or noise (Alon, 2007; Gunawardena, 2005; Wall et al., 2004). Historically, the mechanism for threshold generation was thought to be either the presence of deterministic multistability (Das et al., 2009; Ferrell, 2002; Strogatz, 2014) or zero-order ultrasensitivity (Goldbeter and Koshland, 1981; Melen et al., 2005), both of which require specific regulatory architectures (high-order self-cooperativity with hysteresis and zero-order oppositional reactions, respectively). For example, if a putative activator molecule requires homo-dimerization (i.e., self-cooperativity) to become functional, this automatically generates a molecular threshold—determined by the dimerization disassociation constant—and can lead to deterministic bistability; below the dimerization threshold there is no functional activator, whereas above the threshold activation ensues.

Formally, deterministic multistability requires nonlinearity in the governing differential equations, which can be achieved by self-cooperative positive feedback:

$$\frac{dX}{dt} = \frac{a \bullet X^H}{k + X^H} - r \bullet X \tag{1.1}$$

where X is the activator, a is the feedback strength, k is a Michaelis constant, r is the decay rate, and H is the Hill coefficient (Figure 2A, left). When the positive feedback is self-cooperative (i.e., $H > 1$), the circuit can exhibit deterministic multistability; in particular, if $H = 2$, the system can be bistable having two stable states (ON and OFF) separated by an unstable state, the

'separatrix'. Bistable circuits exhibit a response threshold (specifically, at the unstable separatrix), and are characterized by hysteresis, a type of memory in which the circuit produces different dose-response curves depending on whether signal increases or decreases (Strogatz, 2014). In contrast, positive-feedback circuits lacking self-cooperativity ($H = 1$) are monostable, having no separatrix (or threshold), no hysteresis, and only a single stable state; if this circuit can be turned ON, then the only stable state is the ON state (assuming the biochemical rate constants are not changing), with the OFF state being necessarily unstable (Figure 2A, right).

Gene-regulatory circuits typically achieve $H > 1$ and bistability via cooperative binding of a transcription factor to its promoter (Losick and Desplan, 2008; Mitrophanov and Groisman, 2008). Notable examples of bistable gene-regulatory circuits include the toggle switch (Gardner et al., 2000), phage λ lysis-lyogeny (Arkin et al., 1998; Bednarz et al., 2014), the *lac* operon (Ozbudak et al., 2004), and competence in *B. subtilis* (Maamar and Dubnau, 2005; Süel et al., 2006), all of which have thresholds established by high-cooperativity feedback loops. While other mechanisms for generating a threshold exist, e.g. zero-order ultrasensitivity (Goldbeter and Koshland, 1981; Melen et al., 2005) or buffered threshold-linear responses (Chen and Arkin, 2012; Levine et al., 2007), these rely on an excess of substrate (i.e., the promoter itself) and are not readily applicable to promoter regulation (Dill and Bromberg, 2010).

In stark contrast to these canonical examples, the circuit that controls HIV's fate decision between active replication and proviral latency (Figure 1) has none of the classic mechanisms associated with deterministic bistability or ultrasensitivity (Weinberger, 2015). Latent HIV is the chief barrier to a cure (Richman et al., 2009) and the decision between active replication and latency in HIV is governed primarily by the virus's positive-feedback circuit in which HIV Tat

protein transactivates expression of the HIV long terminal repeat (LTR) promoter, the only promoter in the virus (Figure 1). During latency, the LTR is largely quiescent but establishment of latency is not correlated with viral integration site (Ho et al., 2013; Lewinski et al., 2005; Sherrill-Mix et al., 2013) or progressive cellular silencing (Razooky et al., 2015). Specifically, epigenetic silencing occurs on the order of weeks whereas *in vitro,* while ~50% of infections result in *immediate* establishment of latency (Calvanese et al., 2013; Dahabieh et al., 2013), and *in vivo* latency is established within 3 days (Whitney et al., 2014). Thus, latency *establishment* appears far too rapid for epigenetic silencing, which acts on timescales of a week or more in T cells (Tyagi et al., 2010). Instead, the Tat-LTR positive-feedback circuit appears necessary and sufficient for establishment of latency (Razooky et al., 2015), while long-term stability of latency is likely mediated by epigenetic silencing (Siliciano and Greene, 2011).

Tat acts as a monomeric transactivator, binding to a single site on a nascent RNA hairpin formed by stalled RNA polymerase II at the LTR promoter. Because Tat binds non-cooperatively, classical deterministic models predict that the circuit should have no activation threshold and thus the latent state would be unstable (Weinberger and Shenk, 2007). Thus, it is unclear how, without bistability, HIV generates a molecular threshold in Tat so that it can even temporarily remain in an off state and provide an opportunity for the kinetically slower epigenetic silencing mechanism to act. Given the noisy expression of the HIV LTR promoter (Dar et al., 2012; Dey et al., 2015; Singh et al., 2010), Tat positive feedback should trigger active replication within these first few days. This would preclude establishment of proviral latency, as active replication destroys the cell within hours (Perelson et al., 1996) and silencing of an actively replicating cell cannot overcome active HIV gene expression (Razooky et al., 2015). In

general, it remains unclear how the Tat positive-feedback circuit that lacks deterministic bistability (and ultrasensitivity) can generate a threshold to establish a stable off state.

Here, we examine the HIV Tat-LTR circuit to determine how a threshold can be generated without self-cooperativity. Using a combination of single-cell experimental analyses, both flow cytometry and time-lapse fluorescence microscopy, we find that the LTR circuit exhibits a transient threshold for activation by Tat. The threshold gradually disappears and at ~40 hours, there appears to be no effective threshold such that the LTR-Tat circuit does not exhibit hysteresis or deterministic bistability. The molecular mechanisms enabling this type of transient thresholding remain unclear, but the threshold is tunable via cellular activation (e.g. NF-κB signaling), which modulates the kinetics of promoter toggling.

3.3. Materials and Methods

3.3.1. Cell lines and reagents

The minimal Ld2GITF feedback circuit and the doxycycline-inducible Tat-Dendra cell line have been previously described (Razooky et al., 2015). Here, the lentiviral LTR mCherry reporter from (Razooky et al., 2015) was modified to contain an N-terminal PEST tag, giving LTR mCherry-deg, with mCherry protein half-life 10.7 hours (data not shown). Plasmid maps and cloning details available on request. LTR mCherry-deg was packaged in 293T cells and used to infect Jurkat Tat-Dendra cells at low MOI (mCherry positive cells < 5%). These cells were induced at high Dox (500 ng/mL) for 2 days, then FACS sorted to isolate dual-positive single cells using a FACSAria II (BD Biosciences USA, San Jose, CA) which were grown into isoclonal populations. Isoclones were screened to confirm robust dual-positive response to Dox with negligible expression at baseline. Unless otherwise stated, all chemical reagents were

sourced from Sigma-Aldrich USA (Saint Louis, MO). When specified, the HIV reactivating agents TNF (10 ng/mL tumor necrosis factor alpha) or TSA (400 nM trichostatin A) were supplied at the time of Dox addition.

3.3.2. Flow cytometry data collection and analysis

To generate dose-response plots, each isoclone and condition was tested at eight doxycycline (Dox) levels: seven two-fold dilutions, from 250 to 3.9 ng/mL, plus a zero-Dox control. Data were collected on a MACSQuant™ high-throughput flow cytometer (Miltenyi Biotec, Bergisch Gladbach, Germany), gated for live single cells in FlowJo™ (Tree Star, Ashland, OR). The mCherry positive cutoff was chosen to exclude non-induced cells. All eight Dox dilutions were pooled and cells were grouped by Tat-Dendra signal to estimate the conditional probability of LTR response for the specific Tat level. A schematic of this workflow, with sample data, is presented in Figure 3B-D (all Tat-Dendra values were background-subtracted, using the mean of zero-Dox control as background; clusters with non-positive Tat-Dendra values were not considered in the analysis). The dose-response and dose-mean expression curves obtained by this method were fit to a standard Hill function: $P_{ON} = P_{MAX} \cdot (Tat^H / (K_{50}^H + Tat^H))$. Nonlinear least-squares fitting was performed in R, using the nlsLM function from the minpack.lm package (CRAN).

3.3.3. Immobilization of cells for time-lapse imaging

5-10x10^6 actively dividing (healthy) Jurkat cells were washed twice in regular phosphate buffered saline (PBS), then again in mildly alkalized PBS (pH 8.0). Immediately before use, a single aliquot of biotinylation reagent (1 mg EZ-Link Sulfo-NHS-LC-Biotin, ThermoFisher,

Waltham, MA) was re-suspended in 800 µL PBS (pH 8.0). Of this, 500 µL was used to re-suspend the cells after the final wash, while the rest was added to a collagen-coated coverslip plate (#1.5, 35 mm, MatTek, Ashland, MA). Both cells and coverslip were kept at room temperature. After 30 min, the coverslip was thoroughly rinsed with PBS + 50 mM glycine, then coated with 80 µL streptavidin (1 mg/mL, New England Biolabs, Ipswich, MA). The cells were then washed twice in glycine solution, then again in standard culture medium. During the final wash step (~15 min later), the coverslip was rinsed with PBS to remove unbound streptavidin. The biotinylated cells were resuspended in ~300 µL culture medium, transferred to the coverslip, then placed in the incubator for 30 min to settle by gravity. Unbound cells were then carefully rinsed away, and the plate was refilled with 2.5 mL of culture medium containing 250 ng/mL Dox. The finished plate was placed on the microscope for thermal equilibration (~1 hr) and subsequent imaging.

3.3.4. Microscope setup and imaging conditions

All imaging was performed on a Zeiss AxioVert inverted fluorescence microscope (Carl Zeiss, Jena, Germany), equipped with a Yokogawa spinning disc, CoolSNAP HQ2 14-bit camera (Photometrics, Tucson, AZ), and laser lines for 488nm and 561nm excitation. To facilitate time-lapse imaging, the microscope has a programmable stage with Definite Focus, and also a stage enclosure that maintains samples at 37C and 5% CO2 with humidity. Images were captured every 10 minutes, sampling a 5x5 X-Y grid, one Z-position each. Exposures were 800 ms at 20% power with the 561nm laser, then 400 ms at 10% power with the 488nm laser, then 600 ms for brightfield. The objective used was a 40X oil, 1.3NA, with 2x2 camera binning applied. For all "induced Tat" movies, imaging was started no more than 2.5 hours after Dox addition, and was

continued until 20 hours. For protein half-life measurements, imaging was started 10 minutes after addition of 10 μg/mL cycloheximide and continued for 50 ten-minute intervals. Bleaching half-life was measured with the same image settings, but taken at one location in five-second intervals to minimize changes in total protein level. For HSV-GFP imaging, to maximize the visibility of these very small particles, the 488nm exposure time was increased to 40 s and binning was turned off. For each location in a 7x7 X-Y grid, nine Z-positions were sampled at 0.2 μm intervals; the most in-focus image was chosen for analysis.

3.3.5. Image segmentation analysis to generate single-cell trajectories

The center of each cell was manually marked, using the final brightfield image and a custom script (MATLAB, The MathWorks, Natick, MA). For each cell location, a 23-pixel diameter circle was marked around it, and the mean fluorescence intensity within that circle was recorded at each time point to generate single-cell trajectories. Each trajectory was then subjected to automated quality control (QC): cells in which any two consecutive readings differed by more than 15% in either channel were excluded; upon review of the source images, these events were typically due to cell division, or another cell drifting into view. Cells that began the experiment "on" were also excluded (LTR >2% over background at 2.5 hours post-Dox addition; this was rare, 2-5 cells per condition). Illustrations of the raw image data and QC process are available in Figure 7 (Supporting Materials). For these movies, between 2001 and 2193 cell trajectories passed QC. The trajectories were normalized to set their lowest values to zero, then fit to a smoothing spline in base R (df=10, n=105) to further reduce noise. Tat-Dendra trajectories were also corrected for photobleaching. This was not necessary for mCherry, which did not bleach

under the imaging conditions used (data not shown). The photobleaching correction process is described in Figure 8 (Supporting Materials).

3.3.6. Quantitation of Tat-Dendra molecular number by GFP molecular ruler

For quantitation using the HSV-GFP molecular ruler (Charpilienne et al., 2001; Desai and Person, 1998), the images of viral particles were processed using a custom script (MATLAB, The MathWorks, Natick, MA). Each image was background-subtracted, using the median of all 49 images as background, then thresholded to include the bright particles and the first Airy disk surrounding them. The MATLAB function bwconncomp was used to identify potential features within the images. To set the correct size, TetraSpeck™ beads (ThermoFisher, Waltham, MA) were analyzed by the same method; the 0.2 μm beads were 15-18 pixels (data not shown). Since the HSV-1 capsid is 125 nm (Gibson, 1996), features between 10-14 pixels were selected. For each feature, the total intensity above background was recorded. The mean value was 1424 units. (95% CI 1412-1435; n=5004.). Given that the HSV-GFP images had 100X the exposure time, and 4X as many pixels, relative to the Tat-Dendra images, each intensity unit of HSV-GFP represents 25X less signal. EGFP is also brighter than Dendra2 by 1.47X (Chudakov et al., 2007) such that there are [1424 / 25] intensity equivalents per [900 x 1.47] molecular equivalents, which reduces to 1 intensity unit per 23.2 Tat-Dendra (Figure 9, Supporting Materials). From the single-cell imaging data, the threshold level of Tat proteins required to minimally activate the LTR (i.e., > 2% mCherry positive cells) gives an intensity signal of 5.0 units per pixel, or 1900 units per cell (each cell is 377 pixels). The conversion factor calculated from molecular ruler thus estimates the minimal activation threshold at 4.4×10^4 Tat molecules per cell (Figure 9C).

3.4. Results

3.4.1. The HIV LTR-Tat circuit lacks hysteresis and bistability

Previous studies demonstrated that the HIV Tat-LTR positive-feedback loop has an expression rate that appears non-cooperative and scales linearly with Tat at early time points (Weinberger and Shenk, 2007), as expected for non-cooperative positive feedback (Figure 2A). To confirm that the LTR-Tat circuit does not establish bistability through other mechanisms (e.g., nonlinear degradation), we tested for hysteresis in a minimal Tat-LTR feedback circuit, where LTR drives expression of an unstable (2 hr half-life) GFP reporter (d2GFP) and an IRES enables co-expression of Tat fused to the tunable proteolysis tag FKBP (Figure 2B). In this circuit (hereafter Ld2GITF), Tat can be protected by the small molecule Shield-1 (Banaszynski et al., 2006), thereby allowing feedback strength to be tuned (Razooky et al., 2015) and alternate paths of the circuit—ON-to-OFF versus OFF-to-ON—to be examined. Specifically, cells in the GFP ON state (i.e., pre-incubated in Shield-1) can be exposed to successively decreasing Shield-1 levels to examine turning OFF of the circuit, while cells in the GFP OFF state (i.e., no Shield-1 pre-incubation) can be exposed to successively increasing Shield-1 levels to examine turning ON of the circuit. The difference (Δ) in percentage of GFP ON cells for a specific Shield-1 concentration can be quantified, with $\Delta > 1$ indicating hysteresis. If hysteresis is present, cells beginning in the ON state (i.e., pretreated with high Shield-1) will be more likely remain ON at a specific intermediate dose of Shield-1, as compared to cells that began in the OFF state (i.e., non-pretreated cells); whereas, if hysteresis is not present ($\Delta = 1$), there will no difference in ON-OFF percentages for cells beginning in either the ON or OFF state. We tested five isoclonal Ld2GITF populations carrying single integrations of the Ld2GITF circuit, and measured Δ to be ≈ 1 (Mean

1.008; 95% CI 0.813-1.203; Figure 2C), indicating that hysteresis is unlikely. These hysteresis measurements build upon previous data indicating that the necessary conditions for deterministic bistability are absent in the HIV Tat-LTR circuit (Weinberger and Shenk, 2007).

Figure 2: The HIV LTR-Tat positive-feedback circuit lacks hysteresis and bistability.

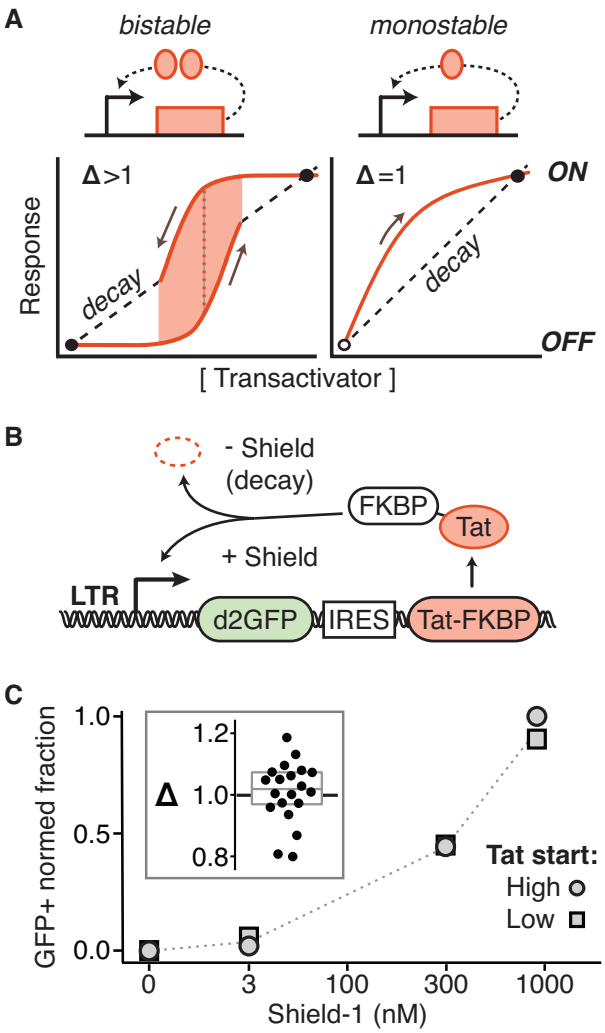

(A) Bistability versus monostability in positive-feedback transcriptional circuits. Formally, deterministic multistability requires nonlinearity in the governing differential equations (Strogatz, 2014); for example, if the activator requires cooperative self-association to bind its promoter, its expression is described by a nonlinear Hill equation (Hill coefficient $H > 1$) (Dill and Bromberg, 2010). Such circuits exhibit bistability, having two attractor states (ON and OFF) separated by a response threshold—at low activator levels, the decay rate (dashed line) dominates over synthesis (solid line), while at high levels the opposite is true—and hysteresis, a type of memory in which the response is history dependent, following different paths from ON-to-OFF versus OFF-to-ON (the difference between paths is $\Delta > 1$). In contrast, circuits lacking self-cooperativity ($H = 1$) are monostable, having neither a threshold nor hysteresis ($\Delta = 1$)—if a monostable circuit can be turned ON, its only stable state is the ON state (assuming the biochemical rate constants are not changing), with the OFF state being necessarily unstable (Strogatz, 2014). (B) Schematic of the minimal HIV "Ld2GITF" positive-feedback circuit used to test for hysteresis (LTR driving a 2-hour half-life GFP reporter and an IRES expressing Tat fused to FKBP, a degradation tag inactivated by the small molecule Shield-1). (C) Hysteresis test by flow cytometry analysis of Ld2GITF. Isoclonal Jurkat Ld2GITF cells were either pretreated with 1 μM Shield-1 for four days to activate cells to start in an ON start (oval data points) or not pretreated to start in an OFF state (square data points). All cells were washed, and then incubated in the specified Shield-1 alongside for an additional four days and the percentage of GFP+ cells measured. Inset: Δ (the ratio of pretreated to not-pretreated GFP+ cells) calculated for five isoclonal populations of Ld2GITF (<Δ> 1).

3.4.2. Single-cell flow cytometry analysis of the HIV LTR-Tat dose-response function shows a threshold-like response that is transient in time

Absent bistability, it was unclear how the Tat-LTR circuit might encode a threshold to temporarily remain OFF in order to provide an opportunity for the kinetically slower epigenetic-silencing mechanisms to act. Importantly, chromatin silencing mechanisms appear unable to silence the actively transcribing promoter (Razooky et al., 2015).

First, to check if the Tat-LTR circuit encodes an activation threshold, we directly quantified LTR activity as a function of Tat levels using an 'open-loop' Tat-LTR dose-response system. In this system, one construct encodes Tat fused to the fluorescent reporter Dendra2 expressed from a doxycycline-inducible tet promoter, while a second construct encodes an mCherry reporter expressed from the LTR promoter (Figure 3A). This open-loop system allows Tat levels to be tuned by doxycycline (Dox) and enables both Tat (dose) levels and LTR (response) levels to be quantified in the same cell (Razooky et al., 2015) so that the dose-response 'transfer' function for Tat and LTR can be fit and an effective Hill coefficient calculated.

To estimate the conditional probability of LTR mean expression level and percentage ON for a given Tat level from flow cytometry data, a binning method similar to previous methods (Krishnaswamy et al., 2014) was used (Figure 3B-C). Examination of the flow cytometry time-course data showed that the LTR appears essentially non-responsive to Tat at low Tat levels, but LTR activity then increases sharply over a narrow range of Tat (Figure 3D). At early times after Dox activation, a pronounced "shoulder" is visible in Tat expression where a substantial percentage of cells express Tat-Dendra but these cells do not express mCherry from the LTR. This delay between Tat-Dendra and mCherry expression is on the order of eight to twelve hours,

which is too long to simply be a temporal delay in expression of mCherry due to activation by Tat-Dendra.

For all LTR isoclones (i.e., integration sites) examined, the dose-response expression curves for both mCherry mean expression and percentage of mCherry ON cells exhibits a conspicuous activation threshold (Figure 3E). The LTR appears essentially non-responsive to Tat at low Tat levels, but LTR activity then increases sharply over a narrow range of Tat. This thresholding behavior appears maximized at intermediate time points of 16-20 hours (Figure 3F-G). At early times the response is incomplete but by 40 hours, the dose-response curves flatten with the K_{50} shifting to lower Tat expression.

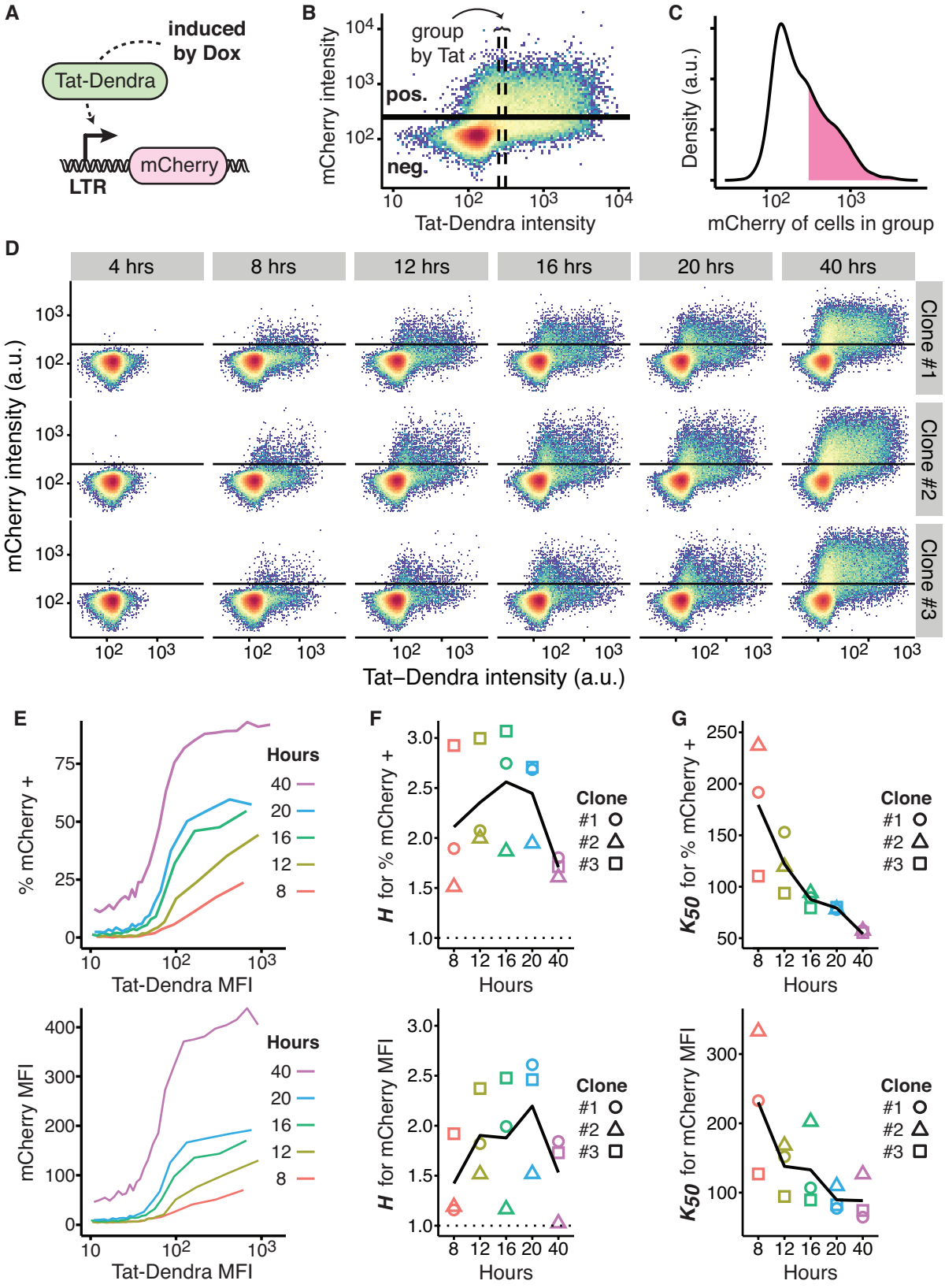

Figure 3. Caption on next page.

Figure 3: The LTR promoter exhibits a transient threshold in its response to Tat.

(A) Schematic of constructs used to directly quantify LTR-Tat dose-response function. A doxycycline-inducible promoter (Tet-ON system) drives expression of a Tat-Dendra2 fusion protein, which activates the LTR promoter to drive expression of destabilized mCherry reporter. (B) Scheme for estimating conditional probability of LTR activity for a given Tat level, with representative two-color flow cytometry dot plot of an isoclonal Jurkat cell line stably expressing constructs in panel A after 20 hours of Dox induction (plot shown is Clone 2). To estimate the conditional probability of LTR expression for a given Tat level, data was combined from eight Dox dilutions (0-250 nM). The dense spot in the lower left corner corresponds to non-induced cells (i.e., auto-fluorescence background), which the mCherry positive cutoff gate excludes (as indicated by the black horizontal line). Cells with similar Tat-Dendra values were grouped, as indicated by the vertical dashed lines, and the percentage of cells above the mCherry positive cutoff and mean mCherry fluorescence was recorded for each group. For visual clarity, this panel depicts a group of 2500 cells, while the analysis uses a tighter group of 1000 cells. (C) Histogram of mCherry intensity for cells in the marked group. Density above the mCherry positive cutoff is shaded. Despite the narrow band of Tat-Dendra intensities, the LTR response is variable. (D) Full flow cytometry time-course for three isoclones of Jurkat encoding both Tet-Tat-Dendra and LTR-mCherry-deg induced with eight Dox dilutions, and measured by flow cytometry over time. The horizontal lines indicate the mCherry positive cutoff. At early times, a pronounced "shoulder" is visible in Tat expression where a substantial percentage of cells express Tat-Dendra but these cells do not express mCherry from the LTR. (E) Calculated dose-response curves for percentage of mCherry+ cells (top) and mCherry mean fluorescence intensity (MFI, bottom) from data in panel D. Clone 1 is shown; the other isoclones, and Hill fits, are presented in Figure 6 (Supporting Materials). (F) Calculated Hill coefficients (H) from dose-response curves over time. The expected non-cooperative response ($H = 1$) is indicated by a dashed line, all data points are above the expected $H = 1$ line. Maximum H-values occur at intermediate time points for both %mCherry cells and MFI. (G) Calculated half-maximal response (K_{50}) from fits of the dose-response curves over time. K_{50} declines over time, indicating that the threshold becomes progressively weaker.

3.4.3. Time-lapse microscopy analysis verifies the threshold-like LTR response to Tat at early times after activation

To verify that this result was not simply a peculiarity of the flow cytometry approach, we next examined activation of this 'open-loop' activation circuit using quantitative time-lapse imaging (Figure 4A). Jurkat isoclones, as above, were imaged for 20 hours after Dox activation and for all isoclones there is a conspicuous delay of approximately seven hours in mCherry expression relative to Tat-Dendra expression (Figure 4A–B). The single-cell trajectories used to

construct Tat-LTR dose-response trajectories via the same conditional binning method as used for flow cytometry (Figure 3) and for all LTR isoclones examined, the dose-response expression curves for both mCherry mean expression and percentage of mCherry ON cells exhibits a conspicuous activation threshold (Figure 4C–D). As observed in flow cytometry, the microscopy imaging shows that the LTR is essentially non-responsive to Tat at low Tat levels, but LTR activity then increases sharply over a narrow range of Tat

We used a previously described 'molecular ruler' approach (Charpilienne et al., 2001; Desai and Person, 1998) to convert Tat-Dendra fluorescence levels to molecular number (Methods and Supporting Materials). For all clones tested, the threshold level of Tat proteins required to minimally activate the LTR (i.e., > 2% mCherry positive cells) is in the tens of thousands of molecules, with the average being 4.4×10^4 Tat/cell (Figure 4C–D). Comparable values for Tat molecules per cell were previously obtained in a minimal Tat-LTR feedback circuit, with quantitation performed by GFP standard beads (Weinberger et al., 2005). Upon accounting for cell size differences, this molecular threshold value is also not dissimilar to those calculated for phage λ, where 55 Cro molecules are required for lytic infection and 145 CI molecules are required for lysogeny (Arkin et al., 1998); human lymphocytes are $\sim 10^3$ times the volume of E. coli (Milo et al., 2010).

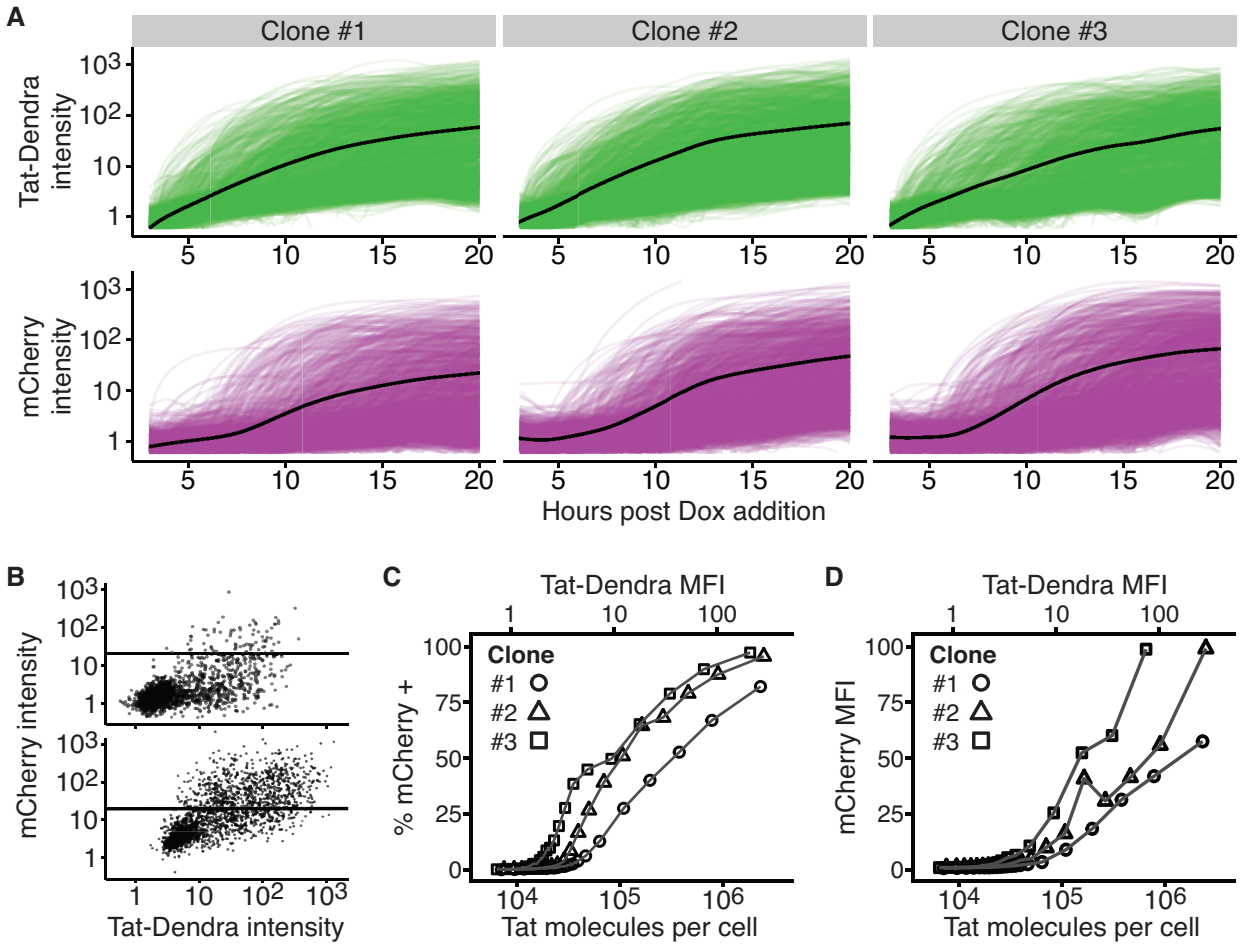

Figure 4: Time-lapse microscopy verifies that the LTR exhibits an activation threshold at early times.

(A) Time-lapse fluorescence microscopy imaging of single cells from three Jurkat cell isoclonal populations each encoding both Tat-Dendra and LTR-mCherry-deg. Cells were activated and then imaged for 20 hours. Tat-Dendra trajectories are green; mCherry trajectories are magenta; mean intensity trace shown in black. ~2000 cell trajectories shown for each clone. (B) Flow-style dot plot of Tat-Dendra versus mCherry intensities from time-lapse images at t = 10 h (upper) and t = 20 (lower) of Clone 2. Each dot represents an individual cell. As in Figure 3, the horizontal line marks the mCherry positive cutoff gate. (C-D) Dose-response curves for %mCherry+ cells (left) and mCherry mean fluorescence intensity (MFI, right) versus Tat MFI and calculated number of Tat molecules per cell. Single-cell intensities extracted from all images were pooled and processed in the same manner as the flow data (each point summarizes 10^4 observations). Tat-Dendra signal intensity was converted to molecular number using a GFP "molecular ruler".

3.4.4. Transcriptional activation by TNF effectively accelerates the transient lifetime of the LTR activation threshold

Based on observations that HIV latency can be partially reversed by transcriptional activators, we next asked if transcriptional activators could alter the observed LTR-activation threshold. To transcriptionally active the LTR, we used the well-characterized cytokine tumor necrosis factor alpha (TNF), which acts through nuclear factor kappa B (NF-κB) signaling to recruit transcriptional activators to the LTR (Jordan et al., 2003; Jordan et al., 2001; Razooky et al., 2015), thereby increasing LTR transcriptional burst frequency (Dar et al., 2012; Dar et al., 2016; Singh et al., 2010)

When the dose-response function is measured at 20 hours post Dox induction in the presence of TNF, the response functions show a markedly reduced threshold (Figure 5A). In fact, when comparing the dose-responses in the presence and absence of TNF, the presence of TNF caused the 20-hour dose-response curve to look similar to the 40-hour non-TNF dose-response curves (compare Figure 5A to Figure 3E). Consistent with this observation, the calculated Hill coefficients, *H*, decreases in the presence of TNF (Figure 5B) and, with the exception of clone 2 MFI, the K_{50} values decline in the presence of TNF (Figure 5C), indicating that the threshold becomes progressively weaker.

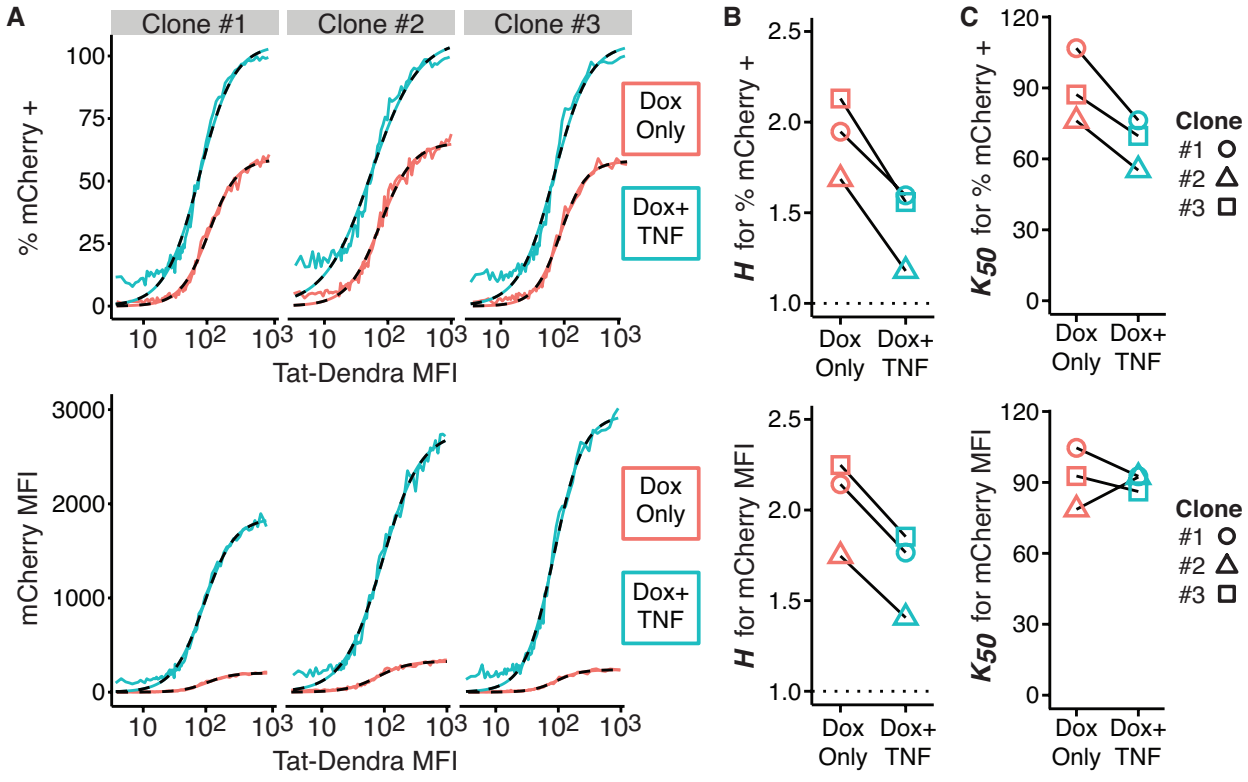

Figure 5: Transcriptional activation by TNF effectively accelerates the transient lifetime of the LTR activation threshold.

(A) Dose-response curves for %mCherry positive cells (top) and mCherry MFI (bottom) from flow cytometry measurements of three isoclones of Jurkat Tet-Tat-Dendra + LTR-mCherry, at 20 hours post Dox induction in the presence or absence of TNF. Each data point depicts a group of 500 cells. These data were fit to a Hill function (dashed lines); numeric results are given in Figure 10 (Supporting Materials). (B) Hill coefficients, *H*, determined from dose-response curve fitting, demonstrate empirical positive cooperativity ($H > 1$) with lowering of *H*-values for cells treated with TNF. The expected non-cooperative response is indicated by the dotted line at $H = 1$. (C) Half-maximal response (K_{50}), determined from dose-response curve fitting.

3.5. Discussion

HIV's ability to establish latency in resting $CD4^+$ T lymphocytes remains the chief barrier to curative therapy (Richman et al., 2009) and an area of active study. Latency establishment is not correlated with viral integration site (Ho et al., 2013; Lewinski et al., 2005; Sherrill-Mix et al., 2013) or progressive cellular silencing, and the Tat positive-feedback circuit is necessary and

sufficient for latency establishment (Razooky et al., 2015), with epigenetic silencing possibly regulating maintenance and stability of the latent state (Siliciano and Greene, 2011). However, given non-cooperative nature of Tat feedback (Weinberger and Shenk, 2007), the circuit was thought to lack an activation threshold so it was unclear how HIV could even temporarily remain in an off state to provide an opportunity for the kinetically slower epigenetic silencing mechanisms to act and stabilize latency.

Here, using combination of single-cell analyses (flow cytometry and time-lapse microscopy), we find that the HIV Tat circuit exhibits a transient threshold in activation that largely disappears after ~40 hours. The transient nature of the threshold accounts for the lack of deterministic bistability and hysteresis in the circuit and previous findings that Tat feedback is non-cooperative (Weinberger and Shenk, 2007). Physiologically, the transient nature of the threshold may allow the Tat circuit to temporarily remain in an off state and buffer stochastic fluctuations from rapidly triggering positive feedback and active replication, thereby providing a 'temporal window' for the kinetically slower epigenetic silencing mechanisms to stabilize the off state.

One caveat to this data is that we only examined three isoclonal integration sites of the LTR promoter. It is possible that these integration sites are somehow unique in their ability to generate a threshold and that higher-throughput analyses of integration sites will produce a different result. Notwithstanding, the cellular and molecular mechanisms that generate this transient threshold in LTR activation remain unclear. Based on the above data, it is possible to exclude two of the simplest classes of gene-activation models. Since the data shows a fractional response of the LTR to despite Tat present in the cell, it is most straightforward to consider chemical-

reaction-type models where fractional responses can be computed. For example, for the simplest Tat-LTR activation model:

$$\begin{gathered} Tat + LTR \rightarrow LTR::Tat \\ LTR::Tat \rightarrow RNA + Tat + LTR \\ RNA \rightarrow RNA + \text{Protein} \\ RNA \rightarrow \varnothing \\ \text{Protein} \rightarrow \varnothing \\ \varnothing \rightarrow Tat \rightarrow \varnothing \end{gathered} \tag{1.2}$$

it is straightforward to show the absence of the necessary conditions for a cooperative response ($H > 1$). Specifically, we consider the fraction of time the system is in the LTR::Tat state ($P_{LTR::Tat}$), which directly generates RNA and Protein. For $H > 1$, $P_{LTR::Tat}$ as a function of Tat levels requires hyperbolic curvature or, more formally, there must be some non-zero value of Tat where $\delta[P_{LTR::Tat}] / [Tat]^2 = 0$. However, in this model, $\delta[P_{LTR::Tat}] / [Tat]^2 \neq 0$ for any non-zero value of Tat. Likewise, for slightly more complex models based on the two-state or random-telegraph model of promoter activity:

$$\begin{gathered} OFF_{LTR} \rightleftharpoons OPEN_{LTR} \\ OPEN_{LTR} + Tat \rightleftharpoons ON_{LTR::Tat} \\ ON_{LTR::Tat} \rightarrow ON_{LTR::Tat} + RNA \\ RNA \rightarrow RNA + \text{Protein} \\ RNA \rightarrow \varnothing \\ \text{Protein} \rightarrow \varnothing \\ \varnothing \rightarrow Tat \rightarrow \varnothing \end{gathered} \tag{1.3}$$

it is also relatively straightforward to algebraically show that $\delta[P_{ON}] / [Tat]^2 \neq 0$ at any non-zero value of Tat.

In order to transiently generate $H > 1$, some form of transient Tat cooperativity is required. This cooperativity could in principle be achieved through homo-multimerization (Dill and Bromberg, 2010; Teng et al., 2012; Wall et al., 2004) of Tat protein, or successive covalent modifications (Ferrell Jr., 1998) of Tat, or successive Tat-dependent steps required for LTR activation. However, to recapitulate the data, it is absolutely critical that the mechanism of cooperativity is transient and disappears over time (or disappears as Tat level increases). The homo-multimerization mechanism is the most difficult to reconcile with this. While it is possible that the active form of Tat multimerizes at early times (low levels of Tat) but then becomes a monomer at later times (high Tat levels) and under TNF stimulation, this scenario would be an exotic departure from the typical biophysical models of concentration-dependent multimerization of a protein (i.e., monomeric at low concentrations with crowding-induced multimerization). In contrast, it may be more appealing to consider models where at early times (low Tat or LTR-expression levels) two successive Tat dependent steps are required for LTR activation but as the promoter increases in transcriptional activity, one of these Tat-dependent steps becomes a Tat-independent step. For example, active and quiescent promoters differentially localize in the nucleus (Cavalli and Misteli, 2013; Simonis et al., 2006) and if the genomic locus where the LTR integrates repositions as LTR activity increases, the LTR may be subject to different activation signals when it reaches a new nuclear microenvironment (Lusic et al., 2013). In other words, at early times during activation the LTR locus is in a quiescent nuclear micro-environment, whereas at later times after activation the LTR may reposition to a more "TNF-like" nuclear micro-environment.

There may also exist additional thresholds in LTR activation, such as in response to chromatin remodeling (Miller-Jensen et al., 2012). However, as discussed above, the epigenetic silencing mechanisms that allow for chromatin-mediated reactivation are dynamically slower effects that cannot explain establishment of latency (Razooky et al., 2015) and thus this chromatin threshold is likely distinct from the early-time transient thresholding results observed here.

Regarding the potential benefits of such transient thresholding relative to multistability, we can only provide speculation. When molecular thresholds are established through self-cooperativity and multistability, it is biochemically difficult to alter the threshold level. In the case of the Tat-LTR circuit, TNF (Figure 5) and other cellular activators (e.g., trichostatin A, Figure 10 in Supporting Materials) can alter the threshold. Thus, somehow the mechanisms that establish the Tat-LTR threshold are distinct and enable 'tuning' of the threshold value. Future work will focus on elucidating the molecular mechanisms that establish the transient threshold and its tunability.

3.6. Acknowledgements

We thank Brandon Razooky for key initial observations and reagents, and Marielle Cavrois of the Gladstone Flow Cytometry Core (supported by NIH P30 AI027763, S10 RR028962) and Kurt Thorn of the UCSF Nikon Imaging Center for technical help and advice. K.H.A. was supported by a NSF Graduate Research Fellowship. M.T. acknowledges support from the NIH Office of the Director, the National Cancer Institute, and the National Institute of Dental and Craniofacial Research (NIH DP5 OD012194). L.S.W. acknowledges support from the NIH Director's New Innovator Award Program (OD006677), and NIH R01 AI109593.

3.7. Supporting Materials

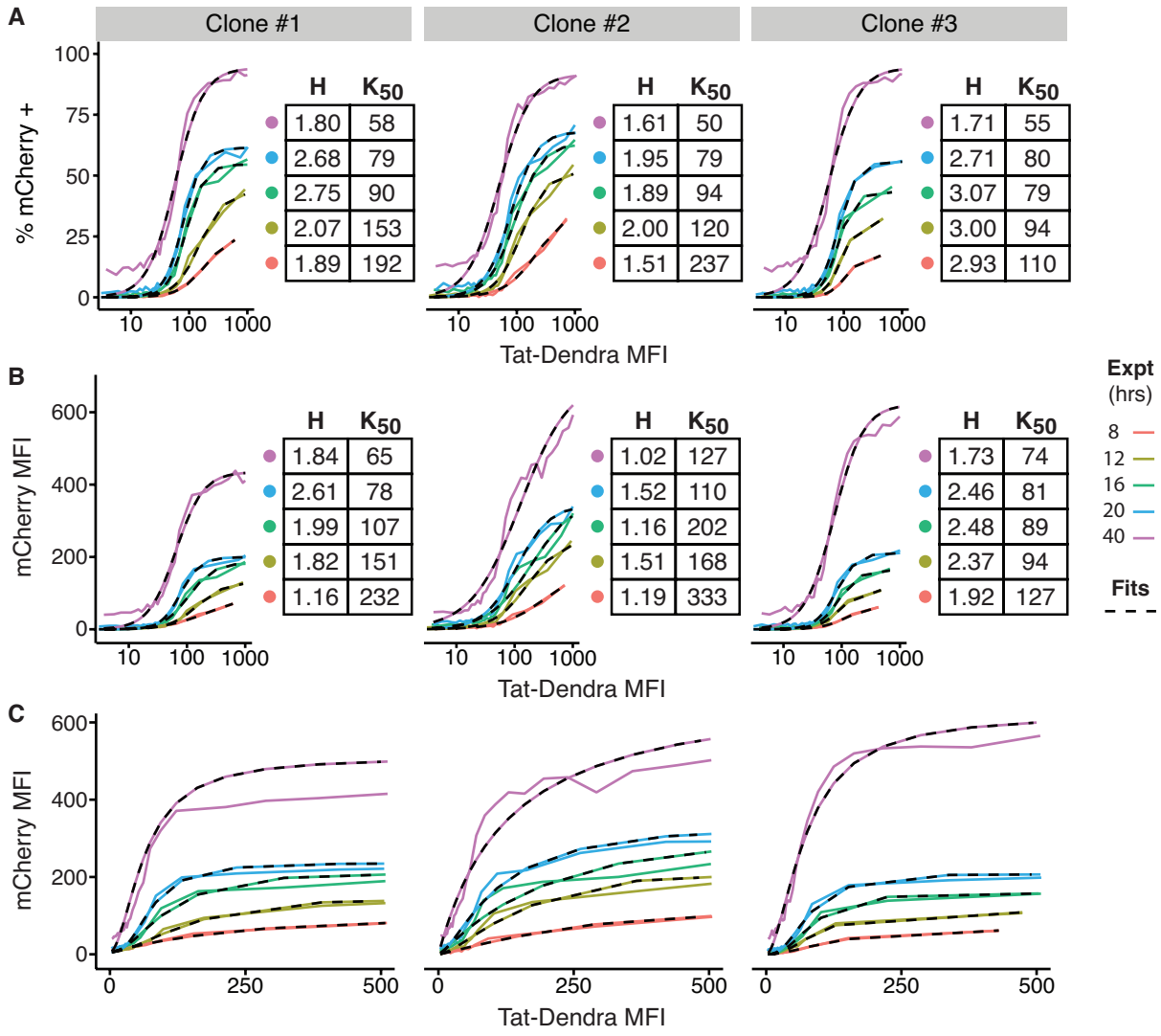

Figure 6: At early times, the open-loop Tat-LTR circuit exhibits a threshold in both activation and mean expression.

(A) Flow data from three isoclones of Jurkat Tat-Dendra + LTR mCherry-deg cells, as shown in raw form in Figure 3D and as dose-response plots in Figure 3E, fit to a Hill function (Methods). The dose-response data and Hill fit lines are depicted for each condition, with Hill coefficient (*H*) and half-maximal binding (K_{50}) values in adjacent table together with goodness of fit (R^2). (B) The equivalent dose-mean expression curves in Figure 3E were analyzed as in panel A. (C) Data and fits from panel B, with Tat-Dendra on a linear scale to emphasize the weakly sigmoidal shape. All fits gave $R^2 > 0.96$.

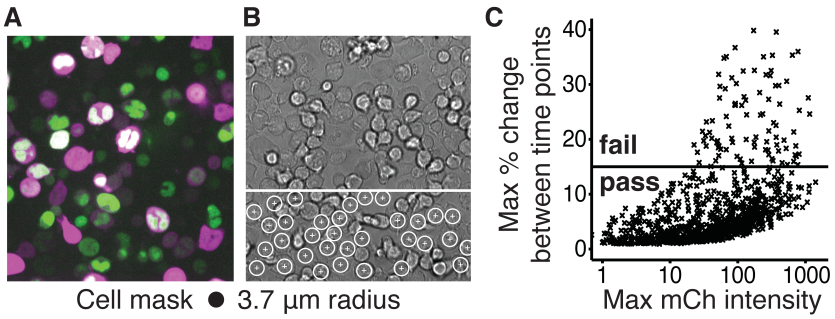

Figure 7: Extraction and QC of single-cell trajectories from time-lapse images.

(A) Jurkat Tat-Dendra + LTR mCherry-deg cells underwent time-lapse microscopy to yield the data described in Figure 4. Briefly, the cells were biotinylated, attached to a streptavidin-coated coverslip, then induced with 250 ng/mL Dox and imaged for 20 hours. Full details of this procedure are in Methods. This two-color fluorescence image is from the final time point of Clone 2, and shows one tile of a 5x5 grid. Tat-Dendra is green; mCherry is magenta. (B) The same location as panel A, in brightfield. Cell locations were marked in brightfield to ensure that dim and non-fluorescent cells are fairly represented. The lower section of the image shows the marked cell centers (white '+') surrounded by a 23-pixel diameter circle, which is taken as the cell's area. Pixels within this area contribute to the fluorescence intensity of the cell. This location is used for all time points to create a single-cell trajectory. (C) To reduce noise in the data, trajectories that showed excessive changes between consecutive time points were discarded. This image shows raw mCherry trajectories from Clone 2 undergoing QC. The maximum percent change between two consecutive time points is plotted as a function of maximum intensity, showing that for both dim and bright cells, most have a percent change under 10%. To pass QC, both Dendra and mCherry channels must be under the 15% noise cutoff shown. These raw trajectories underwent further QC, smoothing, and bleaching correction, as detailed in Methods and Figure 8.

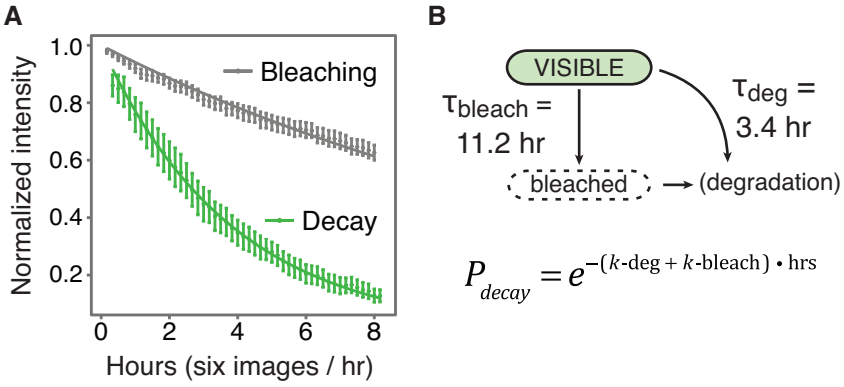

Figure 8: Correcting for photobleaching in Tat-Dendra trajectories.

(A) Single-cell trajectories were constructed from time-lapse imaging of bright Jurkat Tat-Dendra cells. For the decay curve, cycloheximide was added at t=0 to stop protein synthesis, and images were taken every 10 minutes. For the bleaching curve, the same number of images was taken in 5-second intervals to simulate non-decaying protein. Error bars show 95% CI. (B) These trajectories were fit to simple exponential decay models. The bleaching half-time was measured at 11.2 hours. The total rate of visible protein decay can be expressed as the sum of the bleaching and degradation rates; from this equation, the half-life of Tat-Dendra was calculated at 3.4 hours. This value was confirmed by flow cytometry experiments (data not shown). To compute the amount of non-fluorescent protein present, we assume that a fraction of Tat-Dendra enters the bleached state at each time point, and the bleached protein degrades at the normal rate.

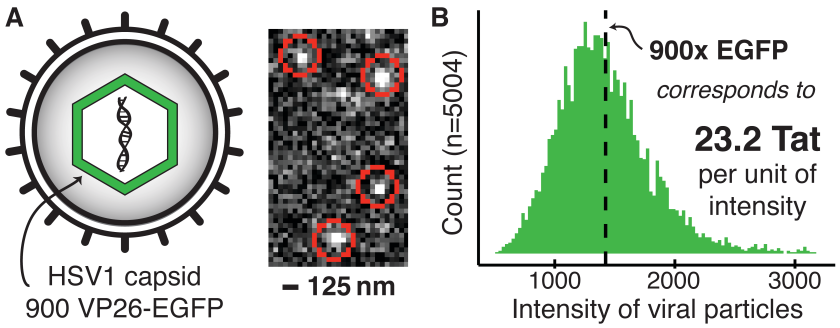

Figure 9: Quantitation of Tat-Dendra by HSV-GFP molecular standard.

(A) HSV-GFP viral particles can serve as a "molecular ruler" to convert fluorescence intensity to molecular number. Since the HSV capsid protein VP26 is fused to EGFP, and each viral particle assembles into an icosahedron with precisely 900 copies of VP26, each viral particle contains 900 EGFP molecules. A small portion of a representative image of HSV-GFP is shown; diffraction-limited viral particles that were successfully segmented are circled in red. (B) Histogram of intensities from all viral particles (n=5004) that were identified, showing a roughly normal distribution with a mean of 1424 intensity units per particle. An increase of one intensity unit corresponds to 23.2 Tat-Dendra molecules; this conversion is detailed in Methods.

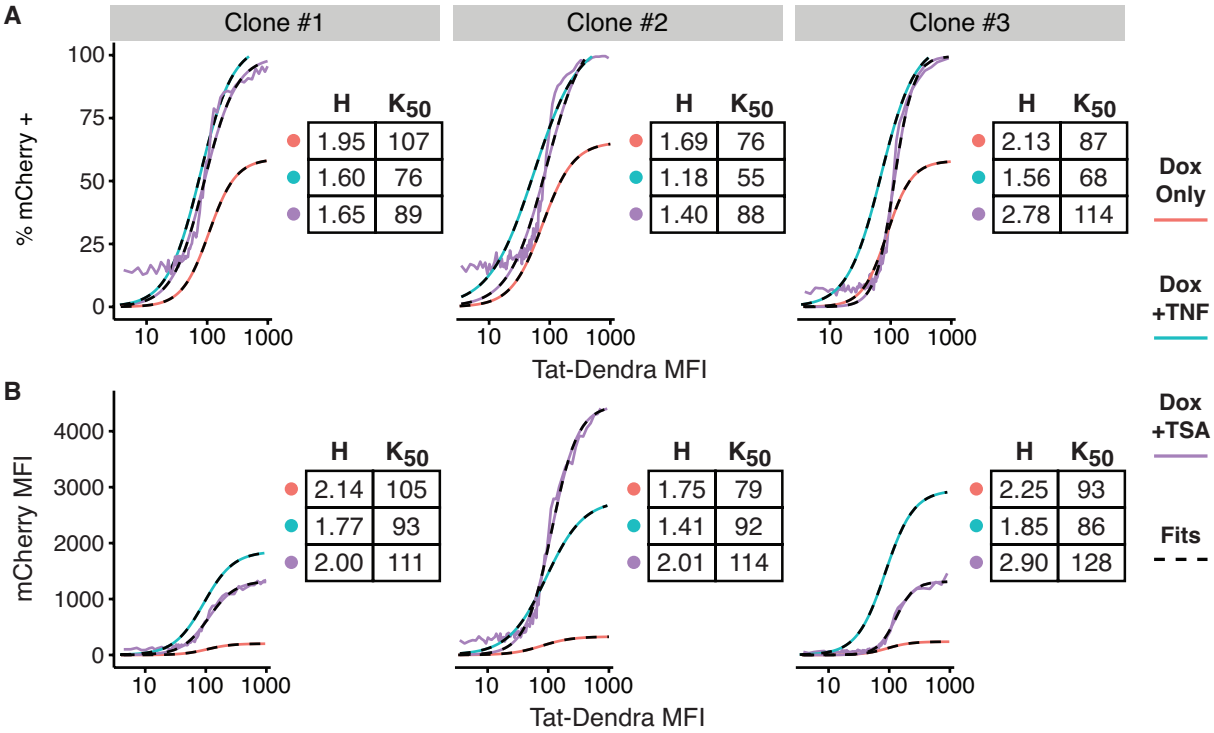

Figure 10: The non-physiological activator TSA and the cytokine TNF have distinct effects on threshold parameters.

(A) Dose-response curves for %mCherry positive cells from flow cytometry measurements of three isoclones of Jurkat Tet-Tat-Dendra + LTR-mCherry, at 20 hours post Dox induction in the presence of TSA (trichostatin A, a histone deacetylase inhibitor). Each data point depicts a group of 500 cells. These data were fit to a Hill function (dashed lines), with Hill coefficient (*H*) and half-maximal binding (K_{50}) values in adjacent table. Hill fits from Figure 5 are presented for comparison. (B) Dose-response curves from the above experiment, showing mCherry MFI. While TNF consistently decreases both *H* and K_{50}, TSA has a less consistent effect on both parameters.

Chapter 4: Promoter toggling generates a tunable threshold in gene activation

4.1. Abstract

It remains unclear how the HIV latency circuit generates a threshold to establish a stable off state. This simple positive feedback circuit lacks cooperative binding or any other known sources of deterministic bistability. Stochastic expression of the HIV activator Tat should always trigger the activation of its own promoter, the HIV LTR, and thus trigger viral replication. Despite noisy expression of LTR, HIV is capable of long-lasting proviral latency. Here, I demonstrate that in a general stochastic model, promoter toggling between on and off expression states can generate an activation threshold without requiring true bistability. Cellular signaling can modulate promoter-toggling frequency and thereby adjust this threshold. Using a combination of single-cell analysis and computational modeling, I demonstrate the applicability of this result to the HIV LTR promoter, which is known to exhibit both intrinsic toggling and an intrinsic activation threshold. These results potentially indicate a functional role for promoter toggling as a general mechanism for tunable threshold generation in regulatory circuits.

4.2. Introduction

The positive-feedback circuit that controls HIV's fate decision between active replication and latency (Figure 1) has none of the classic mechanisms associated with deterministic multistability (Aull et al., 2016; Weinberger, 2015). However, the latent state of HIV is stable, and can persist even when the state of the host cell strongly favors replication (Ho et al., 2013), indicating that this positive-feedback circuit has an activation threshold that must be overcome. This property has clinical significance, as near-total reactivation of latent HIV will be required

for a cure (Hill et al., 2014), and efforts to reduce HIV latency *in vivo* have met with limited success (Deeks, 2012; Shang et al., 2015). Such efforts would benefit from a clearer understanding of how HIV latency is controlled.

The decision between active replication and latency in HIV is governed primarily by the virus's Tat-LTR positive-feedback circuit, in which HIV Tat protein drives its own expression from the long terminal repeat (LTR) promoter, the sole promoter of HIV (Figure 1). This Tat-LTR circuit is necessary and sufficient to activate HIV (Razooky et al., 2015). Tat acts as a monomeric transactivator, binding to a single site on a nascent RNA hairpin formed by stalled RNA polymerase II at the LTR (Weinberger and Shenk, 2007). This architecture excludes most known forms of threshold generation, including self-cooperativity. Because Tat binds non-cooperatively to the LTR promoter, classical deterministic models predict that the circuit should have no activation threshold, and thus the latent state would be unstable (Figure 2A).

While long-term stability of HIV latency is likely mediated by epigenetic silencing (Siliciano and Greene, 2011), immediate latency occurs in ~50% of infections in cell culture (Calvanese et al., 2013; Dahabieh et al., 2013) and *in vivo,* latency is established within 3 days (Whitney et al., 2014). This latency is far too rapid for epigenetic silencing that acts on timescales of a week or more in T cells (Tyagi et al., 2010). Given the noisy expression of the HIV LTR promoter (Dar et al., 2012; Dey et al., 2015), it is unclear how HIV can even temporarily remain in an off state and provide an opportunity for the kinetically slower epigenetic silencing mechanism to act, since Tat positive feedback should trigger active replication within these first few days. This would preclude establishment of proviral latency, since active replication destroys the cell in under 2 days (Perelson et al., 1996), and silencing of an actively replicating cell cannot overcome

active HIV gene expression (Razooky et al., 2015). In general, it remains unclear how a positive-feedback circuit that lacks deterministic bistability and ultrasensitivity can generate the activation threshold required to establish a stable off state.

Here, I use the HIV Tat-LTR circuit as a model system to examine how a threshold can be generated without self-cooperativity. Using a combination of single-cell experimental analysis and *in silico* modeling, I find that intrinsic promoter toggling can stabilize an off state absent bistability. This threshold is tunable via cellular activation (e.g. NF-κB signaling), which modulates the kinetics of promoter toggling and can shift the threshold. A class of general stochastic models of promoter toggling with transactivation recapitulates these observations. These results show that promoter toggling is sufficient to establish a tunable threshold for gene activation, potentially indicating a general mechanism for threshold generation in eukaryotic gene regulatory networks.

4.3. Results

4.3.1. Non-cyclic promoter toggling is sufficient to create a threshold in gene activation but not mean expression

In order to generate a threshold in promoter activation without bistability, we reasoned that the promoter might transiently enter a state that is inaccessible to the transactivator. Then, even provided a large dose of transactivator, the promoter could remain unresponsive. This hypothesis is based on the concept of chromatin 'breathing' (Meshorer et al., 2006)—a process distinct from chromatin 'silencing'—that has been hypothesized to generate episodic, stochastic bursts of transcription. Many eukaryotic promoters toggle between active and inactive states exhibiting burst-like expression (Harper et al., 2011; Suter et al., 2011; Zoller et al., 2015) and the HIV

LTR is no exception (Dar et al., 2012; Singh et al., 2010; Tantale et al., 2016). In the case of HIV, this 'promoter toggling' model predicts that the LTR promoter could remain insensitive to low levels of Tat expression—that deterministically would be predicted to disrupt latency—since Tat protein can proteolytically decay between stochastic expression bursts.

The classical two-state *on-off* (random telegraph) model of promoter toggling (Kepler and Elston, 2001; Ko, 1991; Peccoud and Ycart, 1995) has been invoked to explain bimodal expression in the Tat-LTR circuit (Razooky et al., 2015; Razooky and Weinberger, 2011) and an analogous synthetic feedback circuit with non-cooperative self-activation (To and Maheshri, 2010). In this classical model, the promoter slowly toggles between *on* and *off* states, with expression from the *on* state proportional to the amount of transactivator. Intrinsic bimodality occurs only when expression bursts are large and infrequent; in this 'slow switching' regime, the protein will fully decay between expression bursts, creating a distinct off population. However, this model requires the promoter toggling rate to be much slower than the turnover rate of the protein product (Kaern et al., 2005). Given that Tat has a half-life of 8 hours (Weinberger and Shenk, 2007), 'slow switching' is not consistent with estimated LTR toggling rates of 2-3 hours or less (Dar et al., 2012; Tantale et al., 2016), nor with the relatively fast response of LTR to Tat (Figure 3D-E). The potential of toggling rates in the physiological range to influence the behavior of gene regulatory networks has received less attention.

To test the concept that physiological rates of promoter toggling can generate an activation threshold, I designed a series of increasingly complex stochastic models of a toggling promoter and its transactivator, parameterized based on previous measurements of LTR (Model Definitions). Transactivation of a general two-state promoter model can occur via a number of

different mechanisms: a transactivator molecule (e.g., Tat) could increase the rate of promoter opening (k_{on}); the transactivator could decrease the rate of the promoter turning off (k_{off}); or the transactivator could increase the expression rate of active promoter (k_{max}). In the case of Tat activation of the LTR, Tat appears to increase the size of LTR expression bursts, acting through either k_{max} or k_{off} (Razooky et al., 2015). I find that the full dynamic range of LTR is achieved only when Tat both increases k_{max} and decreases k_{off} (Figure 12A), which as I show later, is required to fit the Tat-LTR experimental dose-response curves.

To provide a natural mechanism for the inverse relationship between transactivator and k_{off}, I extend the classical two-state *on-off* model, adding an intermediate *open* promoter state that is capable of binding the transactivator but which cannot drive transcription (Figure 11A). In this extended model, the promoter slowly toggles between *off* and *open* states; only the *open* promoter is accessible to transactivator, and in the presence of transactivator, it can rapidly transition to the *on* state; efficient expression occurs only in the *on* state, while relaxation to the *off* state occurs only from the *open* state. In this model, the transactivator linearly increases k_{bind}, thus shifting the equilibrium between *open* and *on* states to favor the *on* state and promote expression. Moreover, transactivator-mediated increases in k_{bind} reduce switching to the *off* state due to the reduced effective concentration of the *open* state. This mechanism has the effect of altering the effective rates of both k_{max} and k_{off}; that is, transactivation increases both the intensity and duration of expression bursts.

Simulations of this 'extended' toggling model (Figure 11A) show bimodal expression patterns as the "cells" are induced (Figure 11B), matching flow cytometry data from the open-loop Tat-LTR system (Razooky et al., 2015). As transactivator concentration is increased, the

fraction of cells with expression above the background value also increases, but non-responders persist even at saturating doses (Figure 11B). This partial response is a known property of LTR; no matter how strong the stimulus, a fraction of LTRs will remain off, even when they are capable of reactivation (Ho et al., 2013).

When dose-response curves of these simulations are plotted, the model exhibits a threshold in activation, and also recapitulates the gradual increase in maximum percent positive cells seen over time in the experimental data (Figure 11C). To be sure that the threshold was not due to the particulars of this model, I also examined a simplified two-state model with implicit transactivator binding (Figure 12), a more mechanistically detailed model with explicit non-linear production of the transactivator (Figure 13), and a model that incorporates nucleosome remodeling (Figure 20). All models generated similar dose-response curves exhibiting threshold responses. The near-quantitative match with experimental data (Figure 11C and Figure 11E) gives confidence that our extended toggling model is appropriate for Tat's interaction with LTR.

An important technical point is that the *S* (sigmoidal) shape of these dose-response curves does not imply that the toggling model is cooperative. The likelihood that the promoter is *on* is hyperbolic (Figure 12B), as is the dose-mean expression curve at steady state (Figure 11D), as would be expected for a monostable system (schematic in Figure 2A; see also Analytic Forms). The sigmoidal dose-response in terms of percent positives is achieved through the "inertia" of the protein response; the more long-lived the protein, the more the protein level reflects the average output. A dose that produces an average expression level below the positive cutoff will have fewer positive cells than expected from the number of *on* promoters (see Figure 11B, left),

while a dose with average expression above the positive cutoff will have more positives than expected, creating a stable threshold in gene activation.

Viewed in terms of dose-mean expression curves, the extended model gives a more switch-like response at steady state, as compared to the constitutive or two-state *on-off* models (Figure 11D). However, unlike the experimental results, none of these models have a deterministic threshold at any time point during induction (compare Figure 6B with Figure 15B and Analytic Forms). For the extended model, transactivation extends both the intensity and duration of expression bursts; however, transactivation still only affects the rate of one step, increasing k_{bind} linearly. Thus, the extended model remains non-cooperative, with no threshold; a deterministic threshold implies a separatrix, where the second derivative of the response switches from positive to negative, which is absent here (Analytic Forms). Plotting transactivator dose on a linear scale highlights the hyperbolic response (Figure 11D, right). By contrast, when the flow data from Figure 11C is replotted in terms of mean expression, it shows a threshold, with a consistent sigmoidal shape (Figure 11E) and Hill coefficient above 1 (Figure 3F and Figure 6B). More complex models that provide a threshold in mean expression will be addressed in an upcoming section (Figure 20). However, the present 'extended' model (Figure 11A) is sufficient to reproduce three key behaviors of LTR: bimodal induction in response to transactivator (Figure 11B); a true threshold in gene activation (Figure 11C); and a relatively switch-like (though still hyperbolic) dose-mean expression curve, giving minimal expression at low input without compromising dynamic range at high input (Figure 11E). Thus, in the next section, I use the extended toggling model to explore another key behavior: stochastic reactivation of latent HIV through stimulation of the host cell.

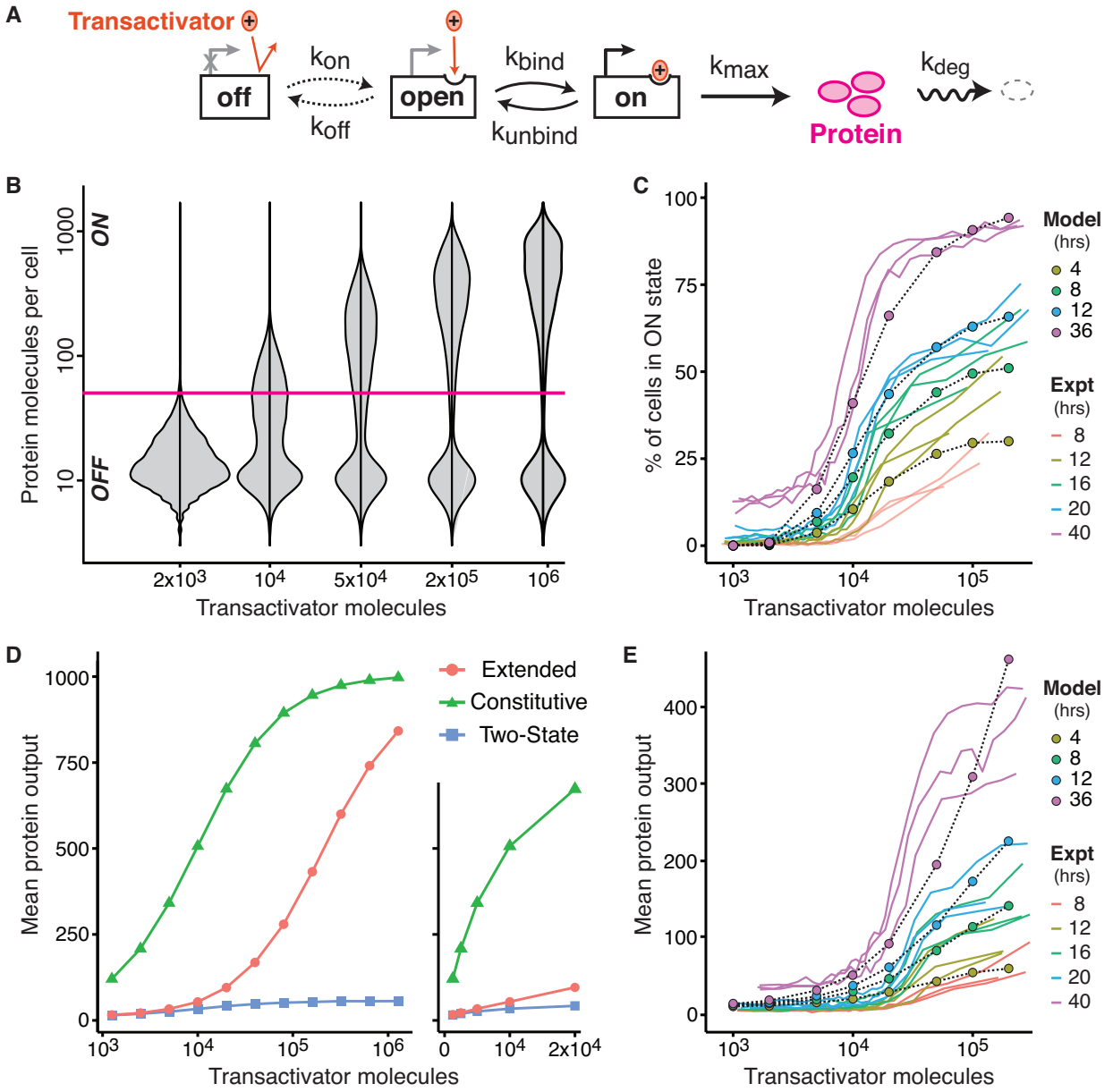

Figure 11: Non-cyclic promoter toggling is sufficient to create a threshold in gene activation but not mean expression.

(A) Schematic of a multi-state toggling promoter model with transactivation (Model 1). In the *off* state, the promoter is "invisible" to transactivator and silent. Only when the promoter toggles into the *open* state can transactivator bind to the promoter, producing a promoter-transactivator complex (the *on* state) that efficiently expresses gene products. Simpler versions of this model which only consider *off* and *on* states also generate thresholds for transactivation (Figure 12). (B) Stochastic simulations of this model. To generate each histogram, 5000 runs were simulated, with Tat added at t=0 and protein output recorded at t=12 hours. Tat input is given as molecular number; the half-maximal binding concentration (K_{50}) is 10^4 units. Parameters were based on published estimates (compiled in Model 1). This model generates bimodality. (C) Results of

simulations shown as % positive trajectories using the cutoff shown in panel B. The resulting dose-response curves, in black, follow the same pattern as experimental data. Data from Figure 6 is reproduced for comparison, with Tat-Dendra intensity scaled to align 12-hour simulations with 20-hour flow. (Dox induction requires 6-8 hours to take effect.) (D) Results of competing models, shown as mean expression at steady state (60 hours). The 'extended' model is that of panel A; the 'constitutive' model lacks the *off* state; the 'two-state' model lacks the *open* state, and k_{max} varies directly with transactivator binding. Data is shown on log (left) and linear (right) plots. The extended model gives the sharpest, most "threshold-like" response, but none of the models are truly bistable. (E) Results from panel C replotted in terms of mean expression. The flow data shows a threshold, but the simulations do not.

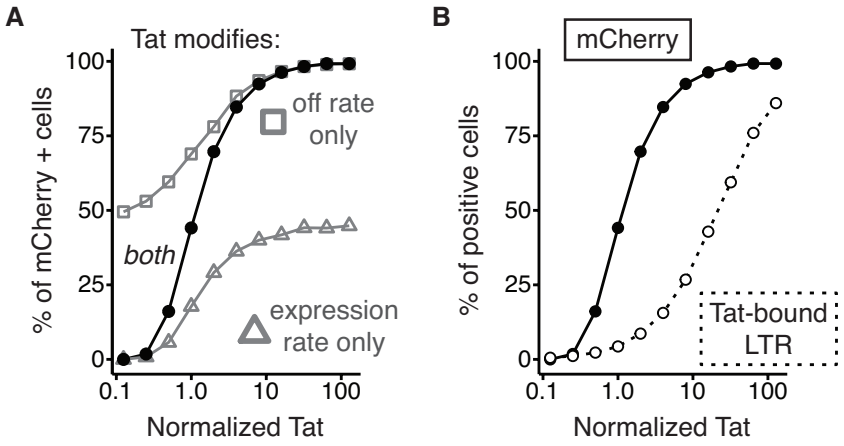

Figure 12: Design constraints for a toggling promoter model with threshold-like activation.

(A) In our 'extended' model (Figure 11), Tat increases the expression from active LTR, and also decreases the rate of transition to the closed state (k_{off}). I simulate this effect directly, using a simplified set of models with implicit transactivation (Model 2). For the "off rate only" version, the model was altered so that transactivator does not change expression rate; both unbound open and bound on promoters express at k_{max}. This model has high background expression, even with minimal transactivator present. In the "expression rate only" version, k_{off} does not change; transactivator-bound promoter can relax to the off state. This model has low expression even at high transactivator, since it cannot remain active for long. The standard model, labeled "both" here, exhibits the full dynamic range of expression. Simulations were performed as in Figure 11, with the 60 hour time point shown. Transactivator input is given as multiples of K_{50}, the half-maximal binding concentration. (B) Due to its stability, a protein output can persist from one burst to the next, creating a cumulative effect that sharpens the dose-response curve. To illustrate this effect, the mCherry protein dose-response (reproduced from panel A) is compared to the percentage of transactivator-bound promoter (dotted line) in the same simulated cells. When fit to a Hill function (Chapter 3 Materials and Methods), the percent positives data gives an apparent cooperativity of $H = 1.769$, while direct measurement of transactivator-bound promoter has $H = 1.002$.

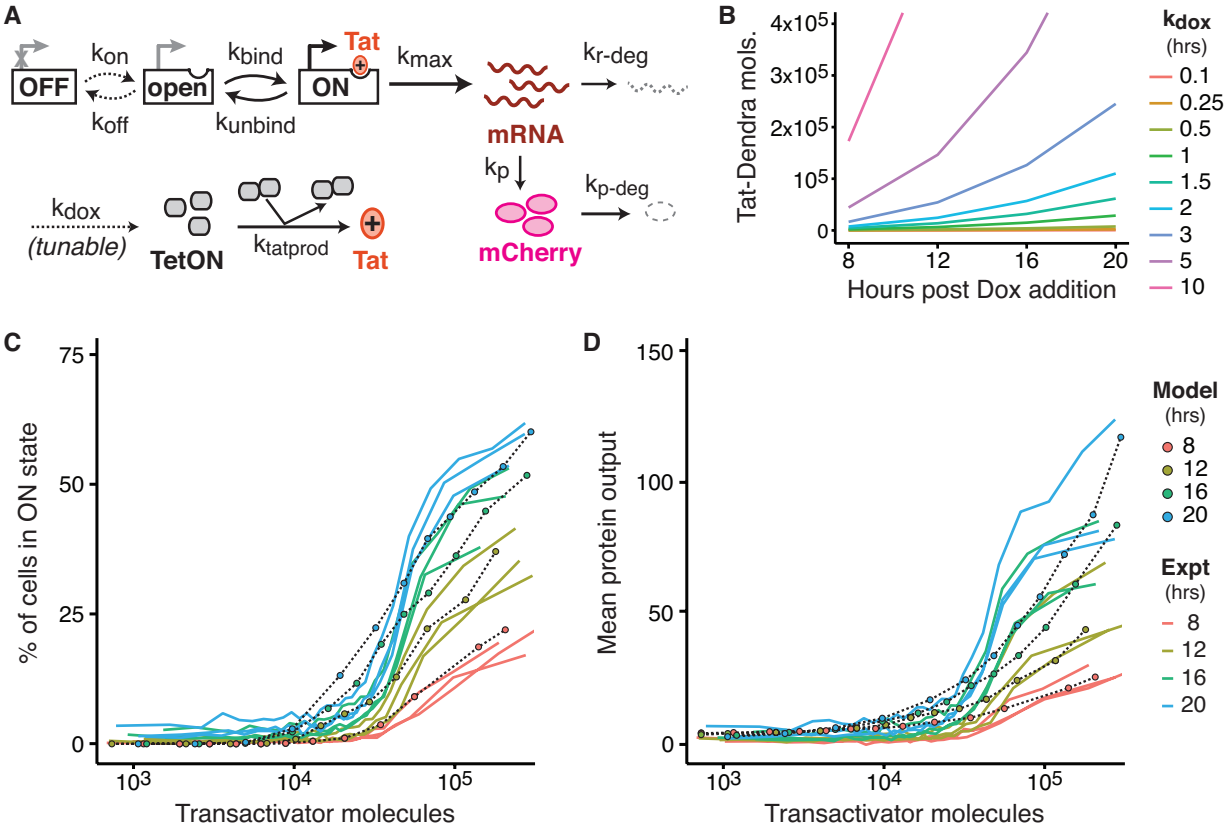

Figure 13: A biochemically detailed model with mRNA and inducible transactivator produces comparable output.

(A) Schematic of a three-state promoter model with inducible transactivator. LTR promoter toggles between *off* and *open* states. The *open* LTR can bind Tat to enter the *on* state, which is required for efficient expression. Unlike the simpler model of Figure 11, both mRNA and protein are simulated for mCherry, as is Dox induction of Tat-Dendra. (B) Stochastic simulations of the model in panel A were performed for 2000 runs at each value of k_{dox} shown. The average Tat-Dendra output for each k_{dox} demonstrates that Tat-Dendra is induced as a quadratic function of time, comparable to experimental time-lapse trajectories obtained by microscopy (Figure 14). (C-D) The mCherry output of the simulations in panel B were processed by the binning method used for flow data (Figure 3B-D and Chapter 3 Materials and Methods). Each data point is based on 1000 runs. The results of these simulations were plotted in terms of percent positives (C) and mean expression (D) and compared to scaled flow data as described in Figure 11C and Figure 11E. The non-linear induction of Tat-Dendra can partially, though not completely, account for the switch-like activation observed in the experimental data.

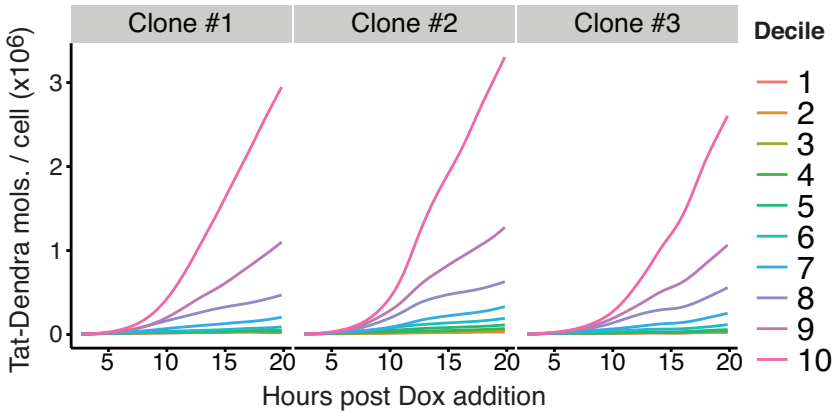

Figure 14: Intensity of Dox-induced Tat-Dendra increases super-linearly with time.

Single-cell trajectories of Tat-Dendra induction in three isoclones of Jurkat Tat-Dendra + LTR mCherry-deg cells were obtained by time-lapse microscopy, as described in Figure 4A, Figure 7, Figure 8, Figure 9, and Chapter 3 Materials and Methods. Briefly, the cells were biotinylated, attached to a streptavidin-coated coverslip, then induced with 250 nM Dox and imaged for 20 hours. These trajectories were ranked by Tat-Dendra intensity at 20 hours and grouped by decile, with the average intensity for each decile plotted over time. Tat-Dendra induction is super-linear and continues to increase over the 20 hour experiment.

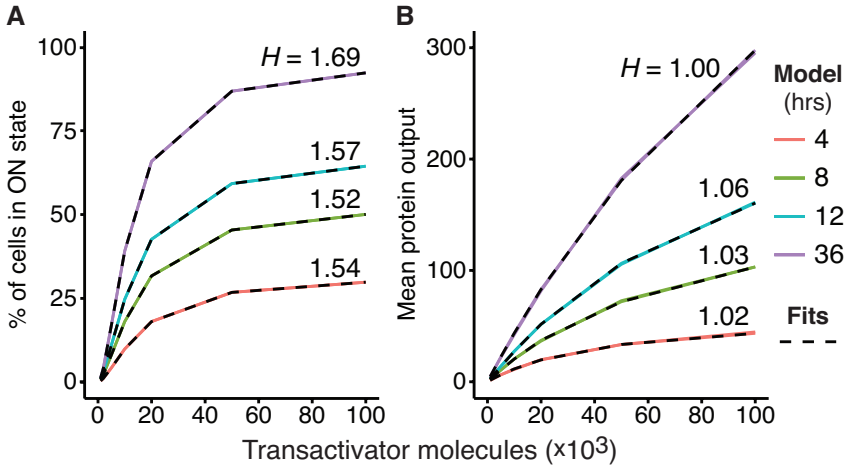

Figure 15: The extended model exhibits a threshold in activation but not mean expression.

(A) The simulations of the extended toggling model from Figure 11C were fit to a Hill function (Chapter 3 Materials and Methods). In terms of percent on, the dose-response curve shows weakly positive empirical cooperativity, with $H > 1$. (B) The equivalent dose-mean expression curves from Figure 11E do not show cooperativity, with $H \approx 1$. For all fits, $R^2 \approx 1$.

4.3.2. A threshold generated by promoter toggling can be tuned by cell state

Molecular thresholds established through multistability and self-cooperativity are often dependent upon protein homo-multimerization (Dill and Bromberg, 2010; Teng et al., 2012; Wall et al., 2004) or successive covalent modifications (Ferrell Jr., 1998), and thus it is biochemically difficult to alter the threshold level. In contrast, I hypothesized that promoter toggling could provide a mechanism for tuning of the molecular activation threshold via modulation of the frequency of toggling. This hypothesis was motivated by observations that latent HIV clones can be partially reactivated by agents that stimulate the host cell (e.g., the cytokine TNF-α, which acts primarily through NF-κB signaling; (Jordan et al., 2003; Jordan et al., 2001; Razooky et al., 2015)), and these agents act via increasing the LTR burst frequency (Dar et al., 2014; Dar et al., 2012; Singh et al., 2010).

To test this prediction, I again used the non-cyclic 'extended' toggling promoter model (Figure 11) and increased k_{on} by three-fold, which is within the measured physiological range of TNF-α stimulation (Dar et al., 2012). Simulations show that this increase in k_{on} sensitizes the LTR response to Tat, with all Tat values with detectable activation giving higher percent positives (Figure 17A). The simulated data agree with experimental dose-response curves taken in the presence or absence of TNF-α (Figure 16; Figure 17A). Activation of the LTR via inhibition of histone deacetylases, using trichostatin A, also produces similar shifts in the dose-response curves (Figure 6). Thus, promoter toggling provides a mechanism for tuning of a molecular activation threshold via cellular activity.

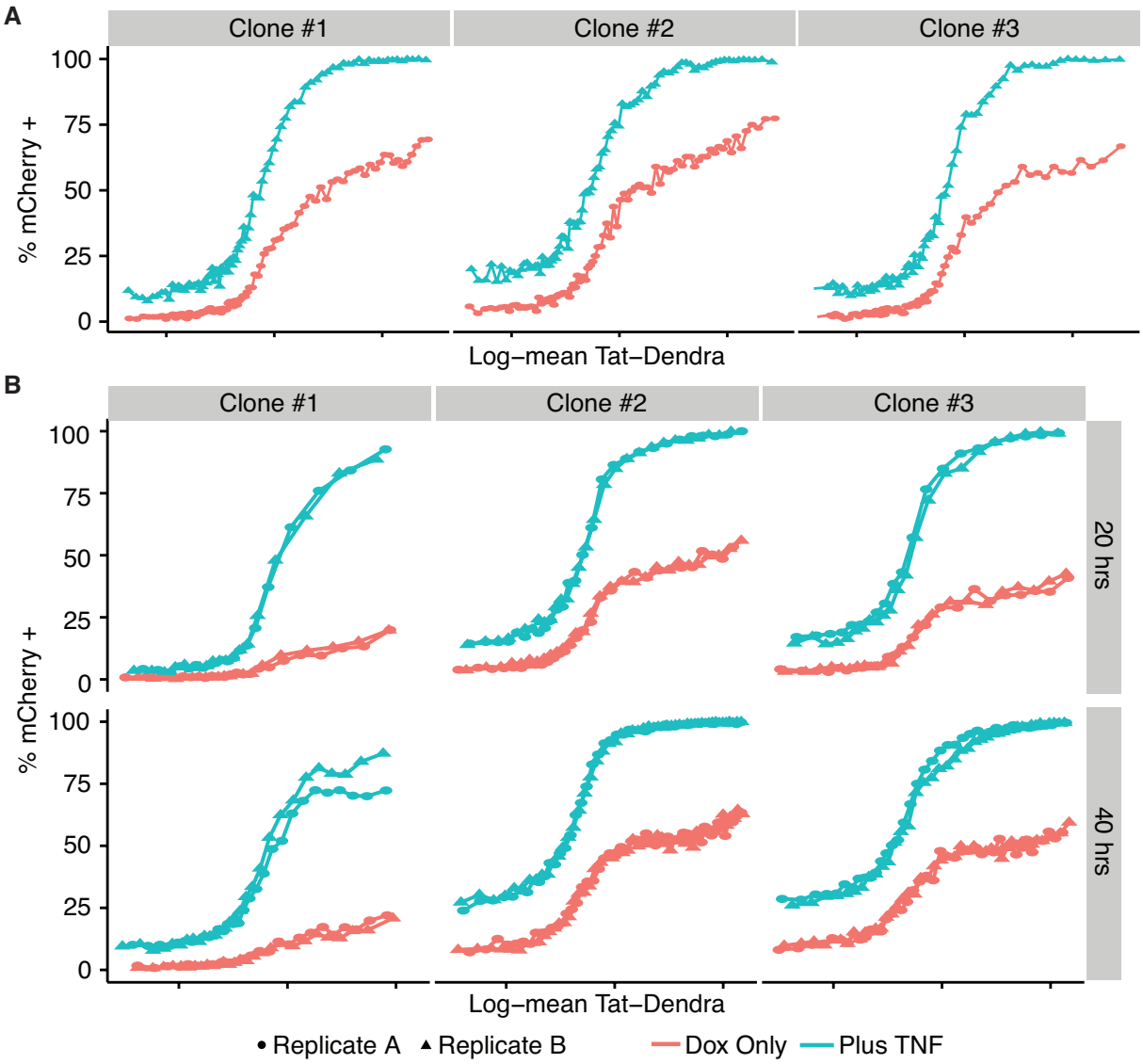

Figure 16: Unscaled dose-response plots showing LTR response to TNF.

(A) Dose-response curves were constructed from three isoclones of Jurkat Tat-Dendra + LTR mCherry-deg cultured in Dox media for 20 hours in the presence or absence of TNF-α, as described in Figure 3. For these plots and in Figure 17A, each group is 500 cells. (B) Two more replicates of panel A, taken at 20 and 40 hours after Dox addition and processed in the same manner. Cells for all replicates were prepared, treated, and measured by flow separately.

Figure 17: A threshold generated by promoter toggling can be tuned by cellular activation.

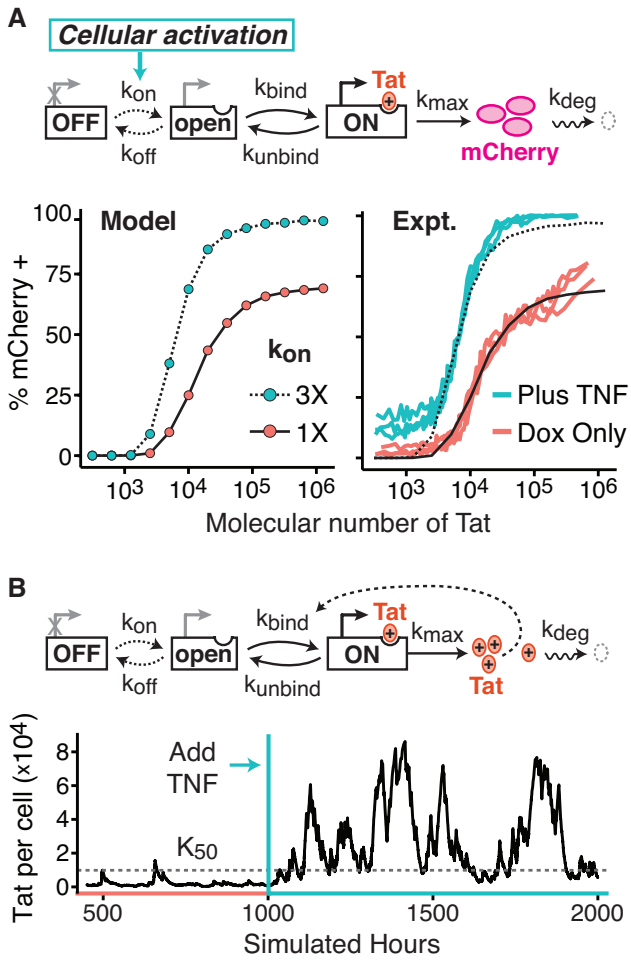

(A) To model the effect of cell state activators (e.g. TNF-α) on LTR response, the k_{on} value was tripled. For comparison, the "Dox Only" simulated dose-response curve at 12 hours (k_{on} = 0.1/hr, solid line) was reproduced from Figure 2C. The "Plus TNF" simulations (k_{on} = 0.3/hr, dotted line) were otherwise matched. The higher k_{on} in the "Plus TNF" condition promotes a stronger and more sensitive response to Tat. Dose-response curves were constructed from three isoclones of Jurkat Tat-Dendra + LTR mCherry-deg, as previously described. The cells were induced with Dox in the presence or absence of TNF-α, then measured by flow at 20 hours. As in Figure 11C, the Tat-Dendra signal was scaled to align with the simulations. There is agreement between these experiments (colored lines) and the models (black lines). (B) To simulate the natural response of latent HIV, the mCherry reporter was replaced with Tat, creating positive feedback. The first 1000 hours were "Dox Only" (baseline) parameters, with the last 550 hours shown. At 1000 hours, k_{on} was increased to "Plus TNF", which notably increased the activity level of LTR.

Next, I asked if this tunable threshold could explain HIV's stochastic reactivation by TNF-α and similar agents. To simulate latent HIV, the open-loop promoter toggling model was modified to include positive-feedback circuitry (Figure 17B and Model 4). In the non-activated latent state (k_{on} = 0.1/hr), the circuit remains mostly at rest. Transient blips of activation occur, but return to baseline quickly. When TNF-α is added to the system (i.e., k_{on} increased by three-fold), the circuit activates. While there is no deterministic "switch" to the on state, there are lengthy excursions to a high Tat level that could support viral replication (Figure 17B). These excursions span multiple burst cycles, and are created by the same mechanism as the activation threshold—

when Tat is strongly expressed, it can persist from one burst to the next, thus providing a form of memory to the system; this requires a Tat half-life comparable to the toggling rate (Figure 18). Notably, tunable activation in response to k_{on} also requires non-cooperative feedback; a bistable version of this model (H = 2) responds erratically and slowly, even with optimized parameters (Figure 19). The dynamics of promoter toggling thus explain another key feature of HIV: stochastic reactivation driven by changes in cell state.

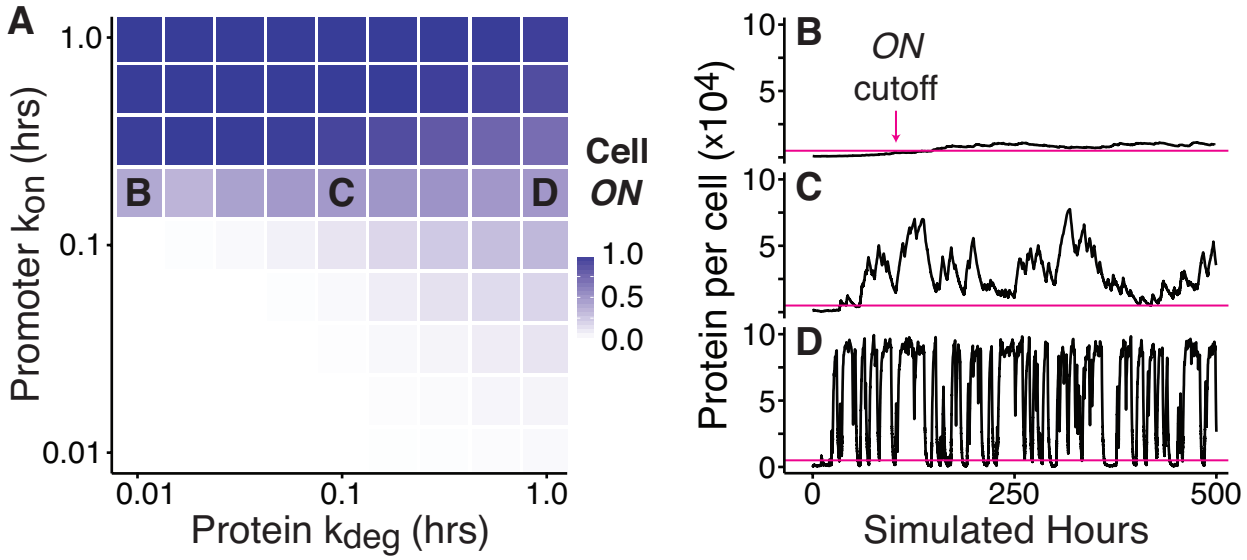

Figure 18: Toggling models show optimal sensitivity to cell state when transactivator decay matches toggling rate.

(A) The toggling Tat-LTR feedback model (Model 4) was run for $5x10^4$ simulated hours using the opening rate (k_{on}) and turnover rate (k_{deg}) indicated. The proportion of this time spent above the "ON" cutoff ($5x10^3$ Tat, or 0.5X $K_{50,}$ as in Figure 17) was recorded. Slow turnover (left) creates a sharp transition between active and inactive promoter as k_{on} increases. Fast turnover (right) creates a more graded response, as the activation threshold disappears in this regime. (B-D) Partial trajectories from the marked squares in panel A. At the slowest turnover rate (B), the response is weak. The moderate rate (C), where $k_{on} \approx k_{deg}$, balances the desired properties of switch-like response to increased k_{on} and strong, fast responses with activation threshold.

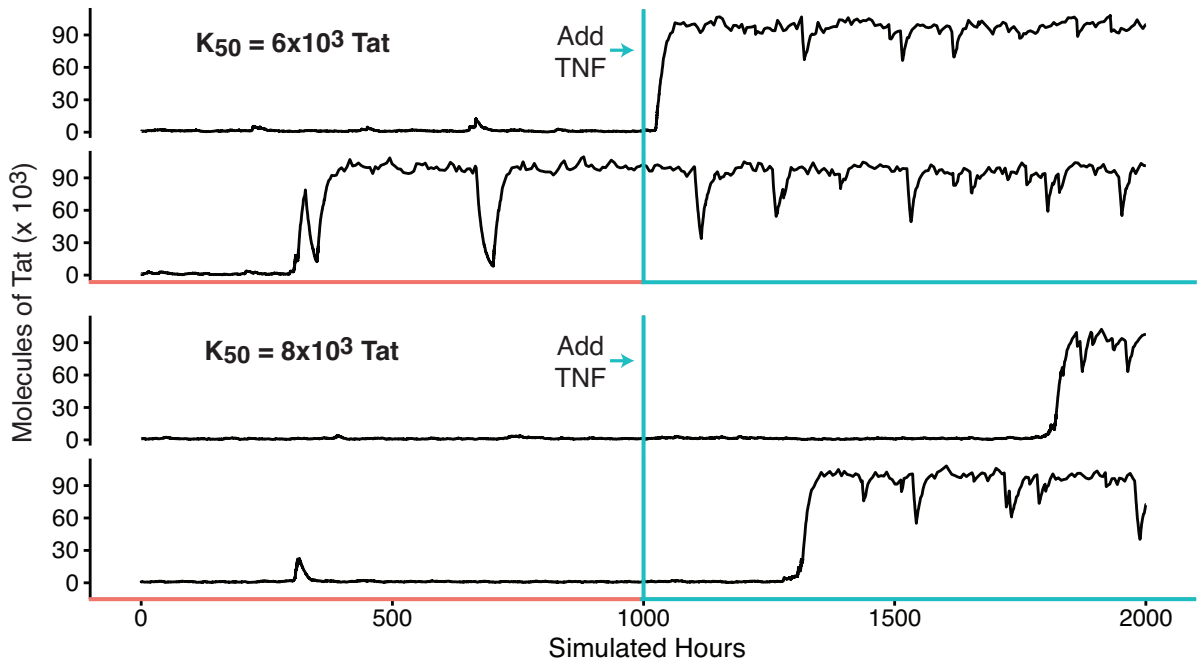

Figure 19: Toggling models with cooperative feedback are poorly responsive to cell state.

The toggling LTR feedback model (Model 4), in which LTR produces Tat, was run under cooperative feedback (H = 2). As in Figure 17B (where N = 1), simulations were run for 1000 hours at "Dox Only" (baseline) parameters, followed by 1000 hours of "Plus TNF". Two independent runs are shown for each condition. Outside a narrow range of K_{50} values, this model is not sensitive to k_{on} changes in the physiological range. Even under optimized values (K_{50} at 6 to 8-fold basal Tat), the response is slow and unreliable. At lower binding affinities ($K_{50} = 6x10^3$, top), the system regularly activates under baseline conditions, while at slightly higher affinities ($K_{50} = 8x10^3$, bottom), the system can remain inactive for several hundred hours in "Plus TNF". Thus, a bistable version of HIV would require extra circuitry to detect cell state.

4.3.3. Cyclic promoter toggling can generate a threshold in mean expression without bistability

While the non-cyclic 'extended' model does not have a threshold in terms of mean expression, the experimental data does (Figure 11E; Figure 6). I suggest three potential reasons for the disparity. First, the induction of Tat-Dendra with Dox is not instantaneous, as this model assumes (Figure 11A). As demonstrated by time-lapse microscopy (Figure 14), Tat-Dendra increases super-linearly with time for the duration of the experiment. In a more realistic model (Figure 13), Tat-Dendra increases as a quadratic function of time, which sharpens both the dose-

response and the dose-mean expression curves. Second, it is likely that promoter toggling works in concert with other mechanisms, e.g. epigenetic silencing, known to stabilize long-term HIV latency (Siliciano and Greene, 2011). A third option, which I explore in this section, is that toggling over more complex geometries (e.g. cyclic) may create a true threshold in mean expression by introducing multiple transactivation-dependent steps (Figure 20).

A minimal model of transactivation-dependent chromatin remodeling, previously used to model the induction of *PHO5* promoter in yeast (Kim and O'Shea, 2008), was adapted to create the 'cyclic' toggling model (Figure 20A). In this model, the promoter toggles between *off*, *open,* and *on* states, as described for the non-cyclic 'extended' model (Figure 11A). For the cyclic model, I also introduce a repressive nucleosome, which must be removed before the *on* state can express. The nucleosome is removed only from *on* promoters, where transactivator is bound; it is replaced only for *open*, unbound promoters. This geometry creates two transactivator-dependent terms: the fraction of *on* promoters, and the fraction of promoters without a nucleosome. Since both of these conditions must be met to achieve expression, the dose-mean expression curve acquires a true deterministic threshold with separatrix (Figure 20B; Analytic Forms), even though no single rate in the model has a super-linear response to transactivation (Figure 20A). Simulations of this cyclic model were performed as described for the extended model (Figure 11), and similarly plotted against the scaled flow data in terms of dose-response (Figure 20C) and dose-mean expression (Figure 20D), demonstrating that in both cases the cyclic model generates empirical cooperativity ($H > 1$) and a threshold (Figure 21), and also better fits the data (Figure 20E). Notably, while this threshold persists at steady state (Figure 20B; Analytic Forms), the cyclic model does not exhibit hysteresis or bistability (Figure 22).

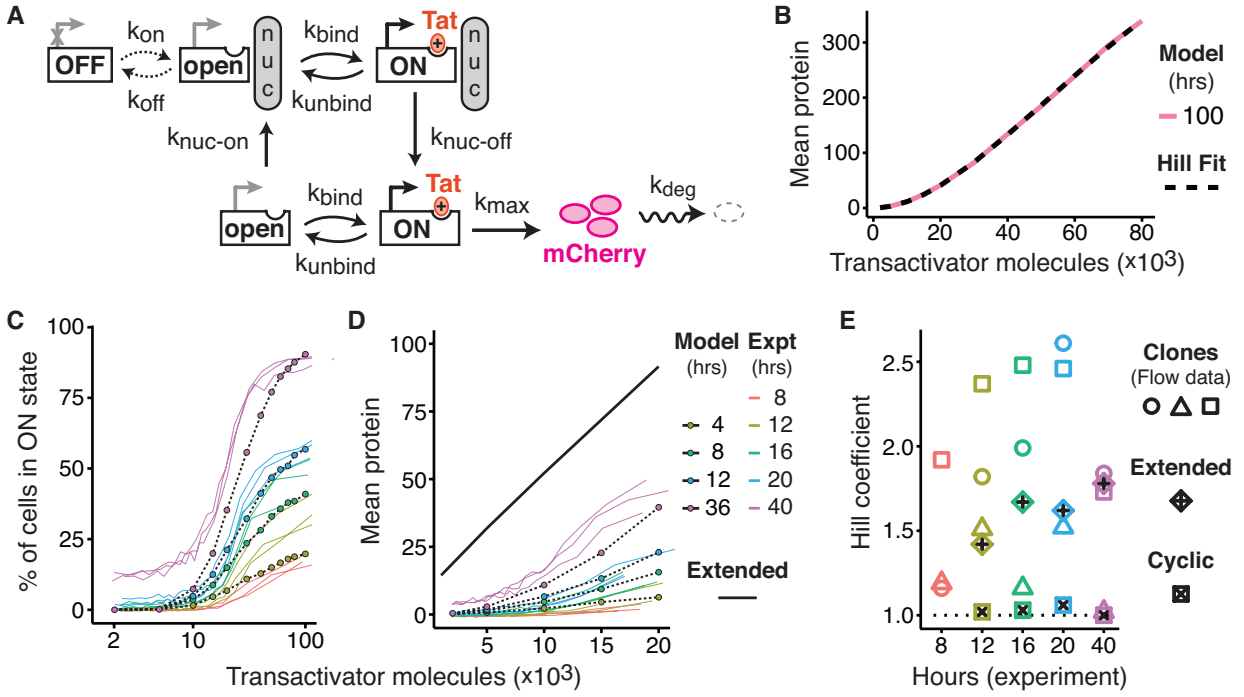

Figure 20: Cyclic toggling can generate a threshold in mean expression without bistability.

(A) Schematic of a five-state promoter model with transactivation (Model 5). The promoter toggles between *off* and *open-nuc* states, with only the *open-nuc* or *open* states able to bind transactivator. Unlike the simpler 'extended' model of Figure 11A, expression also requires a cyclic nucleosome remodeling step that is controlled by transactivation. (B-D) Stochastic simulations of the model in (A), performed as in Figure 11. As compared to the previous models, there is less activity below the K_{50} of 10^4 Tat. When fit to a Hill function, the steady state mean expression curve (B) gives an apparent cooperativity of $H = 1.88$, indicating non-linear activation and a true threshold. Earlier time points (C-D) also show a threshold in both activation and mean expression, with improved fit to data. (E) This flow data, and also extended and current 'cyclic' models, were fit to Hill functions as in panel B. While the extended model gives the non-cooperative result of $H \approx 1$, both the data and cyclic model have positive cooperativity, with average $H = 1.79$ for the data (dotted line; 95% CI 1.52-2.06) and average $H = 1.62$ for the cyclic model (95% CI = 1.47-1.77).

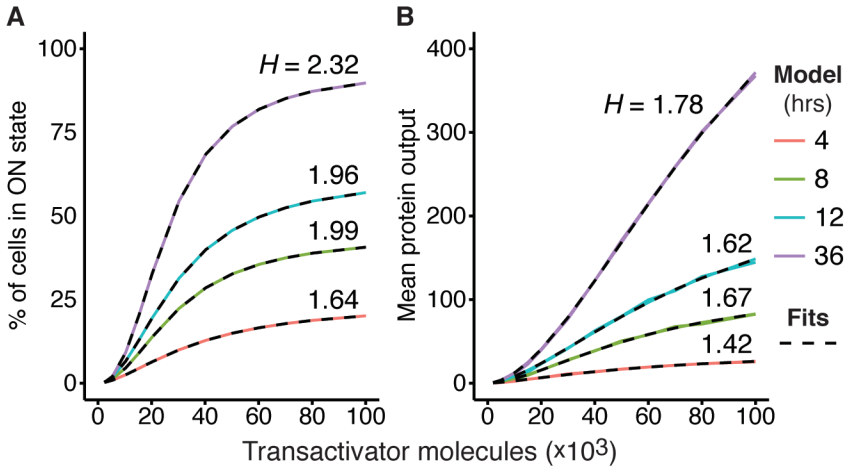

Figure 21: The cyclic nucleosome toggling model exhibits a threshold in both activation and mean expression.

(A) The simulations of the extended toggling model from Figure 20C were fit to a Hill function (Chapter 3 Materials and Methods). In terms of percent on, the dose-response curve shows weakly positive empirical cooperativity, with $H > 1$. (B) The equivalent dose-mean expression curves from Figure 20D also show cooperativity, with $H > 1$. For all fits, $R^2 \approx 1$.

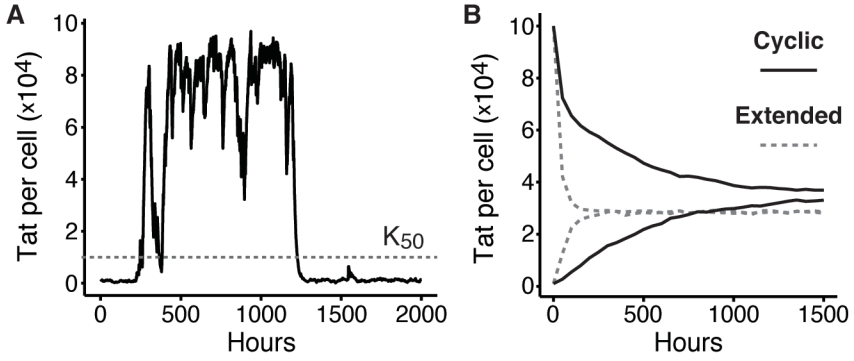

Figure 22: The cyclic nucleosome toggling model has greater state persistence but does not exhibit permanent hysteresis or bistability.

(A) The toggling LTR feedback model with transactivator-dependent nucleosome remodeling (Model 6) was initialized at the basal state with "Plus TNF" parameters and run for 2000 hours. Compared to the non-cyclic extended toggling model (**Figure 17**B), the excursions to the high-Tat state are longer lasting. (B) Both the cyclic and extended feedback models were run 2000 times, from both basal and fully active initial conditions, to give the mean expression over time for each group. The extended model randomizes more quickly, but the cyclic model does ultimately converge to the same mean regardless of starting point.

4.4. Discussion

Overall, these results indicate that that promoter toggling may function as a general mechanism for generating intrinsic molecular thresholds in gene activation. Previous quantitative studies, performed in the context of native regulatory circuits, have revealed threshold-like signal-response curves for LTR (Miller-Jensen et al., 2012) and other eukaryotic promoters (Karttunen and Shastri, 1991; Kim and O'Shea, 2008). This has been attributed to positive feedback increasing the response to strong signals, and to indirect sources of cooperativity, such as slow chromatin remodeling, limiting the response to weak signals. I have attempted to exclude such confounding factors by directly measuring transcriptional inputs and outputs at the single-cell level in a synthetic circuit without feedback. Even when isolated in this manner, LTR retains the intrinsic sharpness of its response to Tat (Figure 6). This result reinforces the previous conclusion that HIV's ability to establish latency is intrinsic to the Tat-LTR circuit and not driven by the cell 'relaxing' or 'retreating' to a resting state (Razooky et al., 2015).

These biologically inspired toggling models match the behavior of the isolated Tat-LTR circuit, and also illustrate a mechanism that would allow HIV to directly respond to changes in cell state. The sensitivity of LTR response to Tat can be tuned by the rate of LTR entering the open state, which increases in the activated cell states that favor HIV replication. This mechanism eliminates the need for complex sensing and control circuits in HIV, allowing the virus to perform a sophisticated fate decision with only one promoter and a modest 9.7 kb genome (Siliciano and Greene, 2011). Indeed, the simplicity of HIV is notable in comparison to phage λ, which requires multiple interwoven cooperative feedback loops to create an analogous

fate decision in *E. coli*, and has a genome five times larger than HIV's (Arkin et al., 1998; Bednarz et al., 2014; Ptashne, 2004).

In a broader context, neither the functional role of promoter toggling, nor its mechanistic basis, are well understood (but see Symmons and Raj, 2016 for an excellent review). One recently identified source of confusion is that, at least in higher eukaryotes, bursting occurs at multiple time scales (Featherstone et al., 2016; Tantale et al., 2016). Studies based on directly imaging transcriptional foci typically report bursts at the scale of a few minutes, with variable intensity among the bursts (Chubb et al., 2006; Corrigan et al., 2016; Larson et al., 2011). In our model, this corresponds to the fast, regulator-dependent movement between *open* and *on* states. By contrast, studies that track expression of reporter genes over time typically report burst cycles of a few hours, with the promoter 'toggling' between discrete active and inactive states (Harper et al., 2011; Suter et al., 2011; Zoller et al., 2015). Studies of LTR expression that infer burst parameters from statistical properties of the distributions of single-cell mRNA or protein measurements also give results consistent with lengthy toggling cycles (Dar et al., 2012; Dey et al., 2015; Singh et al., 2010; Skupsky et al., 2010). This corresponds to the slow, cell-state-dependent toggling between *open* and *off*. In this chapter, I propose a general multi-step model for transactivation of a toggling promoter that unifies these diverse observations, and show that this model has desirable properties for a genetic circuit, including an intrinsic non-deterministic activation threshold and a large dynamic range. I suggest that other eukaryotic circuits may depend on similar design principles for their function, and that systems biologists and modelers should remain alert for the possibilities created by toggling.

4.5. Model Definitions

4.5.1. Extended open-loop model with transactivator and three promoter states.

From Figure 3E, I estimate k_{on} for typical latent LTR at 0.1 / hr. Our clones were chosen for low expression; turn-on rates for LTR in the absence of Tat have been estimated previously at 0.3 / hr (Dar et al., 2012). Turn-off and decay rates were also taken from (Dar et al., 2012).

Turnover time for Tat binding was set at 5 seconds, matching estimates for other transcription factors (Voss et al., 2011). The half-maximal Tat binding value of $K_{50} = 10^4$ is arbitrary, but chosen to match the estimated value from Chapter 3. The 100-fold difference between basal and high output was estimated by (Jeeninga et al., 2000). The mCherry half-life was chosen to match that of Tat (Weinberger and Shenk, 2007). The mCherry reporter used, with its single PEST tag, has a comparable half-life of 10.7 hours (data not shown).

Simulations were initialized at equilibrium for the zero-Tat steady state. For this parameter set, basal mCherry is 10 molecules. The *off* and *open* states were randomly assigned so that they would occur in the expected distribution at t=0.

Reaction	***Description***	***Rate (per hour)***
$OFF \rightarrow OPEN$	Toggling between *OFF* and *OPEN* states	$k\text{-on} = 0.1$ ("Dox Only") $k\text{-on} = 0.3$ ("Plus TNF")
$OPEN \rightarrow OFF$	Toggling between *OPEN* and *OFF* states	$k\text{-off} = 2$
$OPEN + Tat \rightarrow ON$	Toggling between *OPEN* and *ON* states	$k\text{-turn} = 500 \;\; K_{50} = 10^4$ $k\text{-bind} = k\text{-turn} / K_{50}$
$ON \rightarrow OPEN + Tat$	Toggling between *ON* and *OPEN* states	$k\text{-unbind} = k\text{-turn} = 500$
$ON \rightarrow ON + mCherry$	Maximum LTR output	$k\text{-max} = 80$
$\otimes \rightarrow mCherry$	Basal LTR output	$k\text{-min} = 0.8$
$mCherry \rightarrow \otimes$	Protein decay	$k\text{-deg} = 0.08$ (half-life ~8.7 hr)

4.5.2. Simplified model with transactivator-dependent k-off and k-max.

In this simplified (two-state) model, Tat increases the expression from active LTR, and also decreases the rate of transition to the closed state (k_{off}). This produces results indistinguishable from the three-state model in Figure 11A. For the "off rate only" version, the model was altered so that Tat does not change expression rate; both unbound *open* and Tat-bound *on* LTR express at k_{max}. In the "expression rate only" version, k_{off} does not change; Tat-bound LTR can relax to the *off* state. Other parameters were as described in Model 1.

Reactions present in all models

Reaction	***Description***	***Rate (per hour)***
$OFF \rightarrow OPEN$	Toggling between *OFF* and *OPEN* states	$k\text{-on} = 0.1$ ("Dox Only") $k\text{-on} = 0.3$ ("Plus TNF")
$\otimes \rightarrow mCherry$	Basal LTR output	$k\text{-min} = 0.8$
$mCherry \rightarrow \otimes$	Protein decay	$k\text{-deg} = 0.08$ (half-life ~8.7 hr)

Both k-off and k-max are Tat-dependent (standard model)

Reaction	***Description***	***Rate (per hour)***
$OPEN \rightarrow OFF$	Toggling between *OPEN* and *OFF* states	$P\text{-bind} = Tat/(Tat + K_{50})$ $k\text{-off} = 2 \bullet (1 - P\text{-bind})$
$OPEN \rightarrow OPEN + mCherry$	Output from combined *OPEN* and *ON* states	$P\text{-bind} = Tat/(Tat + K_{50})$ $k\text{-max} = 80 \bullet P\text{-bind}$

Only k-off is Tat-dependent

Reaction	***Description***	***Rate (per hour)***
$OPEN \rightarrow OFF$	Toggling between *OPEN* and *OFF* states	$P\text{-bind} = Tat/(Tat + K_{50})$ $k\text{-off} = 2 \bullet (1 - P\text{-bind})$
$OPEN \rightarrow OPEN + mCherry$	Output from combined *OPEN* and *ON* states	$k\text{-max} = 80 \bullet P\text{-bind}$

Only k-max is Tat-dependent (random telegraph model)

Reaction	***Description***	***Rate (per hour)***
$OPEN \rightarrow OFF$	Toggling between *OPEN* and *OFF* states	$k\text{-off} = 2$
$OPEN \rightarrow OPEN + mCherry$	Output from combined *OPEN* and *ON* states	$P\text{-bind} = Tat/(Tat + K_{50})$ $k\text{-max} = 80 \bullet P\text{-bind}$

4.5.3. Detailed model with mRNA and non-linear transactivator production.

In this model, Tat-Dendra induction was designed to match the experimental time-lapse data (Figure 14). In this data, Tat-Dendra intensity is roughly a quadratic function of time. To achieve this in the model, the "TetON" regulator is induced with tunable linear expression; both TetON and Tat-Dendra start at zero, and production of Tat-Dendra requires two units of TetON as a catalyst, giving a quadratic increase of Tat-Dendra with time.

The mRNA half-life for a related LTR reporter construct was previously measured in (Singh et al., 2012). Other parameters were as described in Model 1. Expected mCherry values are 100X higher in this model, so the "mCherry positive" cutoff was rescaled. For computational efficiency, Tat-Dendra was produced in 100-molecule bursts, and mCherry was produced and degraded in 10-molecule bursts.

Reaction	***Description***	***Rate (per hour)***
$OFF \rightarrow OPEN$	Toggling between *OFF* and *OPEN* states	$k\text{-on} = 0.1$ ("Dox Only") $k\text{-on} = 0.3$ ("Plus TNF")
$OPEN \rightarrow OFF$	Toggling between *OPEN* and *OFF* states	$k\text{-off} = 2$
$OPEN + Tat \rightarrow ON$	Toggling between *OPEN* and *ON* states	$k\text{-turn} = 500 \;\; K_{50} = 10^4$ $k\text{-bind} = k\text{-turn} / K_{50}$
$ON \rightarrow OPEN + Tat$	Toggling between *ON* and *OPEN* states	$k\text{-unbind} = k\text{-turn} = 500$
$ON \rightarrow ON + mRNA$	Maximum LTR output	$k\text{-max} = 80$
$\otimes \rightarrow mRNA$	Basal LTR output	$k\text{-min} = 0.8$
$mRNA \rightarrow$ $mRNA + 10 \bullet mCherry$	Translation rate	$k\text{-p} = 30/10$
$mRNA \rightarrow \otimes$	mRNA decay	$k\text{-r-deg} = 0.3$ (half-life ~2.3 hr)
$10 \bullet mCherry \rightarrow \otimes$	Protein decay	$k\text{-p-deg} = 0.08/10$ (half-life ~8.7 hr)
$\otimes \rightarrow TetON$	Dox-regulated intermediate	$k\text{-dox} =$ varies (range 0.1-10)
$2 \bullet TetON \rightarrow$ $2 \bullet TetON + 100 \bullet Tat$	Tat-Dendra expression	$k\text{-tatprod} = 0.1$

4.5.4. Feedback models with non-cooperative and cooperative activation.

For the non-cooperative simulations in Figure 17, N = 1 and the half-maximal binding (K_{50}) was set to 10X basal expression, or 10^4 molecules. For the cooperative simulations in Figure 19, N = 2 and K_{50} was set to the listed values. For computational efficiency, Tat was produced and degraded in 100-molecule bursts. Other parameters were as described in Model 1.

Simulations were initialized at equilibrium for the zero-Tat steady state. For this parameter set, basal Tat is 10^3 molecules. The *off* and *open* states were randomly assigned so that they would occur in the expected distribution at t=0, except in Figure 22, where all runs began in the *open* state with either 10^3 Tat (basal) or 10^5 Tat (active).

Reaction	***Description***	***Rate (per hour)***
$OFF \rightarrow OPEN$	Toggling between *OFF* and *OPEN* states	$k\text{-on} = 0.1$ ("Dox Only") $k\text{-on} = 0.3$ ("Plus TNF")
$OPEN \rightarrow OFF$	Toggling between *OPEN* and *OFF* states	$k\text{-off} = 2$
$OPEN + N \bullet Tat \rightarrow ON$	Toggling between *OPEN* and *ON* states	$k\text{-turn} = 500 \;\; K_{50} = 10^4$ $k\text{-bind} = k\text{-turn}/K_{50}^N$
$ON \rightarrow OPEN + N \bullet Tat$	Toggling between *ON* and *OPEN* states	$k\text{-unbind} = k\text{-turn} = 500$
$ON \rightarrow ON + 100 \bullet Tat$	Maximum LTR output	$k\text{-max} = 80$
$\otimes \rightarrow 100 \bullet Tat$	Basal LTR output	$k\text{-min} = 0.8$
$100 \bullet Tat \rightarrow \otimes$	Protein decay	$k\text{-deg} = 8 \bullet 10^{-4}$ (half-life ~8.7 hr)

4.5.5. Open-loop model with transactivator-dependent nucleosome remodeling.

A minimal model of transactivation-dependent nucleosome remodeling, previously used to model the induction of *PHO5* promoter in yeast (Kim and O'Shea, 2008), was incorporated into the open-loop 'extended' toggling model (Figure 11A). Tat binds the promoter with the same kinetics whether the repressive nucleosome is present or not. Remodeling of the nucleosome occurs only when the promoter is *on*, and is required for expression; this is effectively a second transactivator-dependent step, which generates non-linear activation and a true threshold (Analytic Forms). Other parameters were as described in Model 1.

Reaction	***Description***	***Rate (per hour)***
$OFF \rightarrow OPEN(nuc)$	Toggling between *OFF* and *OPEN* states	$k\text{-on} = 0.1$ ("Dox Only") $k\text{-on} = 0.3$ ("Plus TNF")
$OPEN(nuc) \rightarrow OFF$	Toggling between *OPEN* and *OFF* states	$k\text{-off} = 2$
$OPEN(nuc) + Tat \rightarrow ON(nuc)$ $OPEN + Tat \rightarrow ON$	Toggling between *OPEN* and *ON* states	$k\text{-turn} = 500 \;\; K_{50} = 10^4$ $k\text{-bind} = k\text{-turn} / K_{50}$
$ON(nuc) \rightarrow OPEN(nuc) + Tat$ $ON \rightarrow OPEN + Tat$	Toggling between *ON* and *OPEN* states	$k\text{-unbind} = k\text{-turn} = 500$
$ON(nuc) \rightarrow ON$	Remodeling of *ON* into active state	$k\text{-nuc-off} = 1$
$OPEN \rightarrow OPEN(nuc)$	Remodeling of *OPEN* to inactive	$k\text{-nuc-on} = 4$
$ON \rightarrow ON + mCherry$	Maximum LTR output	$k\text{-max} = 80$
$\otimes \rightarrow mCherry$	Basal LTR output	$k\text{-min} = 0.8$
$mCherry \rightarrow \otimes$	Protein decay	$k\text{-deg} = 0.08$ (half-life ~8.7 hr)

4.5.6. Feedback model with transactivator-dependent nucleosome remodeling.

The 'cyclic' model of transactivation-dependent nucleosome remodeling described in Figure 20A and Model 5 was modified to exhibit feedback, as was done with the 'extended' model of Figure 11A described in Model 1.

For simulations starting at the basal state, initial conditions were 10^3 Tat, and the promoter was in the nucleosome-bound *open-nuc* state. For simulations starting at the fully active state, initial conditions were 10^5 Tat, and the promoter was in the unbound *open* state.

Reaction	***Description***	***Rate (per hour)***
$OFF \rightarrow OPEN(nuc)$	Toggling between OFF and OPEN states	$k\text{-on} = 0.1$ ("Dox Only") $k\text{-on} = 0.3$ ("Plus TNF")
$OPEN(nuc) \rightarrow OFF$	Toggling between OPEN and OFF states	$k\text{-off} = 2$
$OPEN(nuc) + Tat \rightarrow ON(nuc)$ $OPEN + Tat \rightarrow ON$	Toggling between OPEN and ON states	$k\text{-turn} = 500 \;\; K_{50} = 10^4$ $k\text{-bind} = k\text{-turn} / K_{50}$
$ON(nuc) \rightarrow OPEN(nuc) + Tat$ $ON \rightarrow OPEN + Tat$	Toggling between ON and OPEN states	$k\text{-unbind} = k\text{-turn} = 500$
$ON(nuc) \rightarrow ON$	Remodeling of ON into active state	$k\text{-nuc-off} = 1$
$OPEN \rightarrow OPEN(nuc)$	Remodeling of OPEN to inactive	$k\text{-nuc-on} = 1$
$ON \rightarrow ON + 100 \bullet Tat$	Maximum LTR output	$k\text{-max} = 80$
$\otimes \rightarrow 100 \bullet Tat$	Basal LTR output	$k\text{-min} = 0.8$
$100 \bullet Tat \rightarrow \otimes$	Protein decay	$k\text{-deg} = 8 \bullet 10^{-4}$ (half-life ~8.7 hr)

4.6. Methods

The experimental results presented in this chapter were previously described in Chapter 3; thus, experimental methods can be found in Chapter 3: Materials and Methods.

4.6.1. Stochastic simulations

All simulations were performed by the stochastic tau-leaping method, as implemented in StochPy (Maarleveld et al., 2013), on a modified desktop computer. Text descriptions of these models and their chosen parameters are given in Model Definitions. Model specification files in PySCeS, interpretive dance, and SBML formats are available upon request.

4.7. Analytic Forms

For the classic 'random telegraph' model of promoter toggling, in which expression from the *on* state is a function of Tat binding, reporter expression from the open-loop promoter is a hyperbolic function of Tat. Here, k_{on} and k_{off} are the rates of toggling to the *on* and *off* state respectively, k_{max} is the maximum expression rate of the *on* promoter, and K_{50} is the half-maximal binding concentration of Tat.

$$\begin{gathered} OFF \rightleftharpoons ON \\ \frac{dOFF}{dt} = k_{off} \bullet ON - k_{on} \bullet OFF \\ \frac{dON}{dt} = k_{on} \bullet OFF - k_{off} \bullet ON \\ OFF + ON = 1 \end{gathered} \tag{2.1}$$

$$ON = \frac{k_{on}}{k_{on} + k_{off}} \tag{2.2}$$

$$\text{mRNA} = ON \bullet k_{\max} \bullet \frac{Tat}{Tat + K_{50}} \tag{2.3}$$

For the 'extended' toggling model of Figure 11A, the fraction of promoters in the *on* state at steady state is also a hyperbolic function of Tat. Expression is proportional to the time the promoter spends in the *on* state, as in (2.3). (For brevity, k_bTat = k_{bind}, and $k_u = k_{unbind}$.)

$$\begin{gathered} OFF \rightleftharpoons OPEN \rightleftharpoons ON \\ \frac{dOFF}{dt} = k_{off} \bullet OPEN - k_{on} \bullet OFF \\ \frac{dOPEN}{dt} = k_{on} \bullet OFF + k_u \bullet ON - (k_{off} + k_b Tat) \bullet OPEN \\ \frac{dON}{dt} = k_b Tat \bullet OPEN - k_u \bullet ON \\ OFF + OPEN + ON = 1 \end{gathered} \tag{2.4}$$

$$ON = \frac{k_{on} k_b Tat}{k_u k_{off} + k_u (k_{on} + k_{on} Tat)} \tag{2.5}$$

The derivative of this function in terms of Tat is positive everywhere, with the maximum over its defined domain (i.e., non-negative Tat) occurring at Tat = 0. Deterministic bistability requires a 'separatrix' where the second derivative of the dose-mean expression curve goes from positive to negative, so this function cannot be bistable at steady state.

This equation is more easily interpreted in units of K_{50}, the half-maximal binding concentration. When the promoter is *open*, it rapidly reaches equilibrium with the *on* state. When Tat = K_{50}, and the promoter is not *off*, the system is described by:

$$ON = \frac{1}{2} = \frac{k_b K_{50}}{k_b K_{50} + k_u} \quad K_{50} = \frac{k_u}{k_b} \tag{2.6}$$

Equation (2.5) can thus be rephrased in terms of (Tat / K_{50}) = T. Similar hyperbolic expressions can be obtained for the *open* and *off* promoter states.

$$ON = \frac{k_{on} T}{k_{on}(1+T) + k_{off}} \quad OPEN = \frac{k_{on}}{k_{on}(1+T) + k_{off}} \quad OFF = \frac{k_{off}}{k_{on}(1+T) + k_{off}} \tag{2.7}$$

However, in the 'cyclic' nucleosome model of Figure 20A, a higher-order response to Tat is present. Remodeling of the nucleosome occurs only when the promoter is *on*, and is required for expression; this is effectively a second Tat-dependent step, which generates non-linear activation and a true threshold, even though no single reaction rate has a non-linear response to Tat. (For brevity, $k_{nu} = k_{nuc\text{-}off}$, and $k_{nb} = k_{nuc\text{-}on}$.)

$$\begin{aligned}
\frac{dOFF}{dt} &= k_{off} \bullet OPEN(nuc) - k_{on} \bullet OFF \\
\frac{dOPEN(nuc)}{dt} &= k_{on} \bullet OFF + k_u \bullet ON(nuc) + k_{nb} \bullet OPEN - (k_{off} + k_b) \bullet OPEN(nuc) \\
\frac{dON(nuc)}{dt} &= k_b \bullet OPEN(nuc) - (k_u + k_{nu}) \bullet ON(nuc) \\
\frac{dOPEN}{dt} &= k_u \bullet ON - (k_b + k_{nb}) \bullet OPEN \\
\frac{dON}{dt} &= k_b \bullet OPEN + k_{nu} \bullet ON(nuc) - k_u \bullet ON \\
OFF + OPEN(nuc) + ON(nuc) + OPEN + ON &= 1
\end{aligned} \tag{2.8}$$

$$
\begin{aligned}
A &= k_{off} k_{nb} k_u \bullet (k_u + k_{nu}) \\
B &= k_{on} k_{nb} k_u \bullet (k_u + k_{nu}) \\
C &= k_{on} k_{nb} k_u \bullet k_b Tat \\
D &= k_{on} k_{nu} k_u \bullet k_b Tat \\
E &= k_{on} k_{nu} \bullet k_b Tat \bullet (k_b Tat + k_{nb})
\end{aligned}
\tag{2.9}
$$

$$
ON = \frac{k_{on} k_{nu} \bullet k_b Tat \bullet (k_b Tat + k_{nb})}{A + B + C + D + E}
$$

When k_u and k_b are fast relative to other parameters, Tat binding comes to equilibrium, and the 'cyclic' model reduces to a three-state linear system. This system can be solved at steady state, as previously shown.

$$
\begin{gathered}
OFF \rightleftharpoons \textit{Nuc-Bound } (NB) \rightleftharpoons \textit{Nuc-Unbound } (NU) \\
OFF \rightarrow NB \text{ at Tat-independent rate } k_{on} \\
NB \rightarrow NU \text{ at rate } k_{nu} \text{ if Tat bound, } P_{bind} = T/(1+T) \\
NU \rightarrow NB \text{ at rate } k_{nb} \text{ if Tat not bound, } 1\text{-}P_{bind} = 1/(1+T) \\
NB \rightarrow OFF \text{ at rate } k_{off} \text{ if Tat not bound, } 1\text{-}P_{bind} = 1/(1+T)
\end{gathered}
\tag{2.10}
$$

$$
\begin{aligned}
\frac{dOFF}{dt} &= \frac{k_{off} \bullet NB}{(1+T)} - k_{on} \bullet OFF \\
\frac{dNB}{dt} &= k_{on} \bullet OFF + \frac{k_{nb} \bullet NU}{(1+T)} - \frac{(k_{off} + k_{nu} T) \bullet NB}{(1+T)} \\
\frac{dNU}{dt} &= \frac{k_{nu} T \bullet NB}{(1+T)} - \frac{k_{nb} \bullet NU}{(1+T)} \\
OFF + NB + NU &= 1
\end{aligned}
\tag{2.11}
$$

$$
NU = \frac{k_{nu} k_{on} \bullet T(1+T)}{k_{nu} k_{on} \bullet T(1+T) + k_{nb}(k_{off} + k_{on}(1+T))}
\tag{2.12}
$$

$$ON = \frac{NU \bullet T}{(1+T)} = \frac{k_{nu}k_{on} \bullet T^2}{k_{nu}k_{on} \bullet T(1+T) + k_{nb}(k_{off} + k_{on}(1+T))} \tag{2.13}$$

Given the biologically plausible parameter set of $k_{off} = 2$, $k_{nu} = k_{nb} = 1$, the second derivative of this equation reduces to the form below, with a separatrix at T = 2.54 when $k_{on} = 0.1$, in the baseline "Dox Only" state, and at T = 1.50 when $k_{on} = 0.3$, in the activated "Plus TNF" state.

$$\frac{\partial^2 ON}{\partial T^2} = \frac{2k_{on}(k_{on}(-2k_{on} \bullet T^3 - 3(k_{on}+2) \bullet T^2 + k_{on} + 4) + 4)}{(k_{on}(T+1)^2 + 2)^3} \tag{2.14}$$

To understand the responsiveness of Tat-LTR feedback to changing k_{on}, I plot the characteristic curves of these equations (as depicted in Figure 2A), using the feedback model parameters of Model 4 for the 'random telegraph' (2.2) and 'extended' (2.7) models, and the additional nucleosome remodeling parameters of Model 6 for the 'cyclic' (2.14) model. For the random telegraph model (Figure 23A), the steep decrease in slope of the expression curves as Tat increases limits the dynamic range of the response. To achieve the OFF state, the expression curve must be under the decay line; within physiological parameters, this model is either monostable OFF or has a very weak ON state. If the decay constant is shifted downwards to achieve a robust ON state under activated conditions, considerable Tat will be present even under baseline conditions (Figure 23A). For the extended model (Figure 23B), the expression curve has a slope that continues to rise at higher Tat levels; the activated expression curve is well above the decay line, while the baseline curve remains below, explaining the transition from latency to stochastic reactivation observed when TNF-α is added (Figure 17). For the cyclic nucleosome model (Figure 23C), the activated expression curve intersects the decay curve,

giving a true threshold for reactivation. However, because this threshold is relatively weak, the inherent noise of toggling is able to move the system between ON and OFF states (Figure 22).

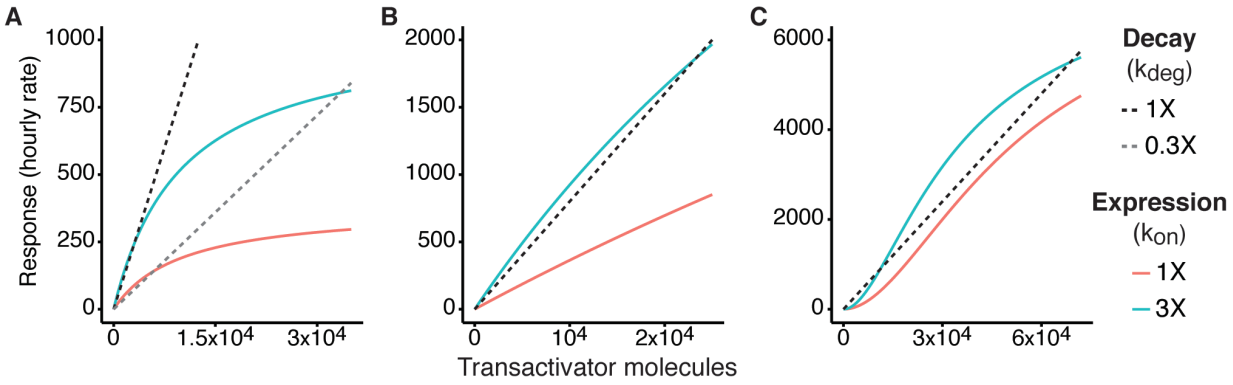

Figure 23: Characteristic curves for toggling models at baseline and activated states.

The expression curves (solid lines) are taken from the applicable equation in Analytic Forms, and parameterized as described in the feedback model of Model 4 for the 'random telegraph' and 'extended' models, and of Model 6 for the 'cyclic' model. The decay rate (black dashed line) is the same in all cases. (A) Random telegraph model (2.2). (B) Extended model (2.7). (C) Cyclic nucleosome model (2.13).

References

Abrams, D., Lévy, Y., Losso, M.H., Babiker, A., Collins, G., Cooper, D.A., Darbyshire, J., Emery, S., Fox, L., Gordin, F.*, et al.* (2009). Interleukin-2 therapy in patients with HIV infection. N Engl J Med *361*, 1548-1559.

Agosto, L.M., Yu, J.J., Dai, J., Kaletsky, R., Monie, D., and O'Doherty, U. (2007). HIV-1 integrates into resting CD4+ T cells even at low inoculums as demonstrated with an improved assay for HIV-1 integration. Virology *368*, 60-72.

Alon, U. (2007). Network motifs: theory and experimental approaches. Nat Rev Genet *8*, 450-461.

Archin, N.M., Cheema, M., Parker, D., Wiegand, A., Bosch, R.J., Coffin, J.M., Eron, J., Cohen, M., and Margolis, D.M. (2010). Antiretroviral intensification and valproic acid lack sustained effect on residual HIV-1 viremia or resting CD4+ cell infection. PLoS One *5*, e9390.

Archin, N.M., Eron, J.J., Palmer, S., Hartmann-Duff, A., Martinson, J.A., Wiegand, A., Bandarenko, N., Schmitz, J.L., Bosch, R.J., Landay, A.L.*, et al.* (2008). Valproic acid without intensified antiviral therapy has limited impact on persistent HIV infection of resting CD4+ T cells. AIDS *22*, 1131-1135.

Arkin, A., Ross, J., and McAdams, H.H. (1998). Stochastic kinetic analysis of developmental pathway bifurcation in phage lambda-infected Escherichia coli cells. Genetics *149*, 1633-1648.

Aull, K.H., Thomson, M., and Weinberger, L.S. (2016). Transient thresholding in the HIV Tat fate-selection circuit. In submission.

Autran, B., Descours, B., and Bacchus, C. (2013). Immune control of HIV-1 reservoirs. Curr Opin HIV AIDS *8*, 204-210.

Bahar Halpern, K., Tanami, S., Landen, S., Chapal, M., Szlak, L., Hutzler, A., Nizhberg, A., and Itzkovitz, S. (2015). Bursty gene expression in the intact mammalian liver. Mol Cell *58*, 147-156.

Balázsi, G., van Oudenaarden, A., and Collins, J.J. (2011). Cellular decision making and biological noise: from microbes to mammals. Cell *144*, 910-925.

Baldauf, H.-M., Pan, X., Erikson, E., Schmidt, S., Daddacha, W., Burggraf, M., Schenkova, K., Ambiel, I., Wabnitz, G., Gramberg, T.*, et al.* (2012). SAMHD1 restricts HIV-1 infection in resting CD4(+) T cells. Nat Med *18*, 1682-1687.

Banaszynski, L.A., Chen, L.-C., Maynard-Smith, L.A., Ooi, A.G.L., and Wandless, T.J. (2006). A rapid, reversible, and tunable method to regulate protein function in living cells using synthetic small molecules. Cell *126*, 995-1004.

Banerjee, C., Archin, N., Michaels, D., Belkina, A.C., Denis, G.V., Bradner, J., Sebastiani, P., Margolis, D.M., and Montano, M. (2012). BET bromodomain inhibition as a novel strategy for reactivation of HIV-1. J Leukoc Biol *92*, 1147-1154.

Barboric, M., Nissen, R.M., Kanazawa, S., Jabrane-Ferrat, N., and Peterlin, B.M. (2001). NF-kappaB binds P-TEFb to stimulate transcriptional elongation by RNA polymerase II. Mol Cell *8*, 327-337.

Barouch, D.H., and Deeks, S.G. (2014). Immunologic strategies for HIV-1 remission and eradication. Science *345*, 169-174.

Barton, K.M., Archin, N.M., Keedy, K.S., Espeseth, A.S., Zhang, Y.-l., Gale, J., Wagner, F.F., Holson, E.B., and Margolis, D.M. (2014). Selective HDAC inhibition for the disruption of latent HIV-1 infection. PLoS One *9*, e102684.

Batada, N.N., and Hurst, L.D. (2007). Evolution of chromosome organization driven by selection for reduced gene expression noise. Nat Genet *39*, 945-949.

Bednarik, D.P., Cook, J.A., and Pitha, P.M. (1990). Inactivation of the HIV LTR by DNA CpG methylation: evidence for a role in latency. EMBO J *9*, 1157-1164.

Bednarz, M., Halliday, J.A., Herman, C., and Golding, I. (2014). Revisiting bistability in the lysis/lysogeny circuit of bacteriophage lambda. PLoS One *9*, e100876.

Bisgrove, D.A., Mahmoudi, T., Henklein, P., and Verdin, E. (2007). Conserved P-TEFb-interacting domain of BRD4 inhibits HIV transcription. Proc Natl Acad Sci U S A *104*, 13690-13695.

Blazkova, J., Murray, D., Justement, J.S., Funk, E.K., Nelson, A.K., Moir, S., Chun, T.-W., and Fauci, A.S. (2012). Paucity of HIV DNA methylation in latently infected, resting CD4+ T cells from infected individuals receiving antiretroviral therapy. J Virol *86*, 5390-5392.

Blazkova, J., Trejbalova, K., Gondois-Rey, F., Halfon, P., Philibert, P., Guiguen, A., Verdin, E., Olive, D., Van Lint, C., Hejnar, J.*, et al.* (2009). CpG methylation controls reactivation of HIV from latency. PLoS Pathog *5*, e1000554.

Boehm, D., Calvanese, V., Dar, R.D., Xing, S., Schroeder, S., Martins, L., Aull, K., Li, P.-C., Planelles, V., Bradner, J.E.*, et al.* (2013). BET bromodomain-targeting compounds reactivate HIV from latency via a Tat-independent mechanism. Cell Cycle *12*, 452-462.

Böhnlein, E., Lowenthal, J.W., Siekevitz, M., Ballard, D.W., Franza, B.R., and Greene, W.C. (1988). The same inducible nuclear proteins regulates mitogen activation of both the interleukin-2 receptor-alpha gene and type 1 HIV. Cell *53*, 827-836.

Bourgeois, C.F., Kim, Y.K., Churcher, M.J., West, M.J., and Karn, J. (2002). Spt5 cooperates with human immunodeficiency virus type 1 Tat by preventing premature RNA release at terminator sequences. Mol Cell Biol *22*, 1079-1093.

Bullen, C.K., Laird, G.M., Durand, C.M., Siliciano, J.D., and Siliciano, R.F. (2014). New ex vivo approaches distinguish effective and ineffective single agents for reversing HIV-1 latency in vivo. Nature medicine *20*, 425-429.

Burnett, J.C., Miller-Jensen, K., Shah, P.S., Arkin, A.P., and Schaffer, D.V. (2009). Control of stochastic gene expression by host factors at the HIV promoter. PLoS Pathog *5*, e1000260.

Cai, L., Friedman, N., and Xie, X.S. (2006). Stochastic protein expression in individual cells at the single molecule level. Nature *440*, 358-362.

Calvanese, V., Chavez, L., Laurent, T., Ding, S., and Verdin, E. (2013). Dual-color HIV reporters trace a population of latently infected cells and enable their purification. Virology *446*, 283-292.

Cavalli, G., and Misteli, T. (2013). Functional implications of genome topology. Nat Struct Mol Biol *20*, 290-299.

Cesbron, F., Oehler, M., Ha, N., Sancar, G., and Brunner, M. (2015). Transcriptional refractoriness is dependent on core promoter architecture. Nat Commun *6*, 6753.

Charpilienne, A., Nejmeddine, M., Berois, M., Parez, N., Neumann, E., Hewat, E., Trugnan, G., and Cohen, J. (2001). Individual rotavirus-like particles containing 120 molecules of fluorescent protein are visible in living cells. J Biol Chem *276*, 29361-29367.

Chavez, L., Calvanese, V., and Verdin, E. (2015). HIV Latency Is Established Directly and Early in Both Resting and Activated Primary CD4 T Cells. PLoS Pathog *11*, e1004955.

Chen, D., and Arkin, A.P. (2012). Sequestration-based bistability enables tuning of the switching boundaries and design of a latch. Mol Syst Biol *8*, 620.

Chong, S., Chen, C., Ge, H., and Xie, X.S. (2014). Mechanism of transcriptional bursting in bacteria. Cell *158*, 314-326.

Chubb, J.R., Trcek, T., Shenoy, S.M., and Singer, R.H. (2006). Transcriptional pulsing of a developmental gene. Curr Biol *16*, 1018-1025.

Chudakov, D.M., Lukyanov, S., and Lukyanov, K.A. (2007). Tracking intracellular protein movements using photoswitchable fluorescent proteins PS-CFP2 and Dendra2. Nat Protoc *2*, 2024-2032.

Chun, T.W., Engel, D., Berrey, M.M., Shea, T., Corey, L., and Fauci, A.S. (1998a). Early establishment of a pool of latently infected, resting CD4(+) T cells during primary HIV-1 infection. Proc Natl Acad Sci U S A *95*, 8869-8873.

Chun, T.W., Engel, D., Mizell, S.B., Ehler, L.A., and Fauci, A.S. (1998b). Induction of HIV-1 replication in latently infected CD4+ T cells using a combination of cytokines. J Exp Med *188*, 83-91.

Chun, T.W., Finzi, D., Margolick, J., Chadwick, K., Schwartz, D., and Siliciano, R.F. (1995). In vivo fate of HIV-1-infected T cells: quantitative analysis of the transition to stable latency. Nat Med *1*, 1284-1290.

Chun, T.W., Stuyver, L., Mizell, S.B., Ehler, L.A., Mican, J.A., Baseler, M., Lloyd, A.L., Nowak, M.A., and Fauci, A.S. (1997). Presence of an inducible HIV-1 latent reservoir during highly active antiretroviral therapy. Proc Natl Acad Sci U S A *94*, 13193-13197.

Civil, A., Rensink, I., Aarden, L.A., and Verweij, C.L. (1999). Functional disparity of distinct CD28 response elements toward mitogenic responses. J Biol Chem *274*, 34369-34374.

Coffin, J., and Swanstrom, R. (2013). HIV pathogenesis: dynamics and genetics of viral populations and infected cells. Cold Spring Harb Perspect Med *3*, a012526.

Corrigan, A.M., Tunnacliffe, E., Cannon, D., and Chubb, J.R. (2016). A continuum model of transcriptional bursting. Elife *5*.

Coull, J.J., Romerio, F., Sun, J.M., Volker, J.L., Galvin, K.M., Davie, J.R., Shi, Y., Hansen, U., and Margolis, D.M. (2000). The human factors YY1 and LSF repress the human immunodeficiency virus type 1 long terminal repeat via recruitment of histone deacetylase 1. J Virol *74*, 6790-6799.

Crooks, A.M., Bateson, R., Cope, A.B., Dahl, N.P., Griggs, M.K., Kuruc, J.D., Gay, C.L., Eron, J.J., Margolis, D.M., Bosch, R.J.*, et al.* (2015). Precise Quantitation of the Latent HIV-1 Reservoir: Implications for Eradication Strategies. J Infect Dis *212*, 1361-1365.

Cuevas, J.M., Geller, R., Garijo, R., López-Aldeguer, J., and Sanjuán, R. (2015). Extremely High Mutation Rate of HIV-1 In Vivo. PLoS Biol *13*, e1002251.

Dahabieh, M.S., Ooms, M., Simon, V., and Sadowski, I. (2013). A doubly fluorescent HIV-1 reporter shows that the majority of integrated HIV-1 is latent shortly after infection. J Virol *87*, 4716-4727.

Dar, R.D., Hosmane, N.N., Arkin, M.R., Siliciano, R.F., and Weinberger, L.S. (2014). Screening for noise in gene expression identifies drug synergies. Science *344*, 1392-1396.

Dar, R.D., Razooky, B.S., Singh, A., Trimeloni, T.V., McCollum, J.M., Cox, C.D., Simpson, M.L., and Weinberger, L.S. (2012). Transcriptional burst frequency and burst size are equally modulated across the human genome. Proc Natl Acad Sci U S A *109*, 17454-17459.

Dar, R.D., Shaffer, S.M., Singh, A., Razooky, B.S., Simpson, M.L., Raj, A., and Weinberger, L.S. (2016). Transcriptional Bursting Explains the Noise-Versus-Mean Relationship in mRNA and Protein Levels. PLoS One *11*, e0158298.

Das, J., Ho, M., Zikherman, J., Govern, C., Yang, M., Weiss, A., Chakraborty, A.K., and Roose, J.P. (2009). Digital signaling and hysteresis characterize ras activation in lymphoid cells. Cell *136*, 337-351.

Davey, R.T., Bhat, N., Yoder, C., Chun, T.W., Metcalf, J.A., Dewar, R., Natarajan, V., Lempicki, R.A., Adelsberger, J.W., Miller, K.D.*, et al.* (1999). HIV-1 and T cell dynamics after interruption of highly active antiretroviral therapy (HAART) in patients with a history of sustained viral suppression. Proc Natl Acad Sci U S A *96*, 15109-15114.

Deaton, A.M., and Bird, A. (2011). CpG islands and the regulation of transcription. Genes & development *25*, 1010-1022.

Deeks, S.G. (2012). HIV: Shock and kill. Nature *487*, 439-440.

Delagrèverie, H.M., Delaugerre, C., Lewin, S.R., Deeks, S.G., and Li, J.Z. (2016). Ongoing Clinical Trials of Human Immunodeficiency Virus Latency-Reversing and Immunomodulatory Agents. Open Forum Infect Dis *3*, ofw189.

Desai, P., and Person, S. (1998). Incorporation of the green fluorescent protein into the herpes simplex virus type 1 capsid. Journal of virology *72*, 7563-7568.

Descours, B., Cribier, A., Chable-Bessia, C., Ayinde, D., Rice, G., Crow, Y., Yatim, A., Schwartz, O., Laguette, N., and Benkirane, M. (2012). SAMHD1 restricts HIV-1 reverse transcription in quiescent CD4(+) T-cells. Retrovirology *9*, 87.

Dey, S.S., Foley, J.E., Limsirichai, P., Schaffer, D.V., and Arkin, A.P. (2015). Orthogonal control of expression mean and variance by epigenetic features at different genomic loci. Mol Syst Biol *11*, 806.

Deymier, M.J., Ende, Z., Fenton-May, A.E., Dilernia, D.A., Kilembe, W., Allen, S.A., Borrow, P., and Hunter, E. (2015). Heterosexual Transmission of Subtype C HIV-1 Selects Consensus-Like Variants without Increased Replicative Capacity or Interferon-α Resistance. PLoS Pathog *11*, e1005154.

Dill, K., and Bromberg, S. (2010). Molecular driving forces: statistical thermodynamics in biology, chemistry, physics, and nanoscience (Garland Science).

Donahue, D.A., Kuhl, B.D., Sloan, R.D., and Wainberg, M.A. (2012). The viral protein Tat can inhibit the establishment of HIV-1 latency. J Virol *86*, 3253-3263.

Doyon, G., Zerbato, J., Mellors, J.W., and Sluis-Cremer, N. (2013). Disulfiram reactivates latent HIV-1 expression through depletion of the phosphatase and tensin homolog. AIDS *27*, F7-F11.

Duh, E.J., Maury, W.J., Folks, T.M., Fauci, A.S., and Rabson, A.B. (1989). Tumor necrosis factor alpha activates human immunodeficiency virus type 1 through induction of nuclear factor binding to the NF-kappa B sites in the long terminal repeat. Proceedings of the National Academy of Sciences *86*, 5974-5978.

Duverger, A., Wolschendorf, F., Zhang, M., Wagner, F., Hatcher, B., Jones, J., Cron, R.Q., van der Sluis, R.M., Jeeninga, R.E., Berkhout, B.*, et al.* (2013). An AP-1 binding site in the

enhancer/core element of the HIV-1 promoter controls the ability of HIV-1 to establish latent infection. J Virol *87*, 2264-2277.

Dybul, M., Hidalgo, B., Chun, T.-W., Belson, M., Migueles, S.A., Justement, J.S., Herpin, B., Perry, C., Hallahan, C.W., Davey, R.T.*, et al.* (2002). Pilot study of the effects of intermittent interleukin-2 on human immunodeficiency virus (HIV)-specific immune responses in patients treated during recently acquired HIV infection. J Infect Dis *185*, 61-68.

Elliott, J.H., McMahon, J.H., Chang, C.C., Lee, S.A., Hartogensis, W., Bumpus, N., Savic, R., Roney, J., Hoh, R., Solomon, A.*, et al.* (2015). Short-term administration of disulfiram for reversal of latent HIV infection: a phase 2 dose-escalation study. Lancet HIV *2*, e520-529.

Elliott, J.H., Wightman, F., Solomon, A., Ghneim, K., Ahlers, J., Cameron, M.J., Smith, M.Z., Spelman, T., McMahon, J., Velayudham, P.*, et al.* (2014). Activation of HIV transcription with short-course vorinostat in HIV-infected patients on suppressive antiretroviral therapy. PLoS Pathog *10*, e1004473.

Elowitz, M.B., and Leibler, S. (2000). A synthetic oscillatory network of transcriptional regulators. Nature *403*, 335-338.

Elowitz, M.B., Levine, A.J., Siggia, E.D., and Swain, P.S. (2002). Stochastic gene expression in a single cell. Science *297*, 1183-1186.

Emiliani, S., Fischle, W., Ott, M., Van Lint, C., Amella, C.A., and Verdin, E. (1998). Mutations in the tat gene are responsible for human immunodeficiency virus type 1 postintegration latency in the U1 cell line. J Virol *72*, 1666-1670.

Eriksson, S., Graf, E.H., Dahl, V., Strain, M.C., Yukl, S.A., Lysenko, E.S., Bosch, R.J., Lai, J., Chioma, S., Emad, F.*, et al.* (2013). Comparative analysis of measures of viral reservoirs in HIV-1 eradication studies. PLoS Pathog *9*, e1003174.

Farrell, M.J., Dobson, A.T., and Feldman, L.T. (1991). Herpes simplex virus latency-associated transcript is a stable intron. Proc Natl Acad Sci U S A *88*, 790-794.

Featherstone, K., Hey, K., Momiji, H., McNamara, A.V., Patist, A.L., Woodburn, J., Spiller, D.G., Christian, H.C., McNeilly, A.S., Mullins, J.J.*, et al.* (2016). Spatially coordinated dynamic gene transcription in living pituitary tissue. Elife *5*, e08494.

Ferrell, J.E. (2002). Self-perpetuating states in signal transduction: positive feedback, double-negative feedback and bistability. Current Opinion in Cell Biology *14*, 140-148.

Ferrell, J.E., and Ha, S.H. (2014a). Ultrasensitivity part I: Michaelian responses and zero-order ultrasensitivity. Trends Biochem Sci *39*, 496-503.

Ferrell, J.E., and Ha, S.H. (2014b). Ultrasensitivity part II: multisite phosphorylation, stoichiometric inhibitors, and positive feedback. Trends Biochem Sci *39*, 556-569.

Ferrell, J.E., and Ha, S.H. (2014c). Ultrasensitivity part III: cascades, bistable switches, and oscillators. Trends Biochem Sci *39*, 612-618.

Ferrell Jr., J.E. (1998). The Biochemical Basis of an All-or-None Cell Fate Switch in Xenopus Oocytes. Science *280*, 895-898.

Finzi, D., Blankson, J., Siliciano, J.D., Margolick, J.B., Chadwick, K., Pierson, T., Smith, K., Lisziewicz, J., Lori, F., and Flexner, C. (1999). Latent infection of CD4+ T cells provides a mechanism for lifelong persistence of HIV-1, even in patients on effective combination therapy. Nature medicine *5*, 512-517.

Finzi, D., Hermankova, M., Pierson, T., Carruth, L.M., Buck, C., Chaisson, R.E., Quinn, T.C., Chadwick, K., Margolick, J., and Brookmeyer, R. (1997). Identification of a reservoir for HIV-1 in patients on highly active antiretroviral therapy. Science *278*, 1295-1300.

Fraser, C., Hollingsworth, T.D., Chapman, R., de Wolf, F., and Hanage, W.P. (2007). Variation in HIV-1 set-point viral load: epidemiological analysis and an evolutionary hypothesis. Proc Natl Acad Sci U S A *104*, 17441-17446.

Fraser, H.B., Hirsh, A.E., Giaever, G., Kumm, J., and Eisen, M.B. (2004). Noise minimization in eukaryotic gene expression. PLoS Biol *2*, e137.

Friedman, N., Cai, L., and Xie, X.S. (2006). Linking stochastic dynamics to population distribution: an analytical framework of gene expression. Phys Rev Lett *97*, 168302.

Fujinaga, K., Irwin, D., Huang, Y., Taube, R., Kurosu, T., and Peterlin, B.M. (2004). Dynamics of human immunodeficiency virus transcription: P-TEFb phosphorylates RD and dissociates negative effectors from the transactivation response element. Mol Cell Biol *24*, 787-795.

García-Rodríguez, C., and Rao, A. (1998). Nuclear factor of activated T cells (NFAT)-dependent transactivation regulated by the coactivators p300/CREB-binding protein (CBP). J Exp Med *187*, 2031-2036.

Gardner, T.S., Cantor, C.R., and Collins, J.J. (2000). Construction of a genetic toggle switch in Escherichia coli. Nature *403*, 339-342.

Gibson, W. (1996). Structure and assembly of the virion. Intervirology *39*, 389-400.

Goldbeter, A., and Koshland, D.E. (1981). An amplified sensitivity arising from covalent modification in biological systems. Proc Natl Acad Sci U S A *78*, 6840-6844.

Golding, I., Paulsson, J., Zawilski, S.M., and Cox, E.C. (2005). Real-time kinetics of gene activity in individual bacteria. Cell *123*, 1025-1036.

Gray, R.H., Wawer, M.J., Brookmeyer, R., Sewankambo, N.K., Serwadda, D., Wabwire-Mangen, F., Lutalo, T., Li, X., vanCott, T., Quinn, T.C*., et al.* (2001). Probability of HIV-1

transmission per coital act in monogamous, heterosexual, HIV-1-discordant couples in Rakai, Uganda. Lancet *357*, 1149-1153.

Greger, I.H., Demarchi, F., Giacca, M., and Proudfoot, N.J. (1998). Transcriptional interference perturbs the binding of Sp1 to the HIV-1 promoter. Nucleic Acids Res *26*, 1294-1301.

Gunawardena, J. (2005). Multisite protein phosphorylation makes a good threshold but can be a poor switch. Proc Natl Acad Sci U S A *102*, 14617-14622.

Ha, S.H., and Ferrell, J.E. (2016). Thresholds and ultrasensitivity from negative cooperativity. Science.

Haase, A.T. (2011). Early events in sexual transmission of HIV and SIV and opportunities for interventions. Annu Rev Med *62*, 127-139.

Hamoen, L.W., Van Werkhoven, A.F., Bijlsma, J.J., Dubnau, D., and Venema, G. (1998). The competence transcription factor of Bacillus subtilis recognizes short A/T-rich sequences arranged in a unique, flexible pattern along the DNA helix. Genes Dev *12*, 1539-1550.

Han, Y., Lassen, K., Monie, D., Sedaghat, A.R., Shimoji, S., Liu, X., Pierson, T.C., Margolick, J.B., Siliciano, R.F., and Siliciano, J.D. (2004). Resting CD4+ T cells from human immunodeficiency virus type 1 (HIV-1)-infected individuals carry integrated HIV-1 genomes within actively transcribed host genes. J Virol *78*, 6122-6133.

Harper, C.V., Finkenstädt, B., Woodcock, D.J., Friedrichsen, S., Semprini, S., Ashall, L., Spiller, D.G., Mullins, J.J., Rand, D.A., Davis, J.R.E.*, et al.* (2011). Dynamic analysis of stochastic transcription cycles. PLoS Biol *9*, e1000607.

Hill, A.L., Rosenbloom, D.I.S., Fu, F., Nowak, M.A., and Siliciano, R.F. (2014). Predicting the outcomes of treatment to eradicate the latent reservoir for HIV-1. Proc Natl Acad Sci U S A *111*, 13475-13480.

Ho, Y.-C., Shan, L., Hosmane, N.N., Wang, J., Laskey, S.B., Rosenbloom, D.I.S., Lai, J., Blankson, J.N., Siliciano, J.D., and Siliciano, R.F. (2013). Replication-competent noninduced proviruses in the latent reservoir increase barrier to HIV-1 cure. Cell *155*, 540-551.

Imamichi, H., Crandall, K.A., Natarajan, V., Jiang, M.K., Dewar, R.L., Berg, S., Gaddam, A., Bosche, M., Metcalf, J.A., Davey, R.T.*, et al.* (2001). Human immunodeficiency virus type 1 quasi species that rebound after discontinuation of highly active antiretroviral therapy are similar to the viral quasi species present before initiation of therapy. J Infect Dis *183*, 36-50.

Ivanov, D., Kwak, Y.T., Guo, J., and Gaynor, R.B. (2000). Domains in the SPT5 protein that modulate its transcriptional regulatory properties. Mol Cell Biol *20*, 2970-2983.

Jeeninga, R.E., Hoogenkamp, M., Armand-Ugon, M., de Baar, M., Verhoef, K., and Berkhout, B. (2000). Functional differences between the long terminal repeat transcriptional promoters of human immunodeficiency virus type 1 subtypes A through G. Journal of virology *74*, 3740-3751.

Jordan, A., Bisgrove, D., and Verdin, E. (2003). HIV reproducibly establishes a latent infection after acute infection of T cells in vitro. EMBO J *22*, 1868-1877.

Jordan, A., Defechereux, P., and Verdin, E. (2001). The site of HIV-1 integration in the human genome determines basal transcriptional activity and response to Tat transactivation. EMBO J *20*, 1726-1738.

Kaern, M., Elston, T.C., Blake, W.J., and Collins, J.J. (2005). Stochasticity in gene expression: from theories to phenotypes. Nat Rev Genet *6*, 451-464.

Kao, S.Y., Calman, A.F., Luciw, P.A., and Peterlin, B.M. (1987). Anti-termination of transcription within the long terminal repeat of HIV-1 by tat gene product. Nature *330*, 489-493.

Karttunen, J., and Shastri, N. (1991). Measurement of ligand-induced activation in single viable T cells using the lacZ reporter gene. Proc Natl Acad Sci U S A *88*, 3972-3976.

Katlama, C., Lambert-Niclot, S., Assoumou, L., Papagno, L., Lecardonnel, F., Zoorob, R., Tambussi, G., Clotet, B., Youle, M., Achenbach, C.J.*, et al.* (2016). Treatment intensification followed by interleukin-7 reactivates HIV without reducing total HIV DNA: a randomized trial. AIDS *30*, 221-230.

Kauder, S.E., Bosque, A., Lindqvist, A., Planelles, V., and Verdin, E. (2009). Epigenetic regulation of HIV-1 latency by cytosine methylation. PLoS Pathog *5*, e1000495.

Ke, R., Lewin, S.R., Elliott, J.H., and Perelson, A.S. (2015). Modeling the Effects of Vorinostat In Vivo Reveals both Transient and Delayed HIV Transcriptional Activation and Minimal Killing of Latently Infected Cells. PLoS Pathog *11*, e1005237.

Kearney, M., Maldarelli, F., Shao, W., Margolick, J.B., Daar, E.S., Mellors, J.W., Rao, V., Coffin, J.M., and Palmer, S. (2009). Human immunodeficiency virus type 1 population genetics and adaptation in newly infected individuals. J Virol *83*, 2715-2727.

Keedy, K.S., Archin, N.M., Gates, A.T., Espeseth, A., Hazuda, D.J., and Margolis, D.M. (2009). A limited group of class I histone deacetylases acts to repress human immunodeficiency virus type 1 expression. J Virol *83*, 4749-4756.

Keele, B.F., Giorgi, E.E., Salazar-Gonzalez, J.F., Decker, J.M., Pham, K.T., Salazar, M.G., Sun, C., Grayson, T., Wang, S., Li, H.*, et al.* (2008). Identification and characterization of transmitted and early founder virus envelopes in primary HIV-1 infection. Proc Natl Acad Sci U S A *105*, 7552-7557.

Kepler, T.B., and Elston, T.C. (2001). Stochasticity in transcriptional regulation: origins, consequences, and mathematical representations. Biophys J *81*, 3116-3136.

Kiernan, R.E., Vanhulle, C., Schiltz, L., Adam, E., Xiao, H., Maudoux, F., Calomme, C., Burny, A., Nakatani, Y., Jeang, K.T.*, et al.* (1999). HIV-1 tat transcriptional activity is regulated by acetylation. EMBO J *18*, 6106-6118.

Kim, H.D., and O'Shea, E.K. (2008). A quantitative model of transcription factor--activated gene expression. Nature structural & molecular biology *15*, 1192-1198.

Kim, Y.K., Bourgeois, C.F., Isel, C., Churcher, M.J., and Karn, J. (2002). Phosphorylation of the RNA polymerase II carboxyl-terminal domain by CDK9 is directly responsible for human immunodeficiency virus type 1 Tat-activated transcriptional elongation. Mol Cell Biol *22*, 4622-4637.

Kinoshita, S., Su, L., Amano, M., Timmerman, L.A., Kaneshima, H., and Nolan, G.P. (1997). The T cell activation factor NF-ATc positively regulates HIV-1 replication and gene expression in T cells. Immunity *6*, 235-244.

Klatt, N.R., Chomont, N., Douek, D.C., and Deeks, S.G. (2013). Immune activation and HIV persistence: implications for curative approaches to HIV infection. Immunol Rev *254*, 326-342.

Ko, M.S. (1991). A stochastic model for gene induction. J Theor Biol *153*, 181-194.

Korin, Y.D., and Zack, J.A. (1998). Progression to the G1b phase of the cell cycle is required for completion of human immunodeficiency virus type 1 reverse transcription in T cells. Journal of virology *72*, 3161-3168.

Krishnaswamy, S., Spitzer, M.H., Mingueneau, M., Bendall, S.C., Litvin, O., Stone, E., Peer, D., and Nolan, G.P. (2014). Conditional density-based analysis of T cell signaling in single-cell data. Science *346*, 1250689.

Lafeuillade, A., Poggi, C., Chadapaud, S., Hittinger, G., Chouraqui, M., Pisapia, M., and Delbeke, E. (2001). Pilot study of a combination of highly active antiretroviral therapy and cytokines to induce HIV-1 remission. J Acquir Immune Defic Syndr *26*, 44-55.

Laird, G.M., Bullen, C.K., Rosenbloom, D.I.S., Martin, A.R., Hill, A.L., Durand, C.M., Siliciano, J.D., and Siliciano, R.F. (2015). Ex vivo analysis identifies effective HIV-1 latency-reversing drug combinations. J Clin Invest *125*, 1901-1912.

Larson, D.R., Zenklusen, D., Wu, B., Chao, J.A., and Singer, R.H. (2011). Real-time observation of transcription initiation and elongation on an endogenous yeast gene. Science *332*, 475-478.

Lassen, K.G., Ramyar, K.X., Bailey, J.R., Zhou, Y., and Siliciano, R.F. (2006). Nuclear retention of multiply spliced HIV-1 RNA in resting CD4+ T cells. PLoS Pathog *2*, e68.

Laughlin, M.A., Zeichner, S., Kolson, D., Alwine, J.C., Seshamma, T., Pomerantz, R.J., and Gonzalez-Scarano, F. (1993). Sodium butyrate treatment of cells latently infected with HIV-1 results in the expression of unspliced viral RNA. Virology *196*, 496-505.

Ledford, H. (2014). HIV rebound dashes hope of Mississippi baby cure. Nature News *10*.

Lehrman, G., Hogue, I.B., Palmer, S., Jennings, C., Spina, C.A., Wiegand, A., Landay, A.L., Coombs, R.W., Richman, D.D., Mellors, J.W., *et al.* (2005). Depletion of latent HIV-1 infection in vivo: a proof-of-concept study. Lancet *366*, 549-555.

Lenasi, T., Contreras, X., and Peterlin, B.M. (2008). Transcriptional interference antagonizes proviral gene expression to promote HIV latency. Cell Host Microbe *4*, 123-133.

Levesque, M.J., and Raj, A. (2013). Single-chromosome transcriptional profiling reveals chromosomal gene expression regulation. Nat Methods *10*, 246-248.

Levine, E., Zhang, Z., Kuhlman, T., and Hwa, T. (2007). Quantitative characteristics of gene regulation by small RNA. PLoS Biol *5*, e229.

Levy, Y., Lacabaratz, C., Weiss, L., Viard, J.-P., Goujard, C., Lelièvre, J.-D., Boué, F., Molina, J.-M., Rouzioux, C., Avettand-Fénoêl, V., *et al.* (2009). Enhanced T cell recovery in HIV-1-infected adults through IL-7 treatment. J Clin Invest *119*, 997-1007.

Lewinski, M.K., Bisgrove, D., Shinn, P., Chen, H., Hoffmann, C., Hannenhalli, S., Verdin, E., Berry, C.C., Ecker, J.R., and Bushman, F.D. (2005). Genome-wide analysis of chromosomal features repressing human immunodeficiency virus transcription. J Virol *79*, 6610-6619.

Li, Z., Guo, J., Wu, Y., and Zhou, Q. (2013). The BET bromodomain inhibitor JQ1 activates HIV latency through antagonizing Brd4 inhibition of Tat-transactivation. Nucleic Acids Res *41*, 277-287.

Losick, R., and Desplan, C. (2008). Stochasticity and cell fate. Science *320*, 65-68.

Lusic, M., Marini, B., Ali, H., Lucic, B., Luzzati, R., and Giacca, M. (2013). Proximity to PML nuclear bodies regulates HIV-1 latency in CD4+ T cells. Cell Host Microbe *13*, 665-677.

Maamar, H., and Dubnau, D. (2005). Bistability in the Bacillus subtilis K-state (competence) system requires a positive feedback loop. Mol Microbiol *56*, 615-624.

Maamar, H., Raj, A., and Dubnau, D. (2007). Noise in gene expression determines cell fate in Bacillus subtilis. Science *317*, 526-529.

Maarleveld, T.R., Olivier, B.G., and Bruggeman, F.J. (2013). StochPy: a comprehensive, user-friendly tool for simulating stochastic biological processes. PLoS One *8*, e79345.

Mandell, G.L., Bennett, J.E., and Dolin, R. (2010). Mandell, Douglas, and Bennett's principles and practice of infectious diseases (Philadelphia, PA: Churchill Livingstone/Elsevier).

Marini, B., Kertesz-Farkas, A., Ali, H., Lucic, B., Lisek, K., Manganaro, L., Pongor, S., Luzzati, R., Recchia, A., Mavilio, F., *et al.* (2015). Nuclear architecture dictates HIV-1 integration site selection. Nature *521*, 227-231.

Marshall, H.M., Ronen, K., Berry, C., Llano, M., Sutherland, H., Saenz, D., Bickmore, W., Poeschla, E., and Bushman, F.D. (2007). Role of PSIP1/LEDGF/p75 in lentiviral infectivity and integration targeting. PLoS One *2*, e1340.

Melen, G.J., Levy, S., Barkai, N., and Shilo, B.-Z. (2005). Threshold responses to morphogen gradients by zero-order ultrasensitivity. Mol Syst Biol *1*, 2005.0028.

Meshorer, E., Yellajoshula, D., George, E., Scambler, P.J., Brown, D.T., and Misteli, T. (2006). Hyperdynamic plasticity of chromatin proteins in pluripotent embryonic stem cells. Dev Cell *10*, 105-116.

Miller, C.J., Li, Q., Abel, K., Kim, E.-Y., Ma, Z.-M., Wietgrefe, S., La Franco-Scheuch, L., Compton, L., Duan, L., Shore, M.D.*, et al.* (2005). Propagation and dissemination of infection after vaginal transmission of simian immunodeficiency virus. J Virol *79*, 9217-9227.

Miller-Jensen, K., Dey, S.S., Pham, N., Foley, J.E., Arkin, A.P., and Schaffer, D.V. (2012). Chromatin accessibility at the HIV LTR promoter sets a threshold for NF-κB mediated viral gene expression. Integr Biol (Camb) *4*, 661-671.

Miller-Jensen, K., Skupsky, R., Shah, P.S., Arkin, A.P., and Schaffer, D.V. (2013). Genetic selection for context-dependent stochastic phenotypes: Sp1 and TATA mutations increase phenotypic noise in HIV-1 gene expression. PLoS Comput Biol *9*, e1003135.

Milo, R., Jorgensen, P., Moran, U., Weber, G., and Springer, M. (2010). BioNumbers--the database of key numbers in molecular and cell biology. Nucleic Acids Res *38*, D750-753.

Mitrophanov, A.Y., and Groisman, E.A. (2008). Positive feedback in cellular control systems. Bioessays *30*, 542-555.

Mousseau, G., Kessing, C.F., Fromentin, R., Trautmann, L., Chomont, N., and Valente, S.T. (2015). The Tat Inhibitor Didehydro-Cortistatin A Prevents HIV-1 Reactivation from Latency. MBio *6*, e00465.

Murphy, K., and Weaver, C. (2017). Janeway's immunobiology.

Nabel, G., and Baltimore, D. (1987). An inducible transcription factor activates expression of human immunodeficiency virus in T cells. Nature *326*, 711-713.

Novis, C.L., Archin, N.M., Buzon, M.J., Verdin, E., Round, J.L., Lichterfeld, M., Margolis, D.M., Planelles, V., and Bosque, A. (2013). Reactivation of latent HIV-1 in central memory $CD4^+$ T cells through TLR-1/2 stimulation. Retrovirology *10*, 119.

Ott, M., Geyer, M., and Zhou, Q. (2011). The control of HIV transcription: keeping RNA polymerase II on track. Cell Host Microbe *10*, 426-435.

Ott, M., Schnölzer, M., Garnica, J., Fischle, W., Emiliani, S., Rackwitz, H.R., and Verdin, E. (1999). Acetylation of the HIV-1 Tat protein by p300 is important for its transcriptional activity. Curr Biol *9*, 1489-1492.

Ozbudak, E.M., Thattai, M., Kurtser, I., Grossman, A.D., and van Oudenaarden, A. (2002). Regulation of noise in the expression of a single gene. Nat Genet *31*, 69-73.

Ozbudak, E.M., Thattai, M., Lim, H.N., Shraiman, B.I., and Van Oudenaarden, A. (2004). Multistability in the lactose utilization network of Escherichia coli. Nature *427*, 737-740.

Pagans, S., Pedal, A., North, B.J., Kaehlcke, K., Marshall, B.L., Dorr, A., Hetzer-Egger, C., Henklein, P., Frye, R., McBurney, M.W.*, et al.* (2005). SIRT1 regulates HIV transcription via Tat deacetylation. PLoS Biol *3*, e41.

Pan, X., Baldauf, H.-M., Keppler, O.T., and Fackler, O.T. (2013). Restrictions to HIV-1 replication in resting CD4+ T lymphocytes. Cell Res *23*, 876-885.

Parada, C.A., and Roeder, R.G. (1996). Enhanced processivity of RNA polymerase II triggered by Tat-induced phosphorylation of its carboxy-terminal domain. Nature *384*, 375-378.

Pearson, R., Kim, Y.K., Hokello, J., Lassen, K., Friedman, J., Tyagi, M., and Karn, J. (2008). Epigenetic silencing of human immunodeficiency virus (HIV) transcription by formation of restrictive chromatin structures at the viral long terminal repeat drives the progressive entry of HIV into latency. J Virol *82*, 12291-12303.

Peccoud, J., and Ycart, B. (1995). Markovian modeling of gene-product synthesis. Theoretical population biology *48*, 222-234.

Perelson, A.S. (2002). Modelling viral and immune system dynamics. Nat Rev Immunol *2*, 28-36.

Perelson, A.S., Neumann, A.U., Markowitz, M., Leonard, J.M., and Ho, D.D. (1996). HIV-1 dynamics in vivo: virion clearance rate, infected cell life-span, and viral generation time. Science *271*, 1582-1586.

Perkins, N.D., Edwards, N.L., Duckett, C.S., Agranoff, A.B., Schmid, R.M., and Nabel, G.J. (1993). A cooperative interaction between NF-kappa B and Sp1 is required for HIV-1 enhancer activation. EMBO J *12*, 3551-3558.

Phiel, C.J., Zhang, F., Huang, E.Y., Guenther, M.G., Lazar, M.A., and Klein, P.S. (2001). Histone deacetylase is a direct target of valproic acid, a potent anticonvulsant, mood stabilizer, and teratogen. Journal of Biological Chemistry *276*, 36734-36741.

Pierson, T.C., Zhou, Y., Kieffer, T.L., Ruff, C.T., Buck, C., and Siliciano, R.F. (2002). Molecular characterization of preintegration latency in human immunodeficiency virus type 1 infection. J Virol *76*, 8518-8531.

Prins, J.M., Jurriaans, S., van Praag, R.M., Blaak, H., van Rij, R., Schellekens, P.T., ten Berge, I.J., Yong, S.L., Fox, C.H., Roos, M.T.*, et al.* (1999). Immuno-activation with anti-CD3 and recombinant human IL-2 in HIV-1-infected patients on potent antiretroviral therapy. AIDS *13*, 2405-2410.

Ptashne, M. (2004). A genetic switch : phage lambda revisited (Cold Spring Harbor, N.Y.: Cold Spring Harbor Laboratory Press).

Rafati, H., Parra, M., Hakre, S., Moshkin, Y., Verdin, E., and Mahmoudi, T. (2011). Repressive LTR nucleosome positioning by the BAF complex is required for HIV latency. PLoS Biol *9*, e1001206.

Raj, A., Peskin, C.S., Tranchina, D., Vargas, D.Y., and Tyagi, S. (2006). Stochastic mRNA synthesis in mammalian cells. PLoS Biol *4*, e309.

Raj, A., and van Oudenaarden, A. (2008). Nature, nurture, or chance: stochastic gene expression and its consequences. Cell *135*, 216-226.

Raser, J.M., and O'Shea, E.K. (2004). Control of stochasticity in eukaryotic gene expression. Science *304*, 1811-1814.

Rasmussen, T.A., Tolstrup, M., Brinkmann, C.R., Olesen, R., Erikstrup, C., Solomon, A., Winckelmann, A., Palmer, S., Dinarello, C., Buzon, M.*, et al.* (2014). Panobinostat, a histone deacetylase inhibitor, for latent-virus reactivation in HIV-infected patients on suppressive antiretroviral therapy: a phase 1/2, single group, clinical trial. Lancet HIV *1*, e13-21.

Razin, A., and Cedar, H. (1977). Distribution of 5-methylcytosine in chromatin. Proc Natl Acad Sci U S A *74*, 2725-2728.

Razooky, B.S., Pai, A., Aull, K., Rouzine, I.M., and Weinberger, L.S. (2015). A hardwired HIV latency program. Cell *160*, 990-1001.

Razooky, B.S., and Weinberger, L.S. (2011). Mapping the architecture of the HIV-1 Tat circuit: A decision-making circuit that lacks bistability and exploits stochastic noise. Methods *53*, 68-77.

Richman, D.D., Margolis, D.M., Delaney, M., Greene, W.C., Hazuda, D., and Pomerantz, R.J. (2009). The challenge of finding a cure for HIV infection. Science *323*, 1304-1307.

Romerio, F., Gabriel, M.N., and Margolis, D.M. (1997). Repression of human immunodeficiency virus type 1 through the novel cooperation of human factors YY1 and LSF. J Virol *71*, 9375-9382.

Rooney, J.W., Sun, Y.L., Glimcher, L.H., and Hoey, T. (1995). Novel NFAT sites that mediate activation of the interleukin-2 promoter in response to T-cell receptor stimulation. Mol Cell Biol *15*, 6299-6310.

Ross, E.K., Buckler-White, A.J., Rabson, A.B., Englund, G., and Martin, M.A. (1991). Contribution of NF-kappa B and Sp1 binding motifs to the replicative capacity of human immunodeficiency virus type 1: distinct patterns of viral growth are determined by T-cell types. Journal of virology *65*, 4350-4358.

Routy, J.P., Tremblay, C.L., Angel, J.B., Trottier, B., Rouleau, D., Baril, J.G., Harris, M., Trottier, S., Singer, J., Chomont, N.*, et al.* (2012). Valproic acid in association with highly active antiretroviral therapy for reducing systemic HIV-1 reservoirs: results from a multicentre randomized clinical study. HIV Med *13*, 291-296.

Rouzine, I.M., Weinberger, A.D., and Weinberger, L.S. (2015). An evolutionary role for HIV latency in enhancing viral transmission. Cell *160*, 1002-1012.

Ruelas, D.S., and Greene, W.C. (2013). An integrated overview of HIV-1 latency. Cell *155*, 519-529.

Sagot-Lerolle, N., Lamine, A., Chaix, M.-L., Boufassa, F., Aboulker, J.-P., Costagliola, D., Goujard, C., Paller, C., Delfraissy, J.-F., and Lambotte, O. (2008). Prolonged valproic acid treatment does not reduce the size of latent HIV reservoir. Aids *22*, 1125-1129.

Said, E.A., Dupuy, F.P., Trautmann, L., Zhang, Y., Shi, Y., El-Far, M., Hill, B.J., Noto, A., Ancuta, P., Peretz, Y.*, et al.* (2010). Programmed death-1-induced interleukin-10 production by monocytes impairs CD4+ T cell activation during HIV infection. Nat Med *16*, 452-459.

Scheller, C., Ullrich, A., Lamla, S., Dittmer, U., Rethwilm, A., and Koutsilieri, E. (2006). Dual activity of phosphorothioate CpG oligodeoxynucleotides on HIV. Annals of the New York Academy of Sciences *1091*, 540-547.

Schröder, A.R.W., Shinn, P., Chen, H., Berry, C., Ecker, J.R., and Bushman, F. (2002). HIV-1 integration in the human genome favors active genes and local hotspots. Cell *110*, 521-529.

Shah, K., and Tyagi, S. (2013). Barriers to transmission of transcriptional noise in a c-fos c-jun pathway. Mol Syst Biol *9*, 687.

Shan, L., Yang, H.-C., Rabi, S.A., Bravo, H.C., Shroff, N.S., Irizarry, R.A., Zhang, H., Margolick, J.B., Siliciano, J.D., and Siliciano, R.F. (2011). Influence of host gene transcription level and orientation on HIV-1 latency in a primary-cell model. Journal of virology *85*, 5384-5393.

Shang, H.-t., Ding, J.-w., Yu, S.-y., Wu, T., Zhang, Q.-l., and Liang, F.-j. (2015). Progress and challenges in the use of latent HIV-1 reactivating agents. Acta Pharmacol Sin *36*, 908-916.

Shearwin, K.E., Callen, B.P., and Egan, J.B. (2005). Transcriptional interference--a crash course. Trends Genet *21*, 339-345.

Sherrill-Mix, S., Lewinski, M.K., Famiglietti, M., Bosque, A., Malani, N., Ocwieja, K.E., Berry, C.C., Looney, D., Shan, L., Agosto, L.M.*, et al.* (2013). HIV latency and integration site placement in five cell-based models. Retrovirology *10*, 90.

Shun, M.-C., Raghavendra, N.K., Vandegraaff, N., Daigle, J.E., Hughes, S., Kellam, P., Cherepanov, P., and Engelman, A. (2007). LEDGF/p75 functions downstream from preintegration complex formation to effect gene-specific HIV-1 integration. Genes Dev *21*, 1767-1778.

Siliciano, J.D., Kajdas, J., Finzi, D., Quinn, T.C., Chadwick, K., Margolick, J.B., Kovacs, C., Gange, S.J., and Siliciano, R.F. (2003). Long-term follow-up studies confirm the stability of the latent reservoir for HIV-1 in resting CD4+ T cells. Nat Med *9*, 727-728.

Siliciano, J.D., Lai, J., Callender, M., Pitt, E., Zhang, H., Margolick, J.B., Gallant, J.E., Cofrancesco, J., Moore, R.D., Gange, S.J.*, et al.* (2007). Stability of the latent reservoir for HIV-1 in patients receiving valproic acid. J Infect Dis *195*, 833-836.

Siliciano, J.D., and Siliciano, R.F. (2005). Enhanced culture assay for detection and quantitation of latently infected, resting CD4+ T-cells carrying replication-competent virus in HIV-1-infected individuals. Methods Mol Biol *304*, 3-15.

Siliciano, R.F., and Greene, W.C. (2011). HIV latency. Cold Spring Harb Perspect Med *1*, a007096.

Simonis, M., Klous, P., Splinter, E., Moshkin, Y., Willemsen, R., de Wit, E., van Steensel, B., and de Laat, W. (2006). Nuclear organization of active and inactive chromatin domains uncovered by chromosome conformation capture-on-chip (4C). Nat Genet *38*, 1348-1354.

Singh, A., Razooky, B., Cox, C.D., Simpson, M.L., and Weinberger, L.S. (2010). Transcriptional bursting from the HIV-1 promoter is a significant source of stochastic noise in HIV-1 gene expression. Biophysical journal *98*, L32-L34.

Singh, A., Razooky, B.S., Dar, R.D., and Weinberger, L.S. (2012). Dynamics of protein noise can distinguish between alternate sources of gene-expression variability. Mol Syst Biol *8*, 607.

Skupsky, R., Burnett, J.C., Foley, J.E., Schaffer, D.V., and Arkin, A.P. (2010). HIV promoter integration site primarily modulates transcriptional burst size rather than frequency. PLoS Comput Biol *6*.

So, L.-H., Ghosh, A., Zong, C., Sepúlveda, L.A., Segev, R., and Golding, I. (2011). General properties of transcriptional time series in Escherichia coli. Nat Genet *43*, 554-560.

Søgaard, O.S., Graversen, M.E., Leth, S., Olesen, R., Brinkmann, C.R., Nissen, S.K., Kjaer, A.S., Schleimann, M.H., Denton, P.W., Hey-Cunningham, W.J.*, et al.* (2015). The Depsipeptide Romidepsin Reverses HIV-1 Latency In Vivo. PLoS Pathog *11*, e1005142.

Spina, C.A., Guatelli, J.C., and Richman, D.D. (1995). Establishment of a stable, inducible form of human immunodeficiency virus type 1 DNA in quiescent CD4 lymphocytes in vitro. J Virol *69*, 2977-2988.

Spivak, A.M., Andrade, A., Eisele, E., Hoh, R., Bacchetti, P., Bumpus, N.N., Emad, F., Buckheit, R., McCance-Katz, E.F., Lai, J.*, et al.* (2014). A pilot study assessing the safety and latency-reversing activity of disulfiram in HIV-1-infected adults on antiretroviral therapy. Clin Infect Dis *58*, 883-890.

Steel, A., Clark, S., Teo, I., Shaunak, S., Nelson, M., Gazzard, B., and Kelleher, P. (2006). No change to HIV-1 latency with valproate therapy. Aids *20*, 1681-1682.

Stellbrink, H.-J., van Lunzen, J., Westby, M., O'Sullivan, E., Schneider, C., Adam, A., Weitner, L., Kuhlmann, B., Hoffmann, C., Fenske, S.*, et al.* (2002). Effects of interleukin-2 plus highly active antiretroviral therapy on HIV-1 replication and proviral DNA (COSMIC trial). AIDS *16*, 1479-1487.

Stevenson, M., Stanwick, T.L., Dempsey, M.P., and Lamonica, C.A. (1990). HIV-1 replication is controlled at the level of T cell activation and proviral integration. EMBO J *9*, 1551-1560.

Stock, P.G., Barin, B., Hatano, H., Rogers, R.L., Roland, M.E., Lee, T.-H., Busch, M., Deeks, S.G., and for Solid Organ Transplantation in HIV Study Investigators (2014). Reduction of HIV persistence following transplantation in HIV-infected kidney transplant recipients. Am J Transplant *14*, 1136-1141.

Strogatz, S.H. (2014). Nonlinear dynamics and chaos: with applications to physics, biology, chemistry, and engineering (Westview press).

Struhl, K., and Segal, E. (2013). Determinants of nucleosome positioning. Nat Struct Mol Biol *20*, 267-273.

Süel, G.M., Garcia-Ojalvo, J., Liberman, L.M., and Elowitz, M.B. (2006). An excitable gene regulatory circuit induces transient cellular differentiation. Nature *440*, 545-550.

Suñé, C., and García-Blanco, M.A. (1995). Sp1 transcription factor is required for in vitro basal and Tat-activated transcription from the human immunodeficiency virus type 1 long terminal repeat. J Virol *69*, 6572-6576.

Suter, D.M., Molina, N., Gatfield, D., Schneider, K., Schibler, U., and Naef, F. (2011). Mammalian genes are transcribed with widely different bursting kinetics. Science *332*, 472-474.

Swiggard, W.J., Baytop, C., Yu, J.J., Dai, J., Li, C., Schretzenmair, R., Theodosopoulos, T., and O'Doherty, U. (2005). Human immunodeficiency virus type 1 can establish latent infection in resting CD4+ T cells in the absence of activating stimuli. J Virol *79*, 14179-14188.

Symmons, O., and Raj, A. (2016). What's Luck Got to Do with It: Single Cells, Multiple Fates, and Biological Nondeterminism. Mol Cell *62*, 788-802.

Taniguchi, Y., Choi, P.J., Li, G.-W., Chen, H., Babu, M., Hearn, J., Emili, A., and Xie, X.S. (2010). Quantifying E. coli proteome and transcriptome with single-molecule sensitivity in single cells. Science *329*, 533-538.

Tantale, K., Mueller, F., Kozulic-Pirher, A., Lesne, A., Victor, J.-M., Robert, M.-C., Capozi, S., Chouaib, R., Bäcker, V., and Mateos-Langerak, J. (2016). A single-molecule view of transcription reveals convoys of RNA polymerases and multi-scale bursting. Nature Communications *7*.

Teng, M.W., Bolovan-Fritts, C., Dar, R.D., Womack, A., Simpson, M.L., Shenk, T., and Weinberger, L.S. (2012). An endogenous accelerator for viral gene expression confers a fitness advantage. Cell *151*, 1569-1580.

Tirosh, I., and Barkai, N. (2008). Two strategies for gene regulation by promoter nucleosomes. Genome Res *18*, 1084-1091.

To, T.-L., and Maheshri, N. (2010). Noise can induce bimodality in positive transcriptional feedback loops without bistability. Science *327*, 1142-1145.

Tyagi, M., Pearson, R.J., and Karn, J. (2010). Establishment of HIV latency in primary CD4+ cells is due to epigenetic transcriptional silencing and P-TEFb restriction. J Virol *84*, 6425-6437.

UNAIDS (2015). Global AIDS Response Progress Reporting 2015. World Health Organization Press: Geneva, Switzerland.

Van Lint, C., Emiliani, S., Ott, M., and Verdin, E. (1996). Transcriptional activation and chromatin remodeling of the HIV-1 promoter in response to histone acetylation. The EMBO journal *15*, 1112.

van Praag, R.M., Prins, J.M., Roos, M.T., Schellekens, P.T., Ten Berge, I.J., Yong, S.L., Schuitemaker, H., Eerenberg, A.J., Jurriaans, S., de Wolf, F.*, et al.* (2001). OKT3 and IL-2 treatment for purging of the latent HIV-1 reservoir in vivo results in selective long-lasting CD4+ T cell depletion. J Clin Immunol *21*, 218-226.

Vandergeeten, C., Fromentin, R., DaFonseca, S., Lawani, M.B., Sereti, I., Lederman, M.M., Ramgopal, M., Routy, J.-P., Sékaly, R.-P., and Chomont, N. (2013). Interleukin-7 promotes HIV persistence during antiretroviral therapy. Blood *121*, 4321-4329.

VandeWoude, S., and Apetrei, C. (2006). Going wild: lessons from naturally occurring T-lymphotropic lentiviruses. Clin Microbiol Rev *19*, 728-762.

Velu, V., Shetty, R.D., Larsson, M., and Shankar, E.M. (2015). Role of PD-1 co-inhibitory pathway in HIV infection and potential therapeutic options. Retrovirology *12*, 14.

Verdin, E., Paras Jr, P., and Van Lint, C. (1993). Chromatin disruption in the promoter of human immunodeficiency virus type 1 during transcriptional activation. The EMBO journal *12*, 3249.

Viñuelas, J., Kaneko, G., Coulon, A., Vallin, E., Morin, V., Mejia-Pous, C., Kupiec, J.-J., Beslon, G., and Gandrillon, O. (2013). Quantifying the contribution of chromatin dynamics to stochastic gene expression reveals long, locus-dependent periods between transcriptional bursts. BMC Biol *11*, 15.

Voss, T.C., Schiltz, R.L., Sung, M.-H., Yen, P.M., Stamatoyannopoulos, J.A., Biddie, S.C., Johnson, T.A., Miranda, T.B., John, S., and Hager, G.L. (2011). Dynamic exchange at regulatory elements during chromatin remodeling underlies assisted loading mechanism. Cell *146*, 544-554.

Wall, M.E., Hlavacek, W.S., and Savageau, M.A. (2004). Design of gene circuits: lessons from bacteria. Nat Rev Genet *5*, 34-42.

Wang, F.-X., Xu, Y., Sullivan, J., Souder, E., Argyris, E.G., Acheampong, E.A., Fisher, J., Sierra, M., Thomson, M.M., and Najera, R. (2005). IL-7 is a potent and proviral strain--specific inducer of latent HIV-1 cellular reservoirs of infected individuals on virally suppressive HAART. The Journal of clinical investigation *115*, 128-137.

Wawer, M.J., Gray, R.H., Sewankambo, N.K., Serwadda, D., Li, X., Laeyendecker, O., Kiwanuka, N., Kigozi, G., Kiddugavu, M., Lutalo, T.*, et al.* (2005). Rates of HIV-1 transmission per coital act, by stage of HIV-1 infection, in Rakai, Uganda. J Infect Dis *191*, 1403-1409.

Wei, P., Garber, M.E., Fang, S.M., Fischer, W.H., and Jones, K.A. (1998). A novel CDK9-associated C-type cyclin interacts directly with HIV-1 Tat and mediates its high-affinity, loop-specific binding to TAR RNA. Cell *92*, 451-462.

Weinberger, L.S. (2015). A minimal fate-selection switch. Curr Opin Cell Biol *37*, 111-118.

Weinberger, L.S., Burnett, J.C., Toettcher, J.E., Arkin, A.P., and Schaffer, D.V. (2005). Stochastic gene expression in a lentiviral positive-feedback loop: HIV-1 Tat fluctuations drive phenotypic diversity. Cell *122*, 169-182.

Weinberger, L.S., Dar, R.D., and Simpson, M.L. (2008). Transient-mediated fate determination in a transcriptional circuit of HIV. Nat Genet *40*, 466-470.

Weinberger, L.S., and Shenk, T. (2007). An HIV feedback resistor: auto-regulatory circuit deactivator and noise buffer. PLoS Biol *5*, e9.

West, M.J., Lowe, A.D., and Karn, J. (2001). Activation of human immunodeficiency virus transcription in T cells revisited: NF-kappaB p65 stimulates transcriptional elongation. Journal of virology *75*, 8524-8537.

Whitney, J.B., Hill, A.L., Sanisetty, S., Penaloza-MacMaster, P., Liu, J., Shetty, M., Parenteau, L., Cabral, C., Shields, J., Blackmore, S.*, et al.* (2014). Rapid seeding of the viral reservoir prior to SIV viraemia in rhesus monkeys. Nature *512*, 74-77.

Williams, S.A., Chen, L.-F., Kwon, H., Ruiz-Jarabo, C.M., Verdin, E., and Greene, W.C. (2006). NF-kappaB p50 promotes HIV latency through HDAC recruitment and repression of transcriptional initiation. EMBO J *25*, 139-149.

Winckelmann, A.A., Munk-Petersen, L.r.V., Rasmussen, T.A., Melchjorsen, J., Hjelholt, T.J., Montefiori, D., Ãstergaard, L., SÃ¸gaard, O.S., and Tolstrup, M. (2013). Administration of a Toll-like receptor 9 agonist decreases the proviral reservoir in virologically suppressed HIV-infected patients. PLoS One *8*, e62074.

Wong, J.K., Hezareh, M., Günthard, H.F., Havlir, D.V., Ignacio, C.C., Spina, C.A., and Richman, D.D. (1997). Recovery of replication-competent HIV despite prolonged suppression of plasma viremia. Science *278*, 1291-1295.

Xing, S., Bullen, C.K., Shroff, N.S., Shan, L., Yang, H.-C., Manucci, J.L., Bhat, S., Zhang, H., Margolick, J.B., and Quinn, T.C. (2011). Disulfiram reactivates latent HIV-1 in a Bcl-2-transduced primary CD4+ T cell model without inducing global T cell activation. Journal of virology *85*, 6060-6064.

Yang, Z., Zhu, Q., Luo, K., and Zhou, Q. (2001). The 7SK small nuclear RNA inhibits the CDK9/cyclin T1 kinase to control transcription. Nature *414*, 317-322.

Yu, J., Xiao, J., Ren, X., Lao, K., and Xie, X.S. (2006). Probing gene expression in live cells, one protein molecule at a time. Science *311*, 1600-1603.

Yu, Q., König, R., Pillai, S., Chiles, K., Kearney, M., Palmer, S., Richman, D., Coffin, J.M., and Landau, N.R. (2004). Single-strand specificity of APOBEC3G accounts for minus-strand deamination of the HIV genome. Nat Struct Mol Biol *11*, 435-442.

Yukl, S., Pillai, S., Li, P., Chang, K., Pasutti, W., Ahlgren, C., Havlir, D., Strain, M., Günthard, H., Richman, D.*, et al.* (2009). Latently-infected CD4+ T cells are enriched for HIV-1 Tat variants with impaired transactivation activity. Virology *387*, 98-108.

Zack, J.A., Arrigo, S.J., Weitsman, S.R., Go, A.S., Haislip, A., and Chen, I.S. (1990). HIV-1 entry into quiescent primary lymphocytes: molecular analysis reveals a labile, latent viral structure. Cell *61*, 213-222.

Zack, J.A., Haislip, A.M., Krogstad, P., and Chen, I.S. (1992). Incompletely reverse-transcribed human immunodeficiency virus type 1 genomes in quiescent cells can function as intermediates in the retroviral life cycle. J Virol *66*, 1717-1725.

Zhong, H., May, M.J., Jimi, E., and Ghosh, S. (2002). The phosphorylation status of nuclear NF-kappa B determines its association with CBP/p300 or HDAC-1. Mol Cell *9*, 625-636.

Zhou, Y., Zhang, H., Siliciano, J.D., and Siliciano, R.F. (2005). Kinetics of human immunodeficiency virus type 1 decay following entry into resting CD4+ T cells. J Virol *79*, 2199-2210.

Zoller, B., Nicolas, D., Molina, N., and Naef, F. (2015). Structure of silent transcription intervals and noise characteristics of mammalian genes. Mol Syst Biol *11*, 823.

Zong, C., So, L.-h., Sepúlveda, L.A., Skinner, S.O., and Golding, I. (2010). Lysogen stability is determined by the frequency of activity bursts from the fate-determining gene. Mol Syst Biol *6*, 440.

Publishing Agreement

It is the policy of the University to encourage the distribution of all theses, dissertations, and manuscripts. Copies of all UCSF theses, dissertations, and manuscripts will be routed to the library via the Graduate Division. The library will make all theses, dissertations, and manuscripts accessible to the public and will preserve these to the best of their abilities, in perpetuity.

Please sign the following statement:

I hereby grant permission to the Graduate Division of the University of California, San Francisco to release copies of my thesis, dissertation, or manuscript to the Campus Library to provide access and preservation, in whole or in part, in perpetuity.

Katherine Aull
Author Signature

12/21/16
Date